Understanding of the kinetic stability of cis-isomer of halogenated azobenzene through structural, kinetic and computational studies

Manish Kumar Yadav

A dissertation submitted for the partial fulfilment of BS-MS dual degree in Science

Indian Institute of Science Education and Research Mohali

May 2020

Certificate of Examination

This is to certify that the dissertation titled **"Understanding of the kinetic stability of cis-isomer of azobenzenes through structural, kinetic and computational studies**" submitted by **Mr. Manish Kumar Yadav** (Reg. No. MS14055) for the partial fulfilment of BS- MS dual degree program of the Institute, has been examined by the thesis committee duly appointed by the Institute. The committee finds the work done by the candidate satisfactory and recommends that the report be accepted.

Dr. Debashis Adhikari Dr. Santanu Kumar Pal Dr. Angshuman Roy Choudhury

(Supervisor)

4th May, 2020

Declaration

The work presented in this dissertation has been carried out by me under the guidance of Dr. Angshuman Roy Choudhury at the Indian Institute of Science Education and Research Mohali.

This work has not been submitted in art or in full for a degree, a diploma, or a fellowship to any other university or institute. Whenever contributions of others are involved, every effort is made to indicate this clearly, with due acknowledgement of collaborative research and discussions. This thesis is a bona fide record of original work done by me and all sources listed within have been detailed in bibliography.

Manish Kumar Yadav

MS14055

May, 04, 2020

In my capacity as the supervisor of the candidate's project work, I certify that the above statements by the candidate are true to the best of my knowledge.

Dr. Angshuman Roy Choudhury

(Supervisor)

Acknowledgements

I would like to express my gratitude to my MS Project supervisor **Dr. Angshuman Roy Choudhury** for giving me this wonderful opportunity to explore the exciting field of Spectroscopy, X-ray Crystallography and for all his guidance, motivation, continuous support and insight which helped in completion of my project. It would never have been possible without his mentorship provided in the Project.

I would like to gratefully acknowledge the help and guidance of **Dr. Debashis Adhikari** and **Dr. Santanu Kumar Pal** members of my MS project committee for kindly reviewing my MS project thesis and for his useful comments, encouraging discussions during my evaluation.

I thank **Dr. Sagarika Dev**, **Dr. P. Balanarayan** for all the support in theoretical calculations and encouragement throughout my project work.

I acknowledge IISER Mohali for central X-ray diffraction, Differential Scanning calorimetry (DSC), FTIR, NMR, UV-visible spectroscopy facilities. I thank **Dr. Samrat Ghosh, Dr. Sanchita Sengupta** and all the faculty members of the department of chemical sciences, **Mr. Mangat Ram** and **Mr. Bahadur** for their help in the teaching laboratory for facilitating the use of various departmental instruments. I also thank to the staff members of library, computing facility, stores and purchase department of the IISER Mohali for their help and co-operation during the course of time.

I would like to take this opportunity to acknowledge IISER Mohali first **Director Prof. N. Sathyamurthy** for all his help and encouragement for their guidance in academic matters during my course of study throughout my BS-MS.

My sincere thanks to lab mates **Dr. Dhiraj Das**, **Ms. Labhini Singla**, **Mr. Mayank Joshi** for their cooperation and support during my project, teaching me different aspects of research including handling of chemicals, usages of different instruments and their software.

Other lab members **Mr. Atul Kumar** and **Mr. Maheshwarao Karanam** are also acknowledged for the support and help for organic synthesis.

I would like to give special thanks to the contribution of my higher secondary teachers and Motivational Guru for building my character. **Mahendra Singh Chouhan Nitin Vijay, Anurag Mishra,Manoj Chauhan,Vineet Khatri.** Without their teaching, motivation and encouragement it was not possible for me to come to this stage of my life.

I deeply express my gratitude to my parents **Gajendra Prasad Yadav, Pramila Devi** for never-ending support and inspiration throughout my life. I sincerely acknowledge my brother **Prashant** and sisters **Sonika** and **Monika.** I wish to thank all my friends for their cheerful companionship and special thanks to **Jagbir** for encouragement, love and affection for me.

Mr. Manish Kumar Yadav

(MS 14055)

Contents

List of Figures

List of Tables

Abstract

As we know that Azobenzene (AB) derivatives are widely used as photo switchable systems for various applications. Aromatic azobenzenes are excellent candidates as molecular switches, their capability to undergo fast, efficient, and reversible photo-isomerization (trans→cis). Our study focuses on synthesis of symmetrically as well as unsymmetrically halogen substituted AB derivatives with the focus on the kinetics of spontaneous *cis*- to *trans*- isomerization in the presence of visible light. A library of halogen-substituted azobenzenes (ABs) have been synthesized and structurally characterized by single crystal X-ray diffraction technique and various other spectroscopic technique like IR, NMR, PXRD, DSC after that their solid-state interactions has been studied. Halogenated azobenzenes studies herein display fast photo switching properties. Kinetics of *cis*- → *trans*- isomerization has been studied using UV-VIS spectroscopy and the rate constant for this transformation were determined. Theoretical studies like Intrinsic Reaction Coordinate (IRC) was followed to establish the transformation TS to *trans*- and TS to *cis*- isomers. The optimizations of the *trans*-, *cis*- isomers and the probable transition states were conducted using DFT/B3LYP level of theory and 6-311++G(d,p) as basis set. The effect of the solvents (DMSO) were modelled with the polarizable continuum model (PCM). Optimization of probable conformers of the *cis*- isomer and the corresponding transition state (TS) were carried out to determine the energy of activation. The Time-Dependent Density Functional Theory (TD-DFT) calculations were also performed to gain insight into the photo-isomerization by comparing the wavelength and the nature of transitions observed in the experimental UV-Vis spectra. Our results indicate that the fluorinated compounds display better kinetic stability of the *cis*- isomer compared to the corresponding chloro and bromo analogues.

CHAPTER 1

Introduction

1.1Historical Perspective

The existence of the *cis*- isomer of azobenzene was first reported in Nature by Hartley in 1937 in the article entitled "The Cis- form of Azobenzene" a result of their study on the determination of the solubility of azobenzene, using a photometric method of analysis.[1] They traced an increase in the light absorption of standard prepared solution on exposure to UV light. Thus he identified, for the first time the photochemical isomerization of azobenzene. Since then the photo-isomerization of azobenzene has become an example of unimolecular photochemical reaction and through this work *cis-trans* isomerization by excited state mechanism has been a famous subject to investigation for ultra-fast spectroscopy.[1] Azobenzene (AB) derivatives are widely used as photo switchable systems for various applications.[2-5] Most interesting features of ABs are their capability to undergo fast, efficient, and reversible photo-isomerization (*trans*- → *cis*-) without sufficient photo bleaching. The AB moiety is generally incorporated in a wide variety of systems due to their useful and versatile nature. Their unique photo-isomerization property is utilized for applications in photo-orientation of materials,[6-9] photo switching properties of materials[10,11] and all-optical surface patterning.[12-14] AB moiety has a potential application in controlling enzyme activities by the incorporation into the biological system.[15] It has been observed that *trans*- and *cis*- isomers of AB have different interaction with polymerase enzyme. Incorporation of *cis*- isomer of AB into the DNA sequence results in the disruption of duplex formation.[16] Thus by incorporating AB unit in the new system one can generate systems, which can be triggered by visible light and this strategy can be applied to resolve the problems in the chemical dynamics, with biological systems being the explicit targets. In addition, researchers are still trying to increase the lifetime of *cis* – isomer. Researchers have reported the lifetime of the *cis*- isomer up to 6 years.[17-22] Synthetic protocols have also been reported to synthesize exclusively the *cis*- isomer.[23]

Azobenzenes have two geometrical isomers around N=N like alkenes. The *trans*- isomer energy is more stable than the *cis* isomer by around 12 Kcal/mol.[24] The energy barrier between these two states is around 23 Kcal/mol.[25] If we irradiate the *trans*- isomer using UV light of wavelength between 320-365nm, it is converted to the *cis*- isomer ($S_1 \leftarrow S_0$ or $S_2 \leftarrow S_0$ excitation) and the *cis*- isomer is spontaneously converted to the *trans*- isomer when irradiated at 400-450nm (exciting S_1 or S_2) or by heating. While the *trans*- azobenzene do not have any dipole

moment, *cis*– isomer, having an angular geometry, has a dipole moment of 3.0 D, and one of the rings is flipped to minimize the π-cloud repulsion of one another. This type of rearrangement affect the proton nuclear magnetic resonance spectrum (^{1}H NMR), signal of *cis*-isomer appear higher field strength than the *trans*- isomers due-to the anisotropic effect of the π-cloud of the aromatic rings of azobenzene. When the isomerization process occurs then the distance between the two carbon atoms in the position 4 of the aromatic rings of azobenzenes from 9.0 Å in the transform to 5.5 Å in the *cis* form (Figure 1.1)[26] The azobenzenes in UV-Visible spectrum having two characteristics absorption bands the first one is π→π*(UV-region) and n→π*(Visible region) electronic transitions.[27]

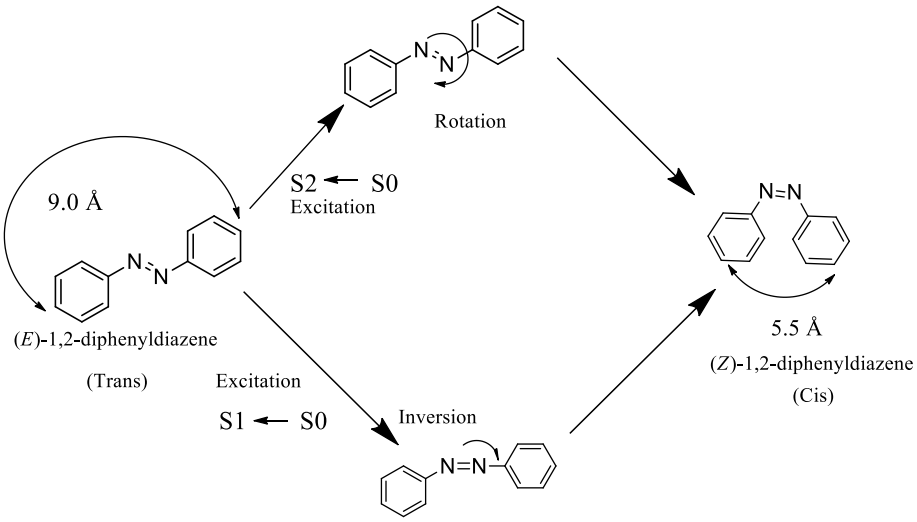

Figure 1.1: Photo-isomerization process of azobenzene.

1.2 Recent developments on azobenzene photo-switching

In the last couple of decades, many research groups across the oceans have contributed in the area related to azobenzene photoisomerization.[28-34] While Karanam & Choudhury reported structural analysis of halogen substituted Azobenzenes and reported the significance of weak interactions in those,[28] Zharnikov group have reported the photoisomerization of azobenzene-substituted thiolates on Au(111) substrate in context of work function variation: the effect of structure and packing density.[29] Hong-Xing Zhang group theoretically studied the *cis-trans* isomerization mechanism of a pendant metal-bound azobenzene[30] and theoretical study of substituent and charge effects on the thermal *cis-trans* isomerization of ortho-fluoroazobenezenes photoswitches.[31] In 2018 Rafal Klajn group reported Reversible photoswitching of encapsulated azobenzenes in water and investigated the behaviour of azobenzene-the key building block of light controlled molecular machine[32] and also published

their research work on Supramolecular Control of Azobenzene Switching on Nanoparticals in journal of the American Chemical Society.[33] Recently Jonathen E. Beves group from School of Chemistry, UNSW Sydney Australia reported their work on Visible-light Photoswitching by azabenzazoles.[34]

1.3 Foreword

Based on the literature reports available on azobenzene, we aimed to study and understand the kinetic stability of *cis*-isomer of halogenated azobenzene derivatives. Our study focuses on synthesis of symmetrically as well as unsymmetrically halogen substituted AB derivatives with the focus on the kinetics of spontaneous *cis*- to *trans*- isomerization in the presence of visible light. This study may lead to a strategy to develop ABs with kinetically stable *cis*- isomer in solution and in the solid state as well. Herein, we have successfully synthesized a series (fifteen) of both symmetrical and unsymmetrical halogen derivatives of azobenzene. We have structurally characterized the *trans*- isomers of azobenzene derivatives by single crystal and powder X-ray diffraction technique and studied their photo-isomerization process by UV/Vis and NMR spectroscopy. In addition, we have conducted computational study to verify the experimental result by density functional theory method and spectral signatures were explained by time dependent density functional theory (TD-DFT) using Gaussian09.[35]

CHAPTER 2

Methodology

2.1 Experimental

2.1.1 Synthesis

All the substituted aniline derivatives were purchased from Sigma Aldrich, India, and were used without further purification. Solvents and reagents were purchased from Merck Chemicals, India, and used as received. All the unsymmetrical azo compounds (**1a, 1b, 1c, 2a, 2b,** and **2c**) and symmetrical azo compounds (**3a, 3b, 3c, 4a, 4b, 4c, 5a, 5b,** and **5c**) as indicated in Scheme S1 and Scheme S2 were synthesized using the procedure reported in the literature.[36,37]

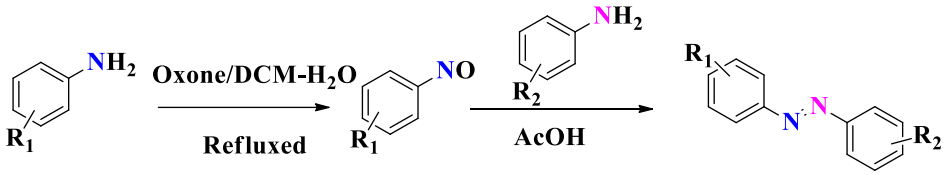

R_1 = H, R_2 = 3-F - (1a)
R_1 = H, R_2 = 3-Cl - (1b)
R_1 = H, R_2 = 3-Br - (1c)
R_1 = 4-F, R_2 = 3-F - (2a)
R_1 = 4-Cl, R_2 = 3-Cl - (2b)
R_1 = 4-Br, R_2 = 3-Br - (2c)

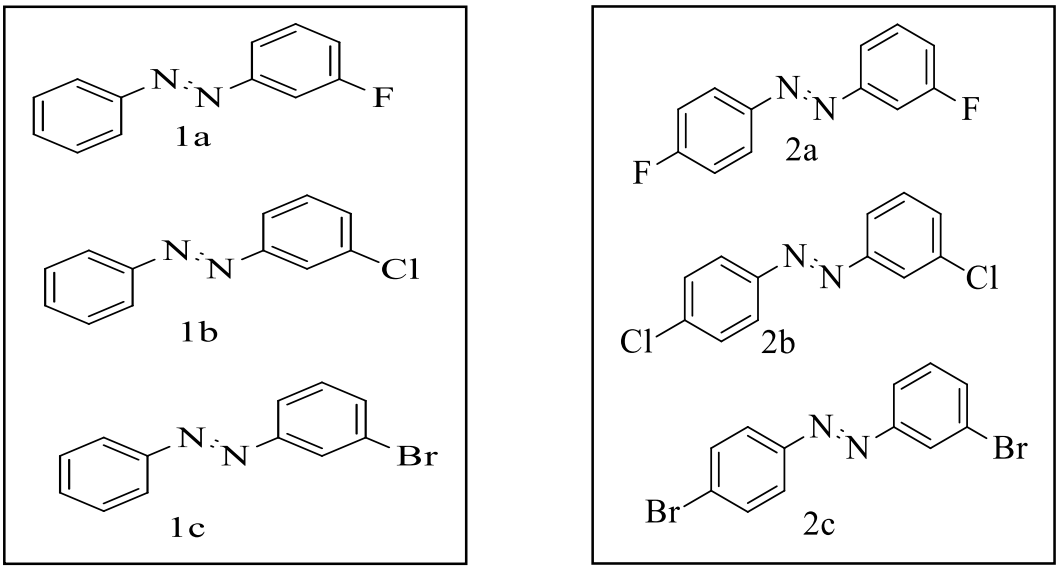

Scheme S1: Synthetic Scheme for unsymmetrical Azobenzene

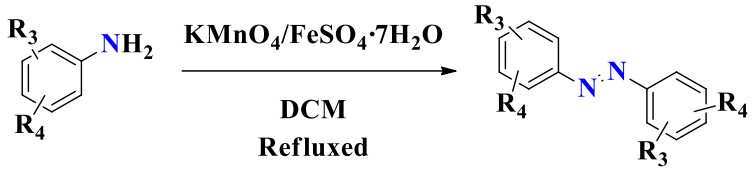

R_3 = 2-F, R_4 = 5-F - (3a)
R_3 = 2-Cl, R_4 = 5-Cl - (3b)
R_3 = 2-Br, R_4 = 5-Br - (3c)
R_3 = 2-F, R_4 = 4-F - (4a)
R_3 = 2-Cl, R_4 = 4-Cl - (4b)
R_3 = 2-Br, R_4 = 4-Br - (4c)
R_3 = 3-F, R_4 = 5-F - (5a)
R_3 = 3-Cl, R_4 = 5-Cl - (5b)
R_3 = 3-Br, R_4 = 5-Br - (5c)

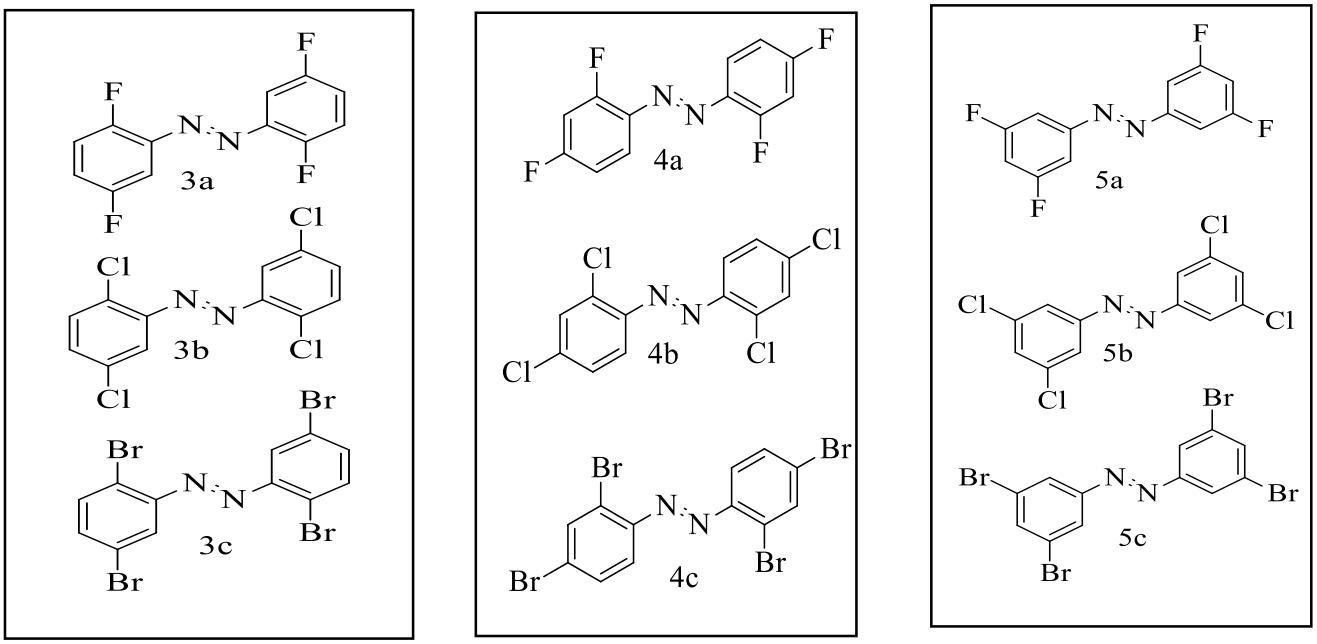

Scheme S2: Synthetic Scheme for symmetrical Azobenzenes

For the synthesis of unsymmetrical (**1a, 1b, 1c, 2a, 2b,** and **2c**) azobenzenes, at first the nitroso compound of one aniline was synthesized using oxone, and then second aniline (1 eqiv.) was added to the acetic acid solution of nitroso compounds (1.2 eqiv.). The symmetrical azo compounds (**3a, 3b, 3c, 4a, 4b, 4c, 5a, 5b,** and **5c**) were synthesized by taking corresponding aniline derivatives (2 mmol) and a freshly ground mixture of $KMnO_4$ (1 g) and $FeSO_4{\cdot}7H_2O$ (1 g) in DCM (20 mL). The reaction mixture was refluxed overnight. Then reaction mixture was filtered through Whatman 40 filter paper and concentrated under reduced pressure. The obtained crude product from the reaction was purified by flash chromatography on a short silica gel (100-200 mesh size) column using hexane as an eluent. .

2.1.2 Characterization

2.1.2(A) Spectroscopic Characterization

All the compounds were characterized by FT-IR (PerkinElmer Spectrum 2) and [^{1}H and ^{13}C] NMR (400 MHz for ^{1}H, 100 MHz for ^{13}C) Bruker ultra shield plus Avance-III NMR spectrometer

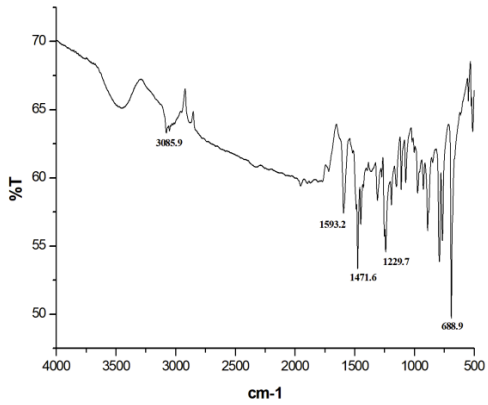

1a

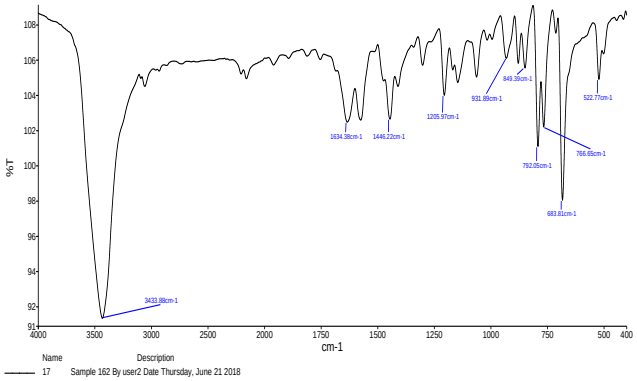

1b

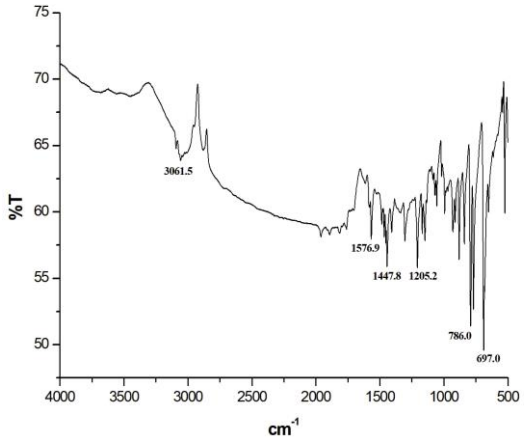

1c

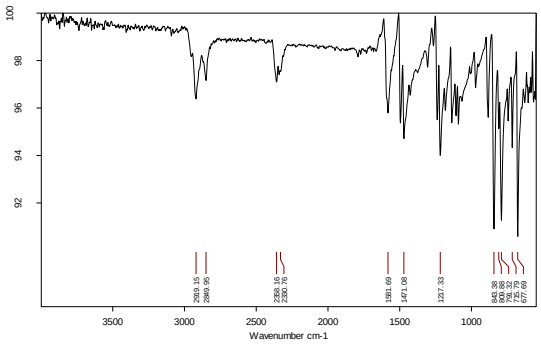

2a

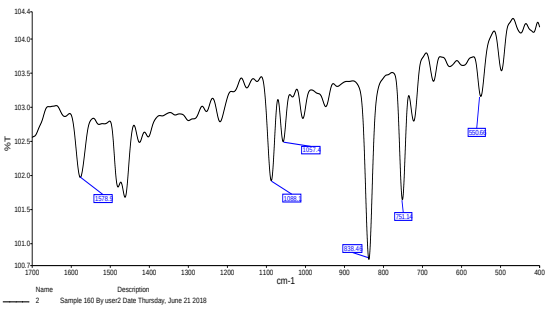

2b

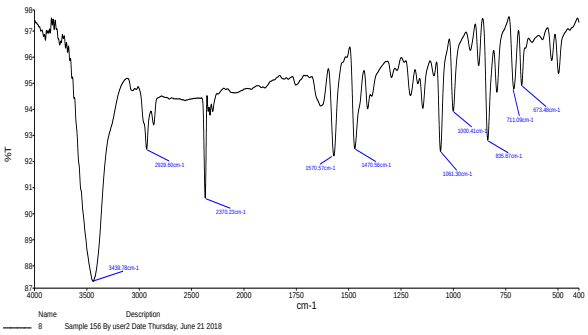

2c

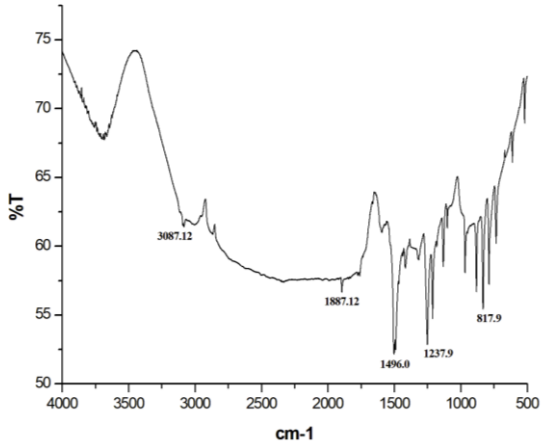

3a

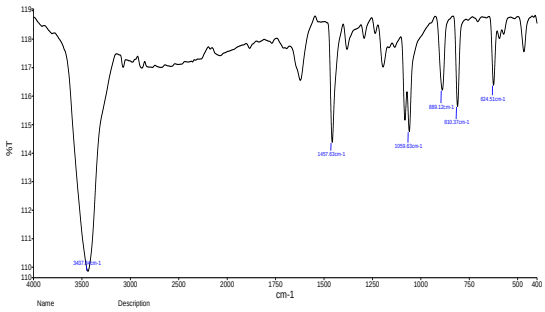

3b

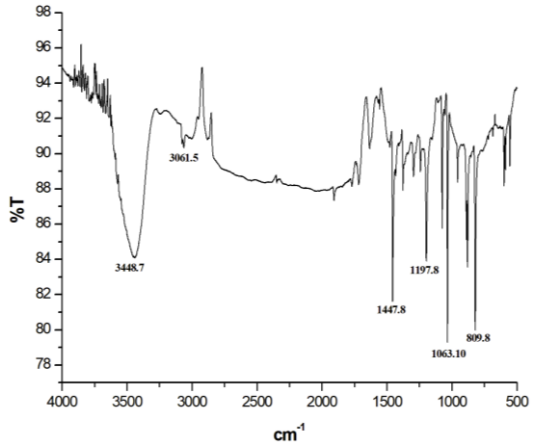

3c

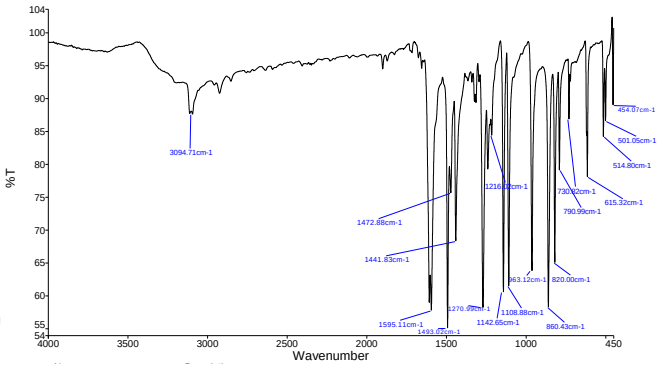

4a

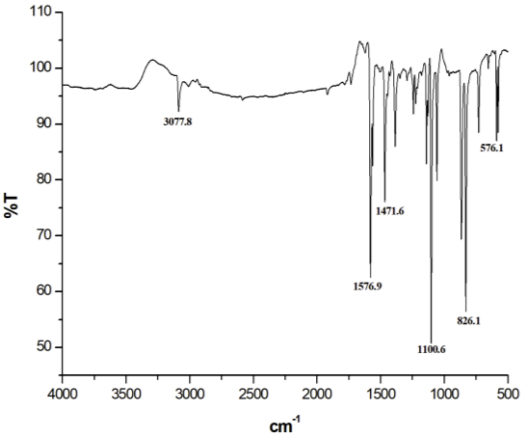

4b

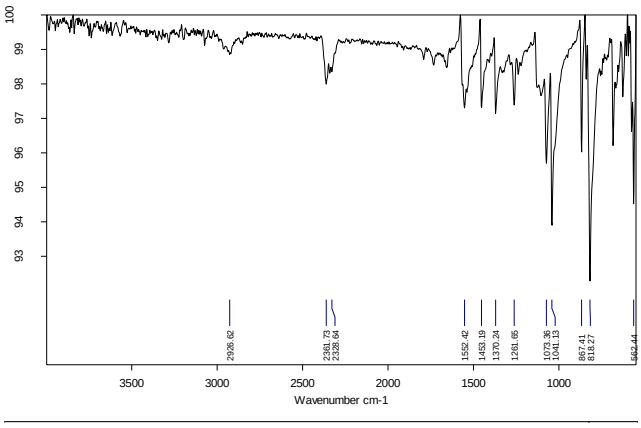

4c

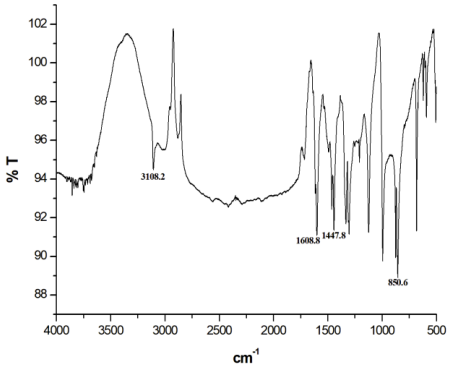

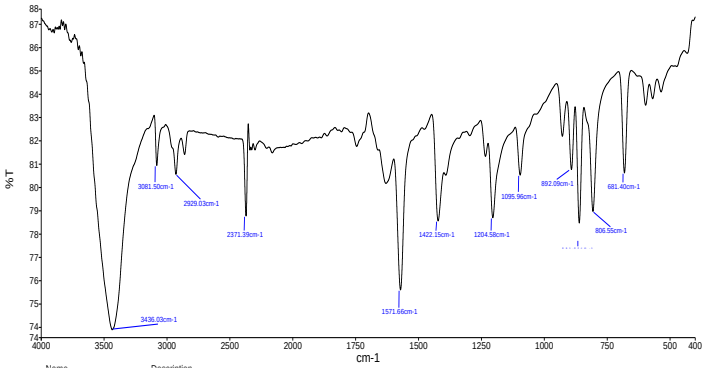

5a **5b**

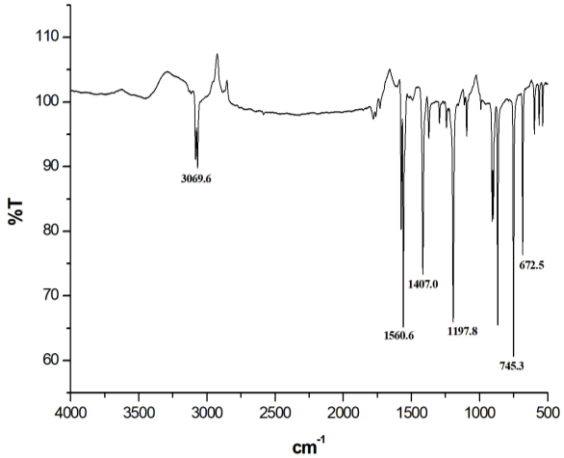

5c

Figure 2.1: FT-IR spectrum of all 5 set of compound **(1a,1b,1c), (2a,2b,2c), (3a,3b,3c), (4a,4b,4c)** and **(5a,5b,5c**)

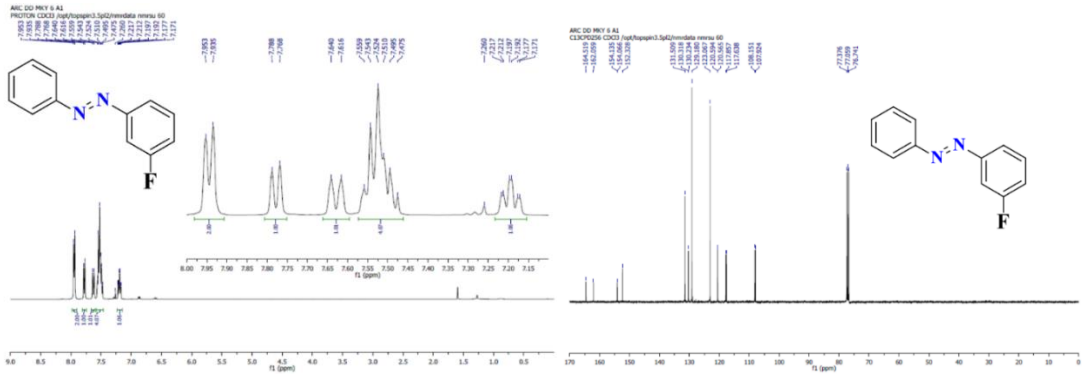

^{1}H, ^{13}C NMR spectrum of **1a**

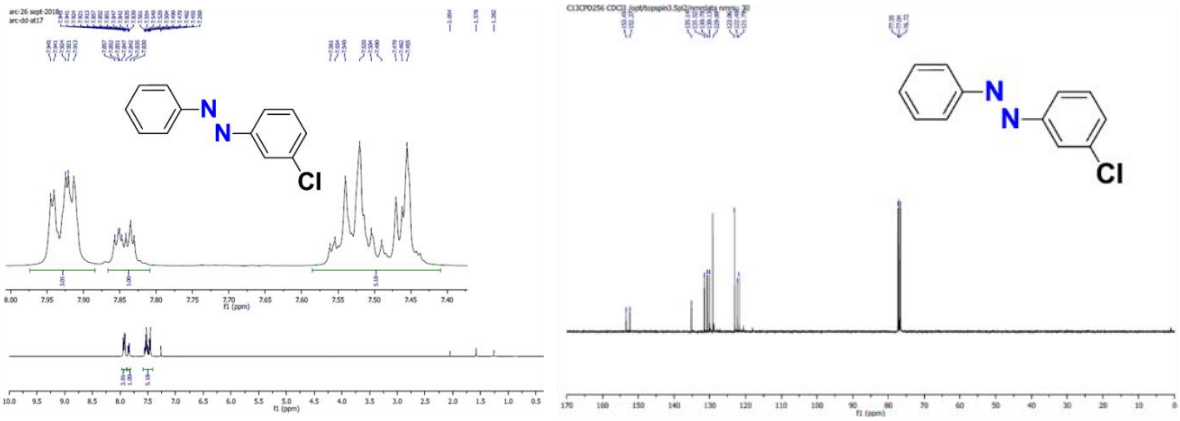

^{1}H, ^{13}C NMR spectrum of **1b**

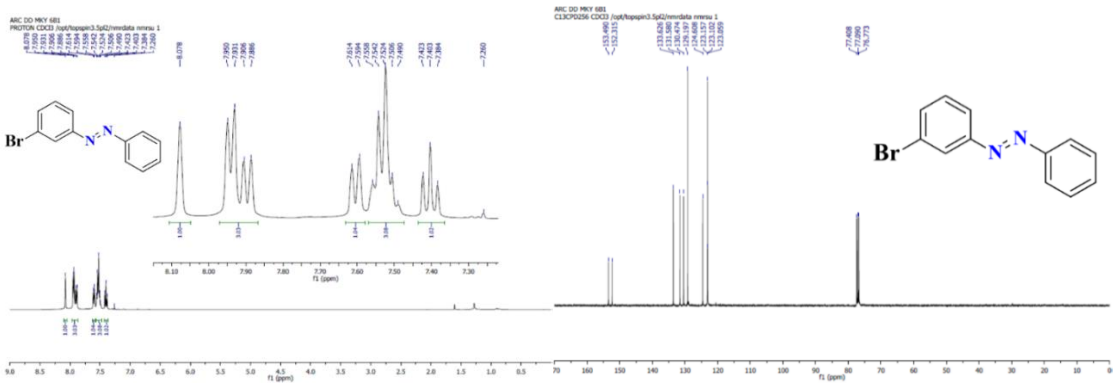

^{1}H, ^{13}C NMR spectrum of **1c**

Figure2.2: ^{1}H, ^{13}C NMR spectrum of compound **1a,1b,1c**.

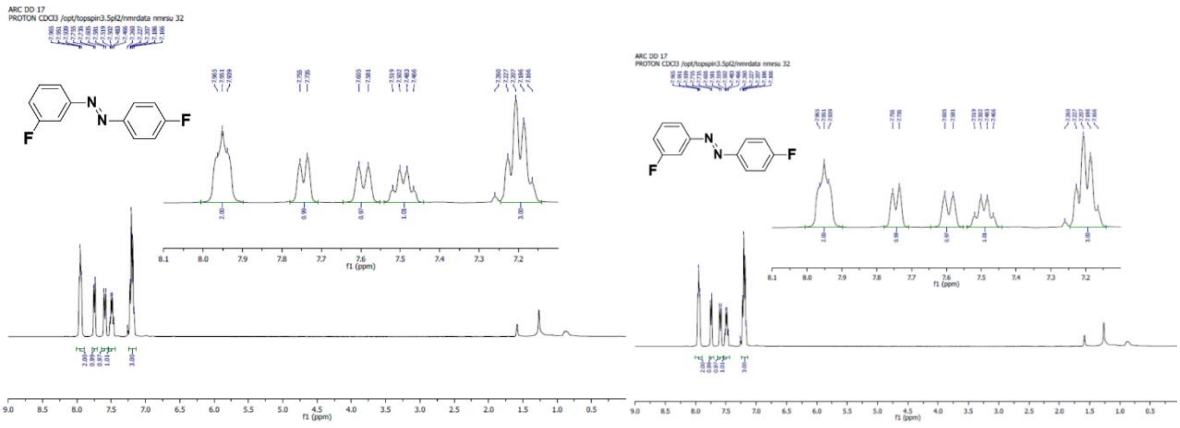

^{1}H NMR spectrum of **2a**

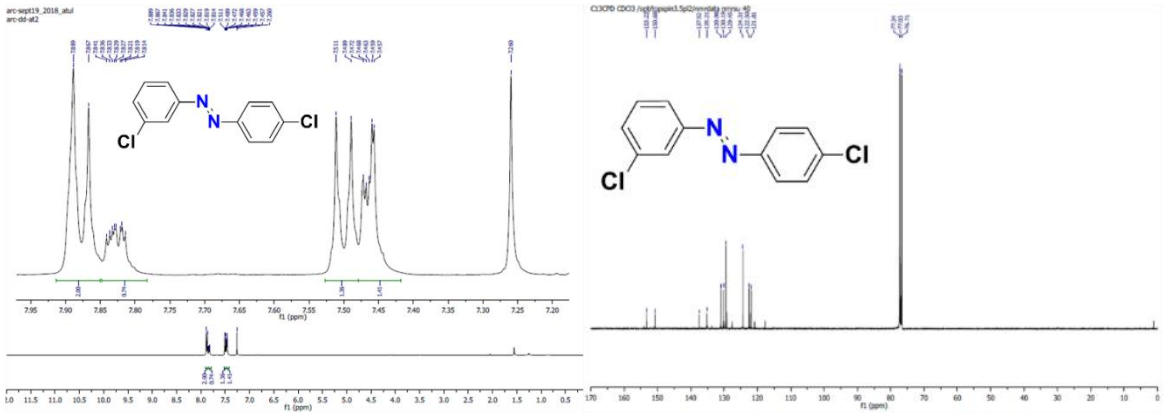

^{1}H, ^{13}C NMR spectrum of **2b**

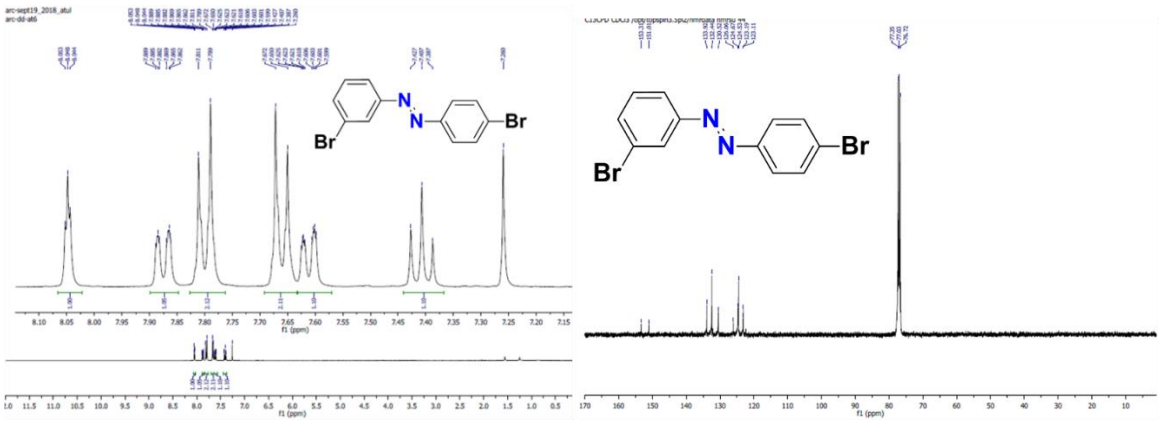

^{1}H, ^{13}C NMR spectrum of **2c**

Figure2.3: ^{1}H, ^{13}C NMR spectrum of compound **2a,2b,2c**

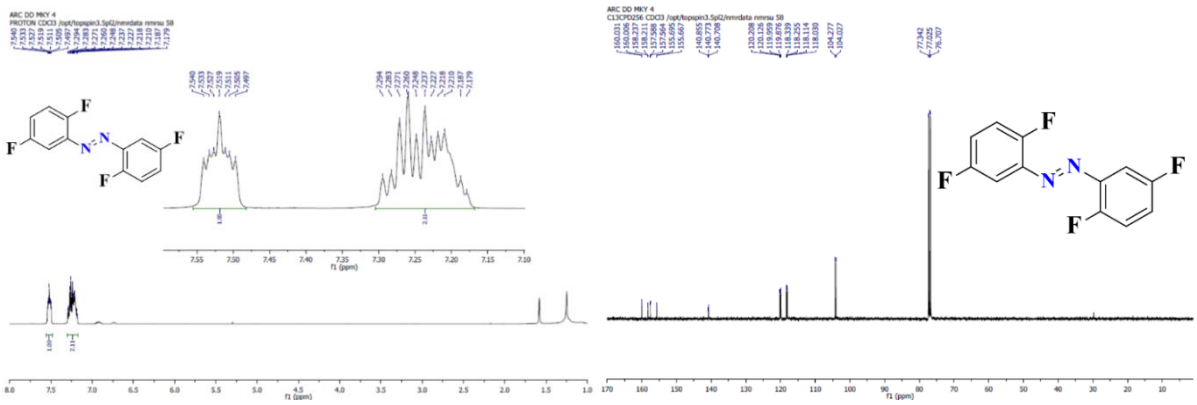

^{1}H, ^{13}C NMR spectrum of **3a**

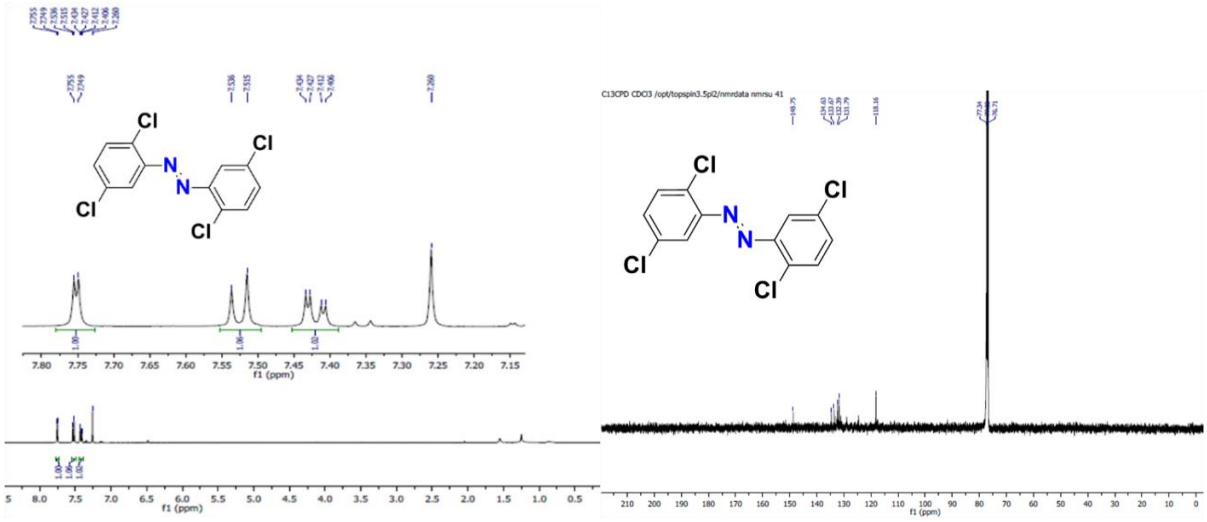

^{1}H, ^{13}C NMR spectrum of **3b**

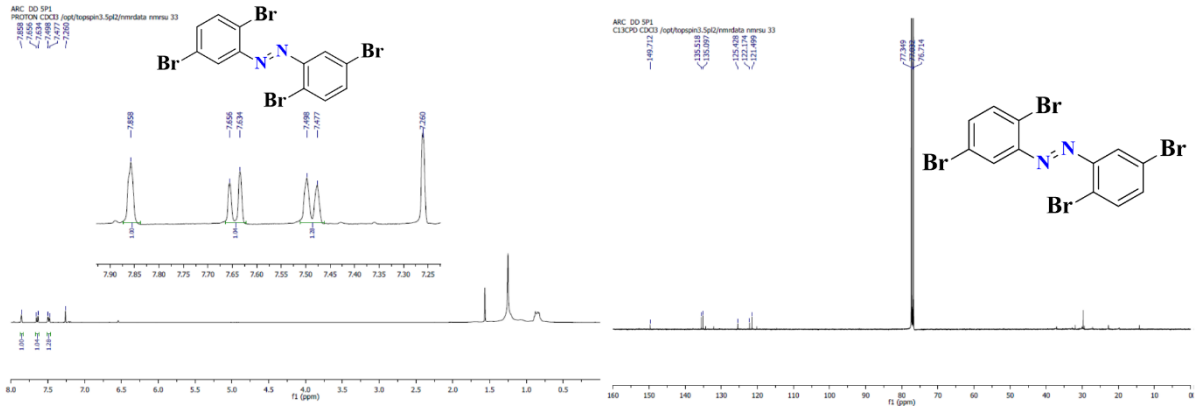

^{1}H, ^{13}C NMR spectrum of **3c**

Figure2.4: ^{1}H, ^{13}C NMR spectrum of compound **3a,3b,3c.**

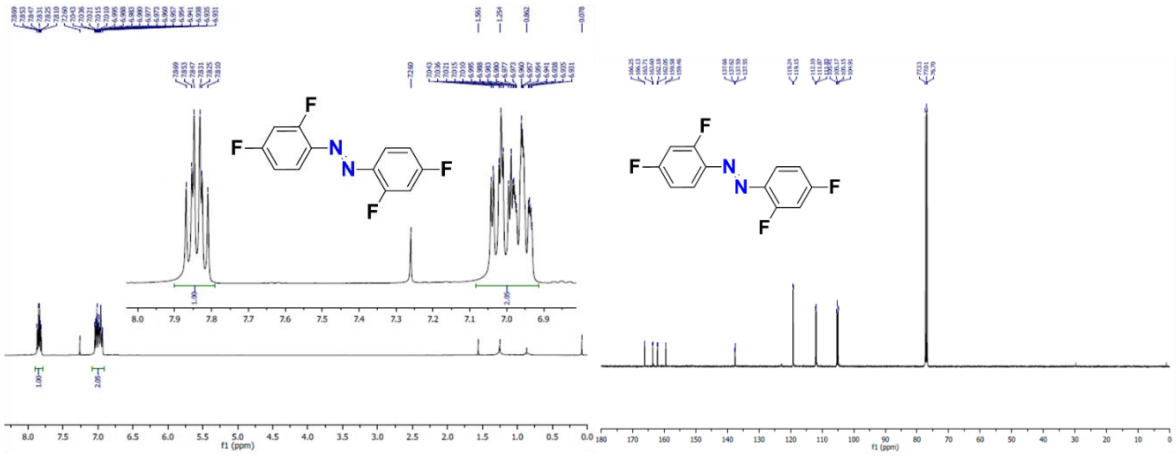

^{1}H, ^{13}C NMR spectrum of **4a**

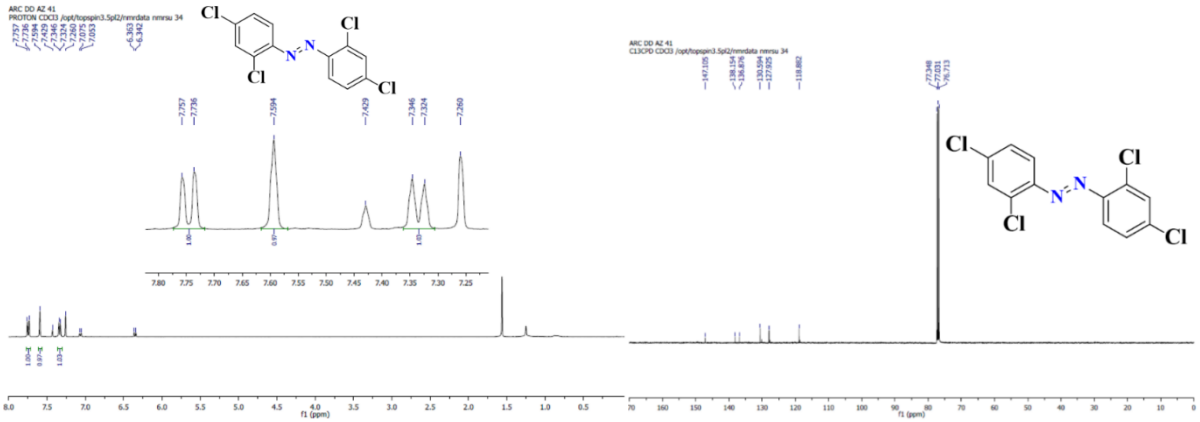

^{1}H, ^{13}C NMR spectrum of **4b**

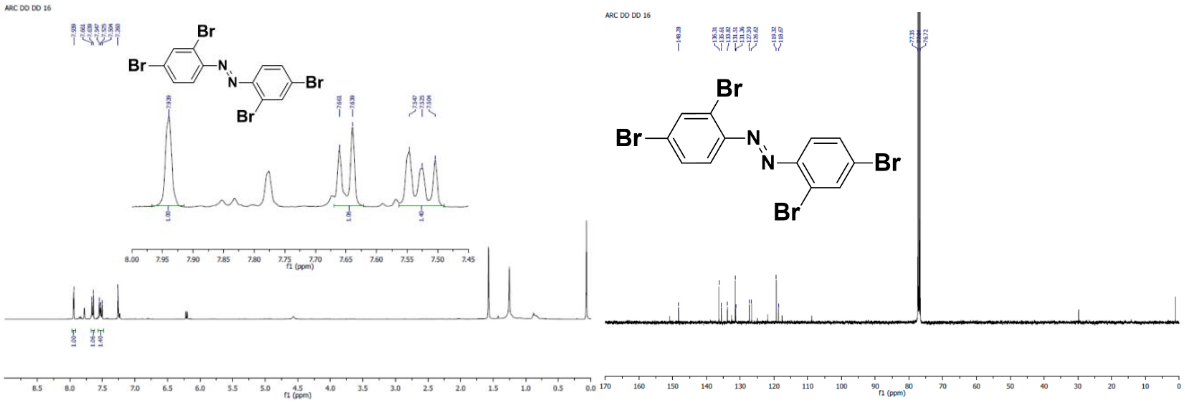

^{1}H, ^{13}C NMR spectrum of **4c**

Figure2.5: ^{1}H, ^{13}C NMR spectrum of compound **4a,4b,4c**.

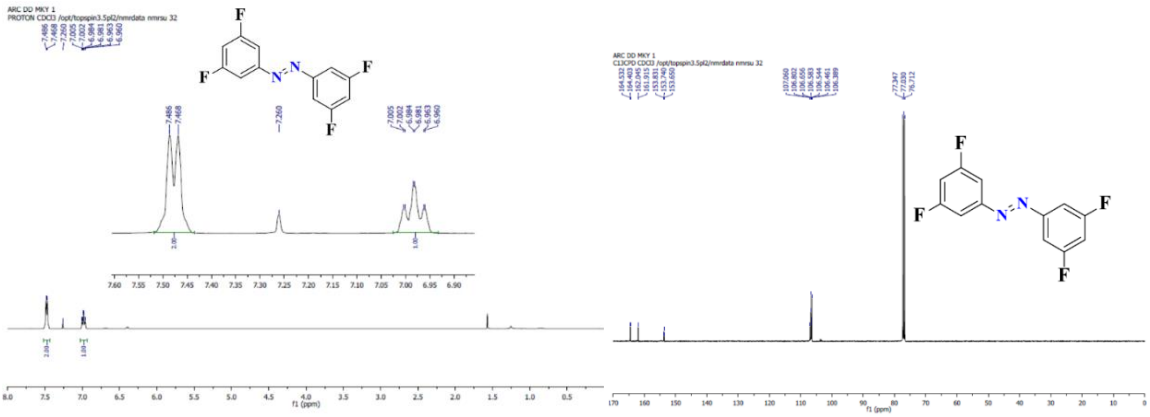

^{1}H, ^{13}C NMR spectrum of **5a**

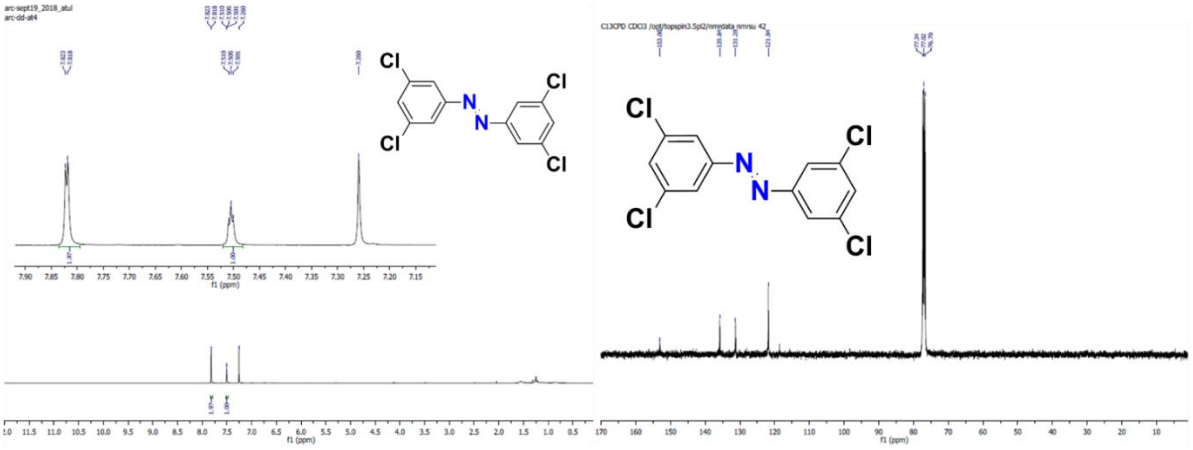

^{1}H, ^{13}C NMR spectrum of **5b**

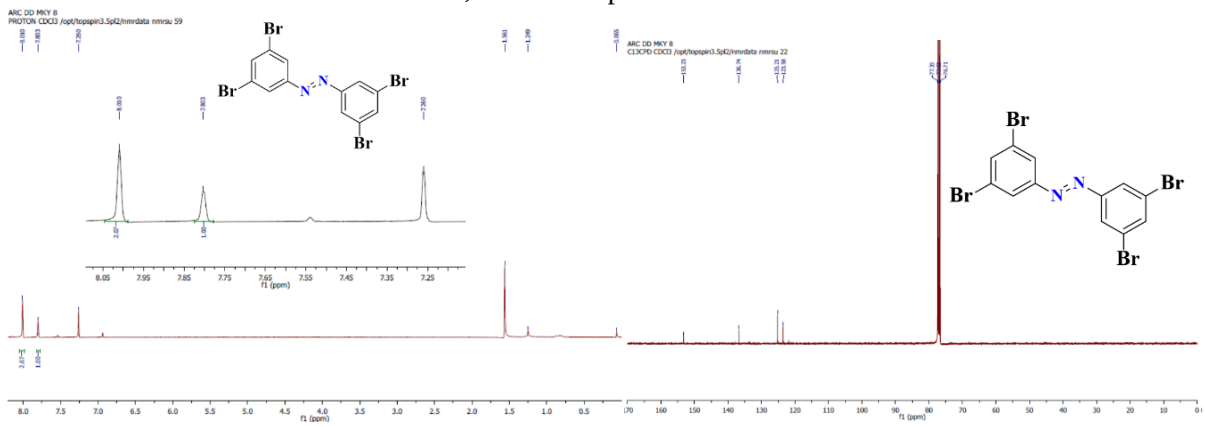

^{1}H, ^{13}C NMR spectrum of **5c**

Figure2.6: ^{1}H, ^{13}C NMR spectrum of compound **5a,5b,5c**.

NMR analysis of *cis-trans*- isomerization of all the compounds

We studied photo-isomerization of all the halogenated azobenene through NMR spectroscopy and analysed ^{1}H NMR spectra during our analysis we observed that small peaks along with the peaks corresponding to the peaks of the *trans*- isomer in the aromatic region. To verify we irradiated sample by 365 nm UV light and recorded the spectra again and we found that those small peaks become prominent. This confirmed that very small amount of the *cis*- isomer was present even in the as synthesized raw material at room temperature.

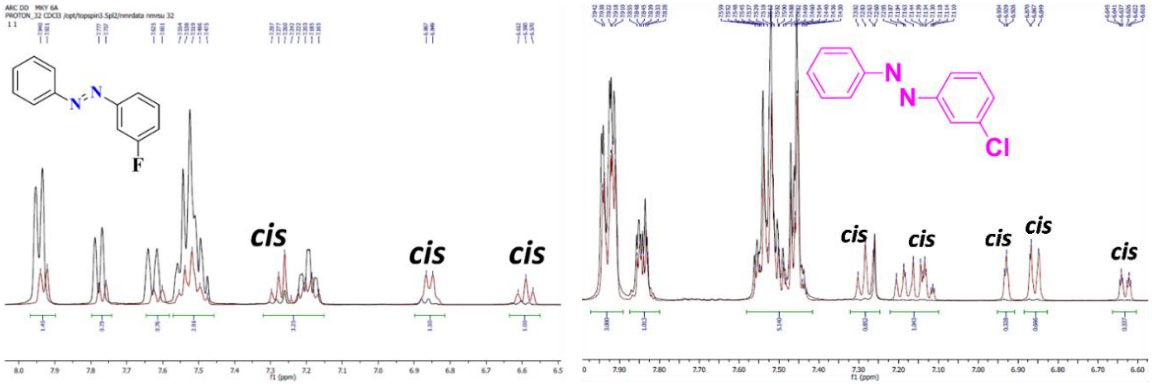

^{1}H NMR spectra of before (black) and after (brown) irradiation of **1a,1b**

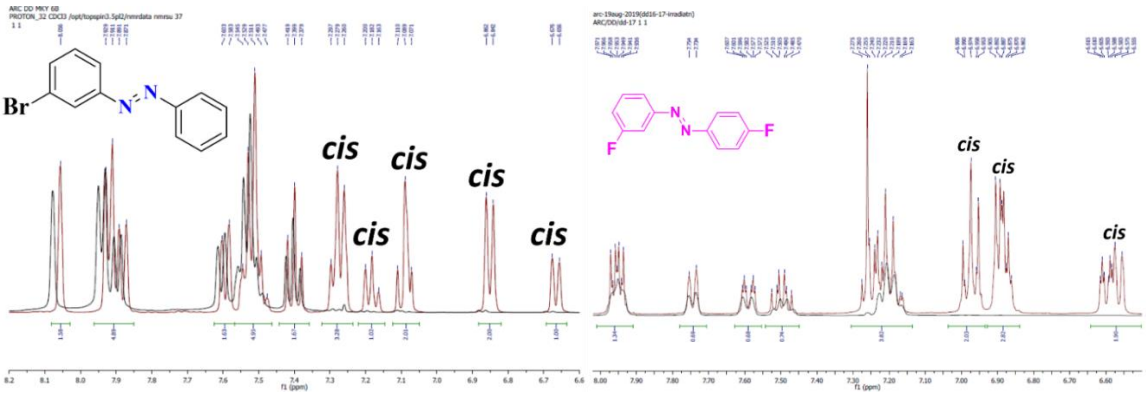

^{1}H NMR spectra of before (black) and after (brown) irradiation **1c,2a**

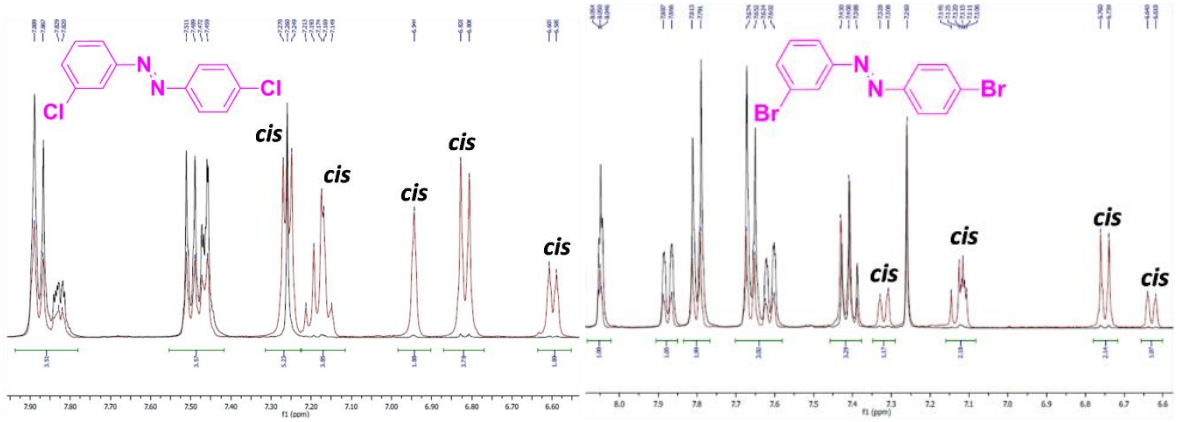

^{1}H NMR spectra of before (black) and after (brown) irradiation **2b,2c**

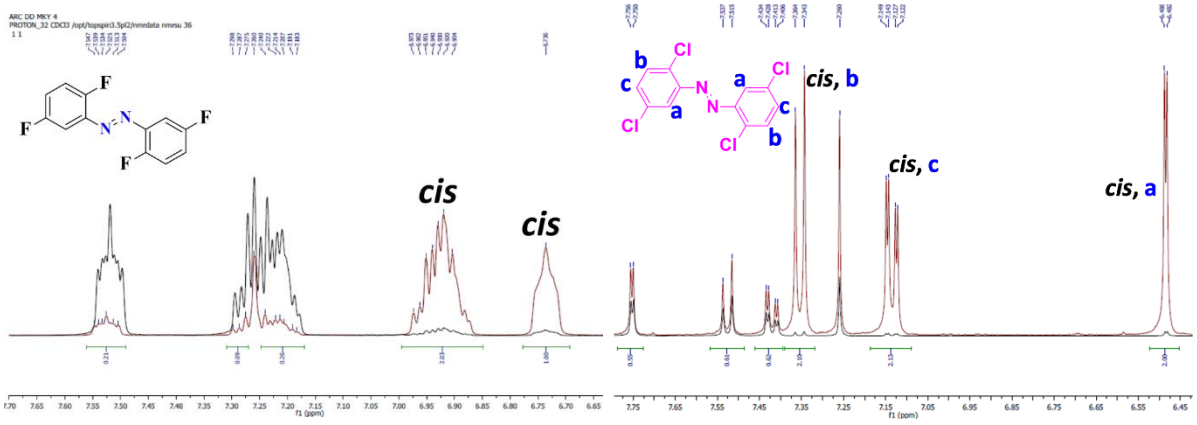

^{1}H NMR spectra of before (black) and after (brown) irradiation **3a,3b**

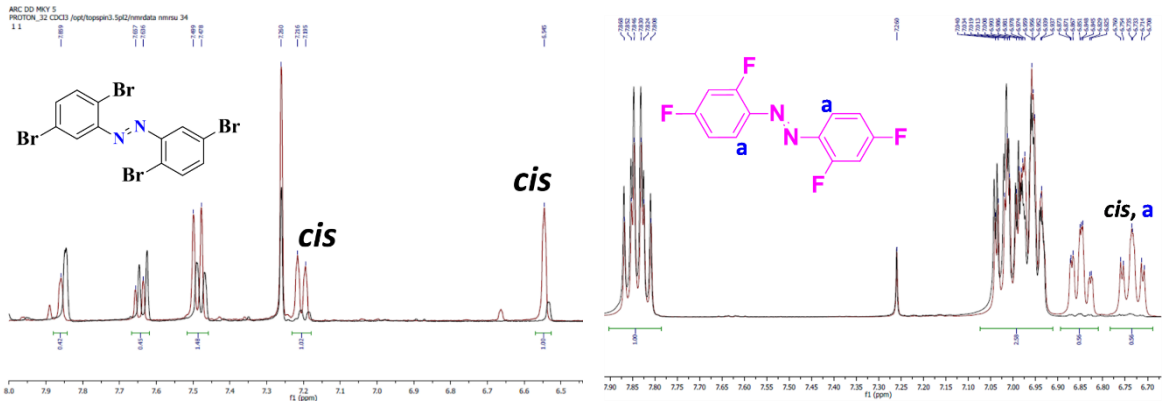

^{1}H NMR spectra of before (black) and after (brown) irradiation **3c,4a**

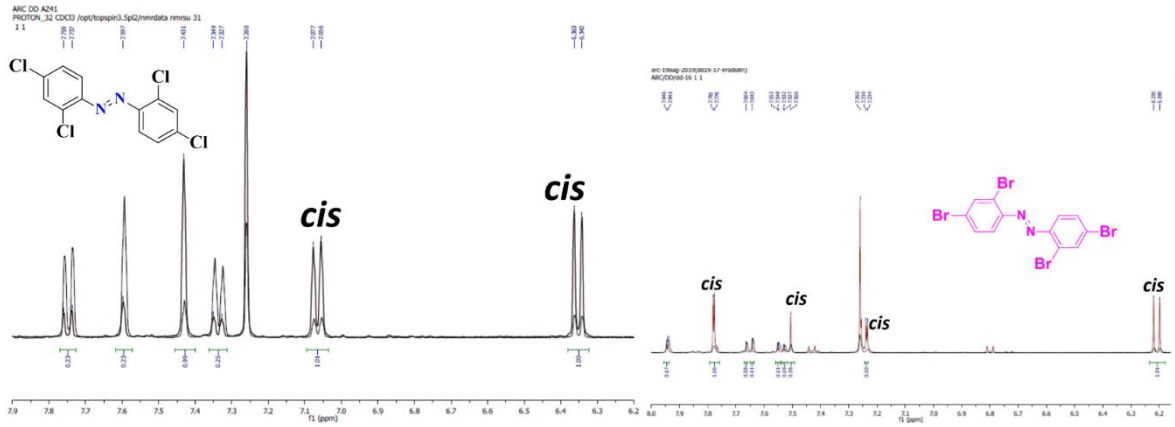

^{1}H NMR spectra of before (black) and after (brown) irradiation **4b,4c**

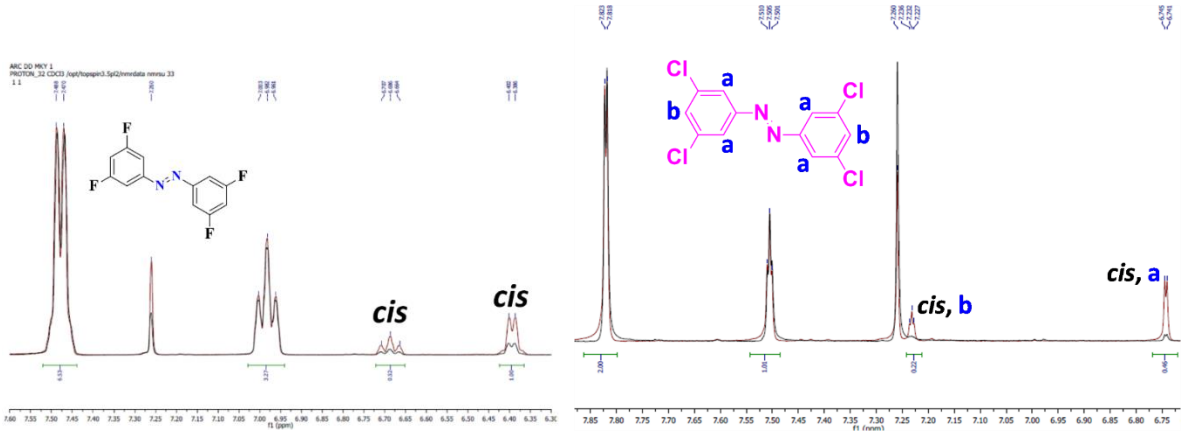

^{1}H NMR spectra of before (black) and after (brown) irradiation **5a,5b**

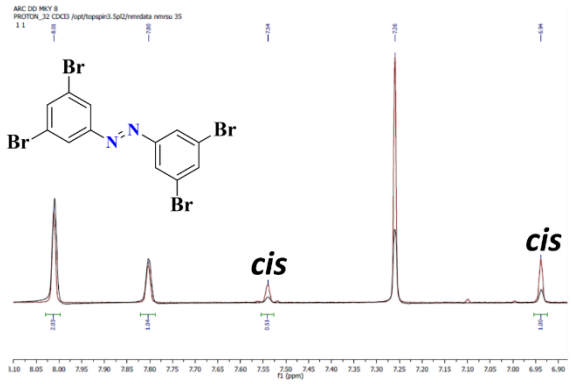

^{1}H NMR spectra of **5c** before (black) and after (brown) irradiation

Figure2.7: ^{1}H NMR spectra of of compound **(1a,1b,1c), (2a,2b,2c), (3a,3b,3c), (4a,4b,4c)** and **(5a,5b,5c)** before (black) and after (brown) irradiation.

2.1.2(B) Differential Scanning Calorimetry

The melting points and melting enthalpies (Table 1) were determined based on DSC (Figure-2.8) (PerkinElmer DSC 8000) traces recorded at a rate of 5 ºC min^{-1} under nitrogen atmosphere.

Table 1. Melting Points of all synthesised compounds from DSC analysis.

Samples	**Melting range (ºC)**	**Enthalpy of melting ($J\ g^{-1}$)**
1a	43-46	87.92
1b	66-69	95.93
1c	64-67	33.87
2a	84-87	99.42
2b	112-114	95.78
2c	123-126	47.10
3a	126-130	80.83
3b	129-131	7.25
3c	254-256	36.36
4a	147-150	100.18
4b	163-166	32.84
4c	212-214	41.94
5a	88-91	68.85
5b	195-197	95.28
5c	248-250	56.15

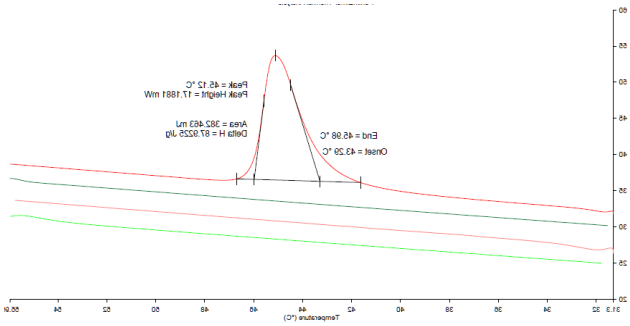

1a

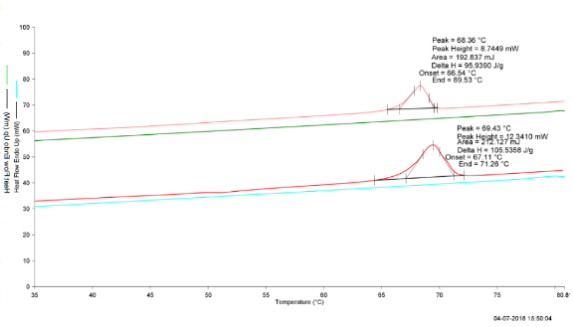

1b

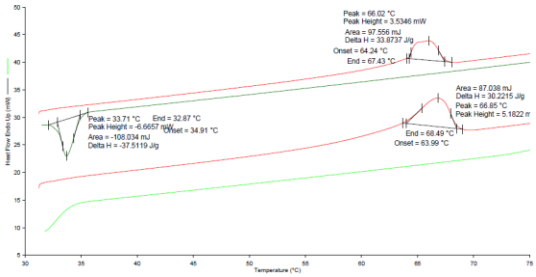

1c

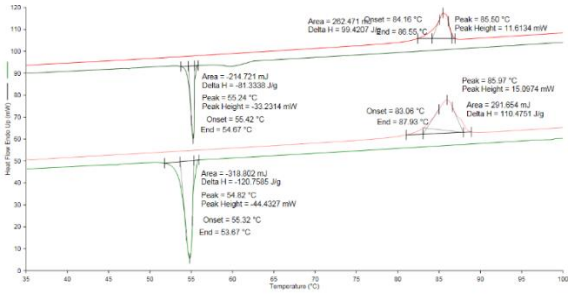

2a

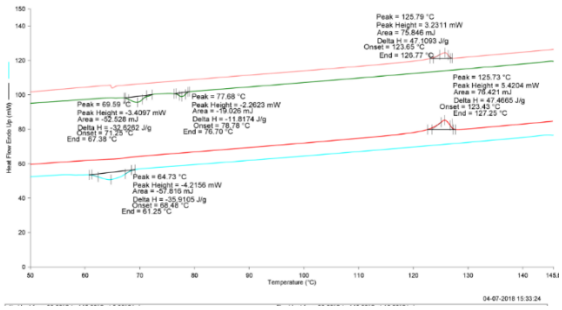

2b

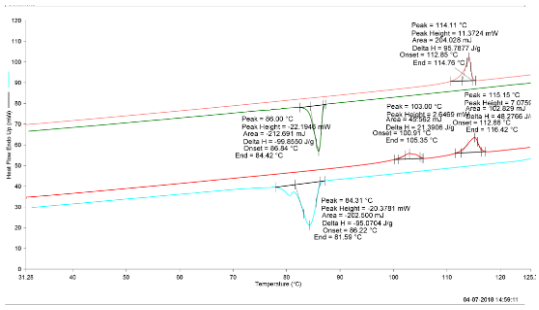

2c

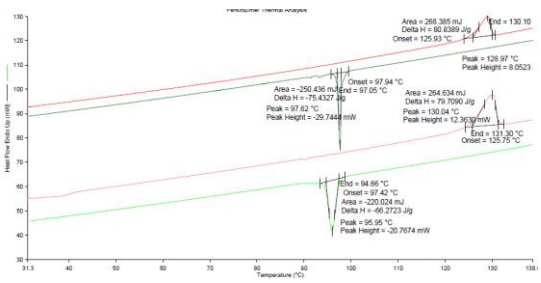

3a

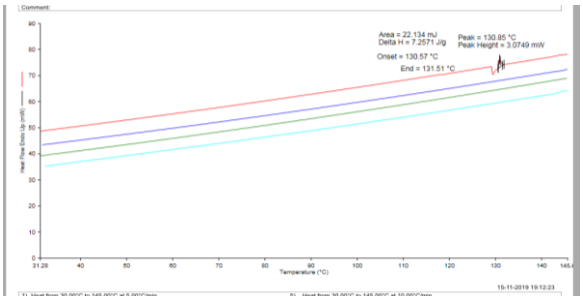

3b

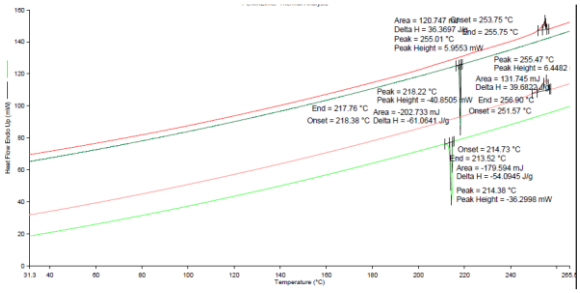

3c

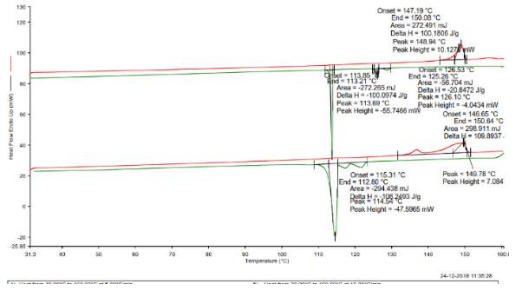

4a

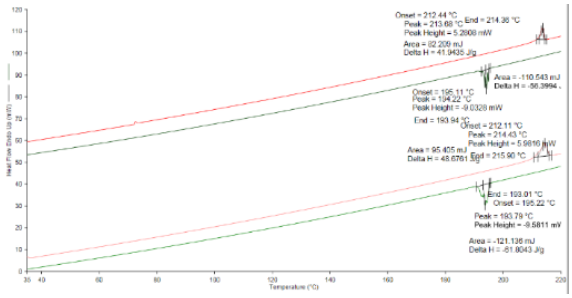

4b

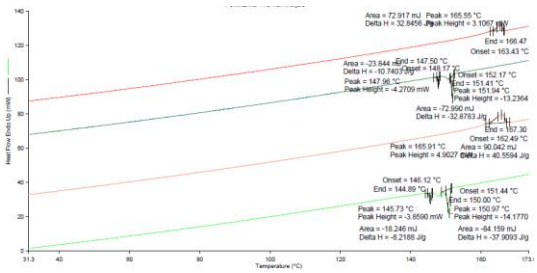

4c

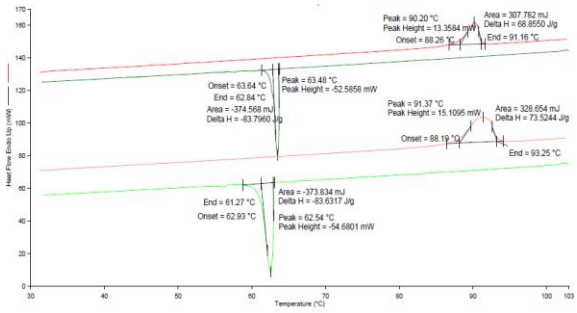

5a

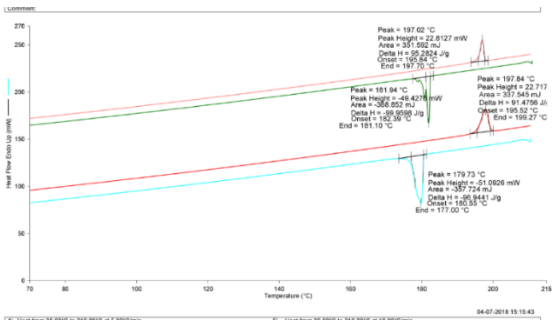

5b

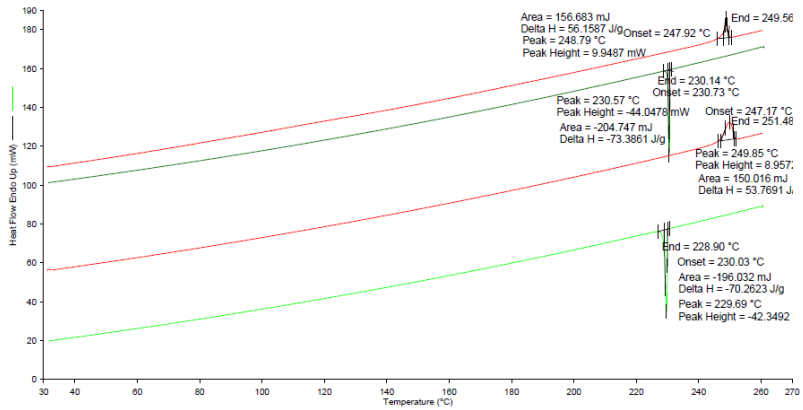

5c

Figure2.8: DSC curve for all 5 set of compound **(1a,1b,1c), (2a,2b,2c), (3a,3b,3c), (4a,4b,4c)** and **(5a,5b,5c)**

2.1.3 Powder X-ray Diffraction Analysis

The powder X-ray diffraction (PXRD) data were determined based on Rigaku Ultima IV diffractometer with a parallel beam geometry, Cu K_α radiation, 2.5º primary and secondary solar slits, a 0.5º divergance slit with a 10 mm height limit slit, sample rotation stage (120 rpm) attachment and DTex Ultra detector at a tube voltage of 40 kV and current of 40 mA. The data sets were collected over 2θ values ranging from 3º to 50º with a scanning speed of 3º min^{-1} and a 0.02º per step for all compounds. The simulated PXRD spectra were generated using Mercury. Raw materials after the purification through column chromatography were ground using agate morter and pestle and were used to record the PXRD patterns.

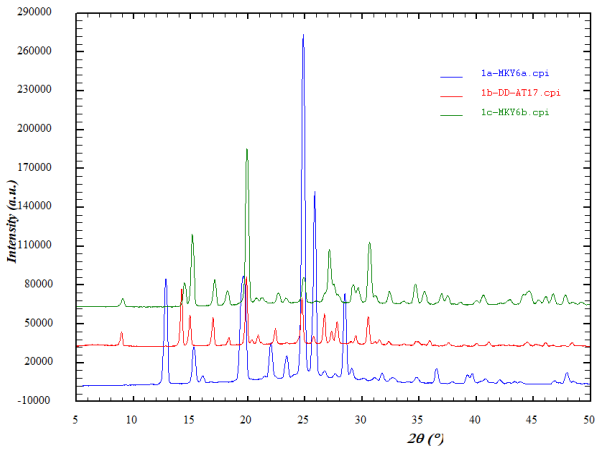

Experimental PXRD pattern of **1(a, b, c)**

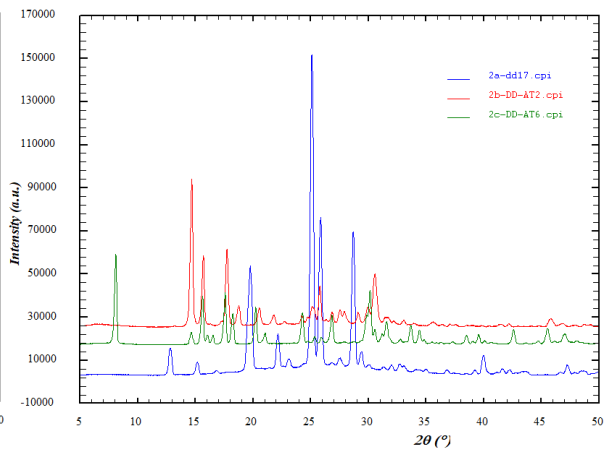

Experimental PXRD pattern of **2(a, b, c)**

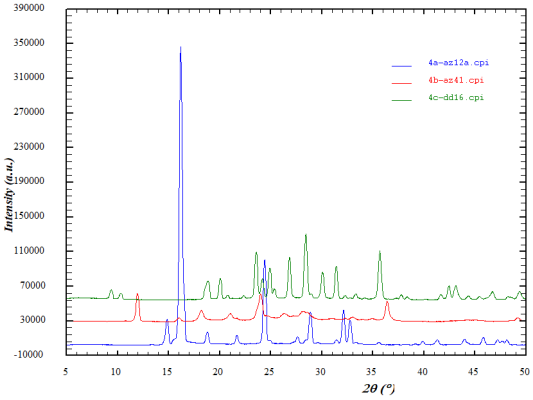

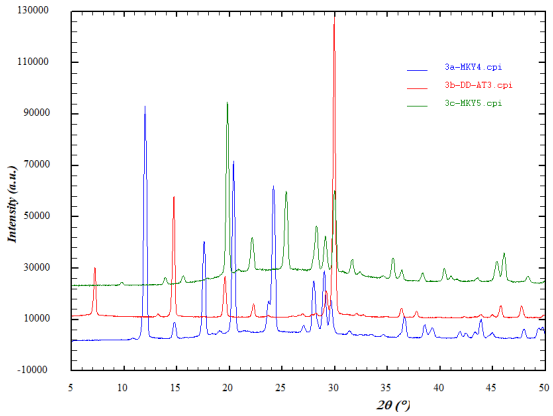

Experimental PXRD pattern of **3(a, b, c)** Experimental PXRD pattern of **4(a, b, c).**

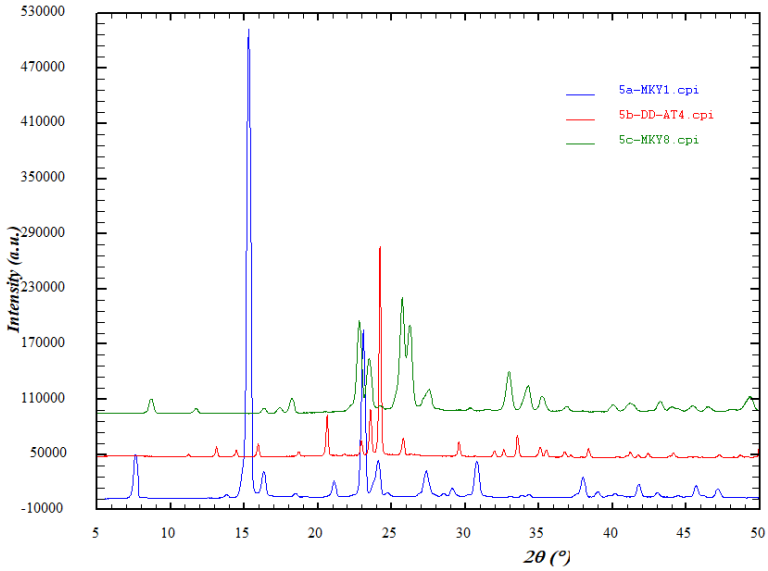

Experimental PXRD pattern of **5(a, b, c).**

Figure 2.9 Experimental PXRD pattern for all 5 set of compound **(1a,1b,1c), (2a,2b,2c), (3a,3b,3c), (4a,4b,4c)** and **(5a,5b,5c)**

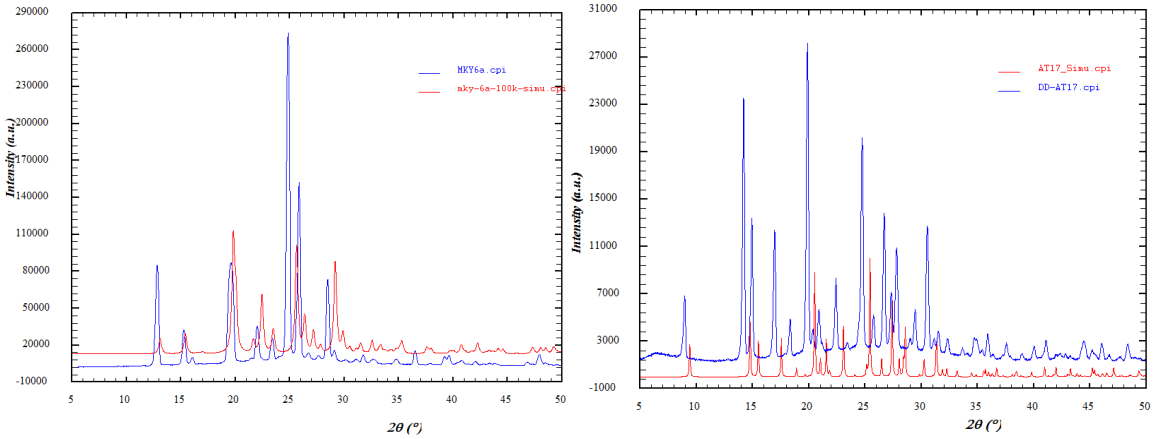

Experimental (blue) and simulated (red) PXRD pattern of **1a,1b**

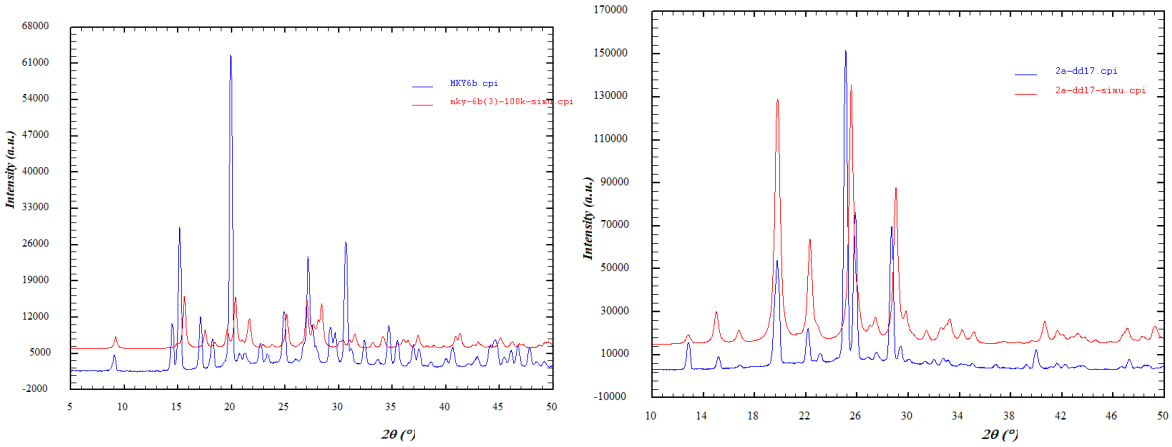

Experimental (blue) and simulated (red) PXRD pattern of **1c,2a**

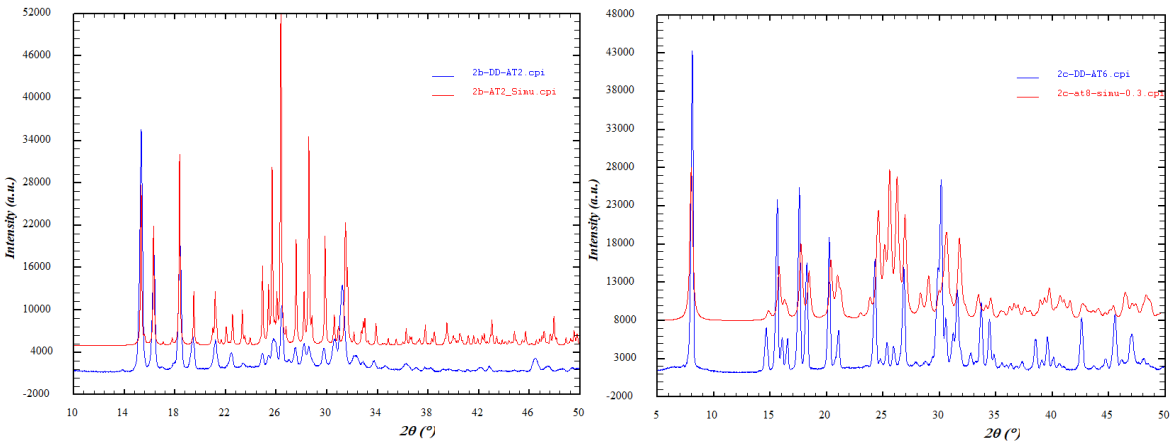

Experimental (blue) and simulated (red) PXRD pattern of **2b,2c**

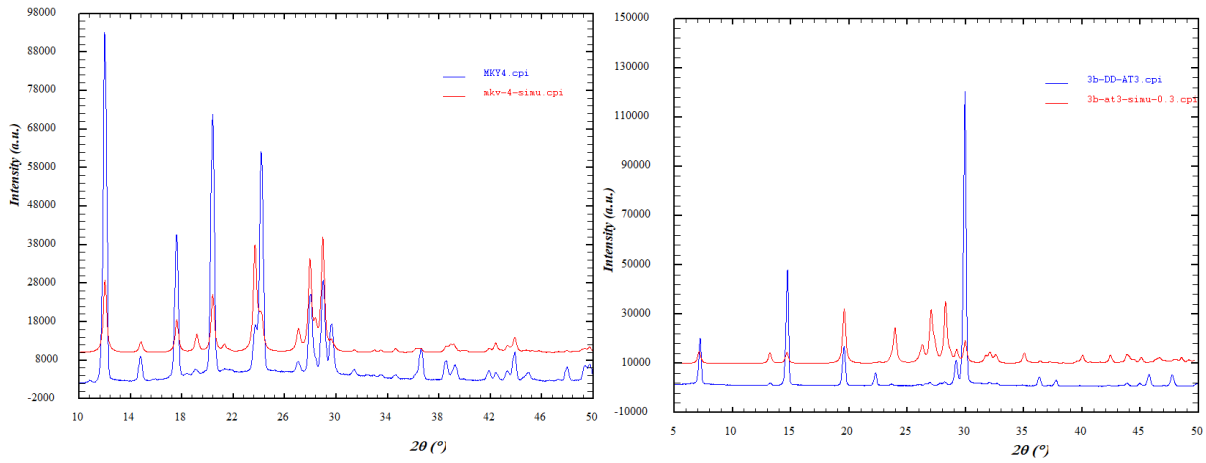

Experimental (blue) and simulated (red) PXRD pattern of **3a,3b**

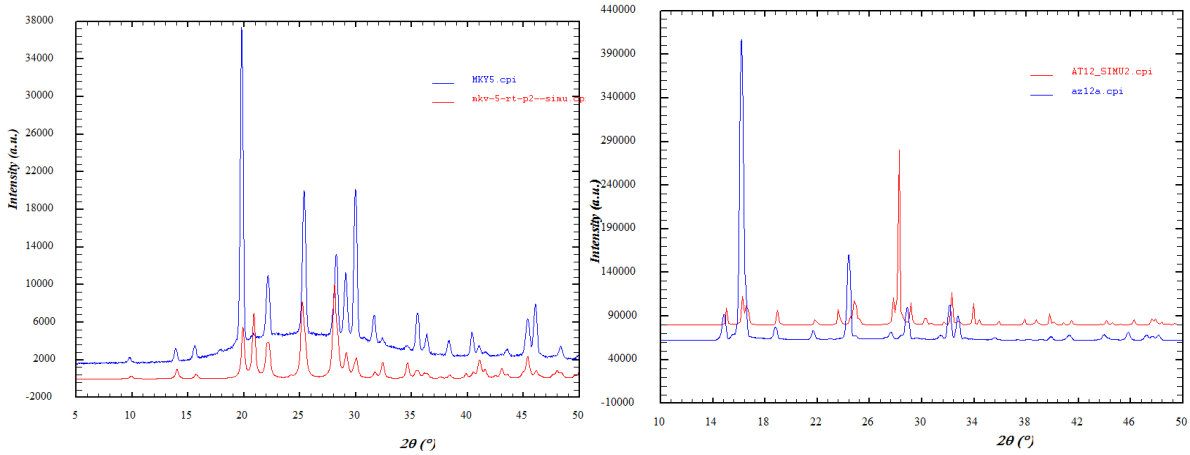

Experimental (blue) and simulated (red) PXRD pattern of **3c,4a**

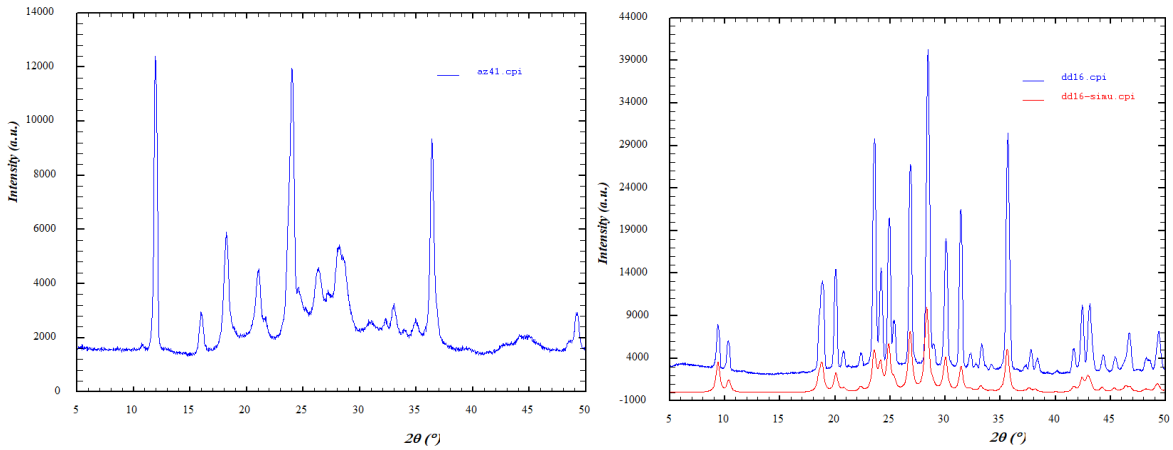

Experimental PXRD pattern of **4b,** Experimental (blue) and simulated (red) PXRD pattern of **4c**.

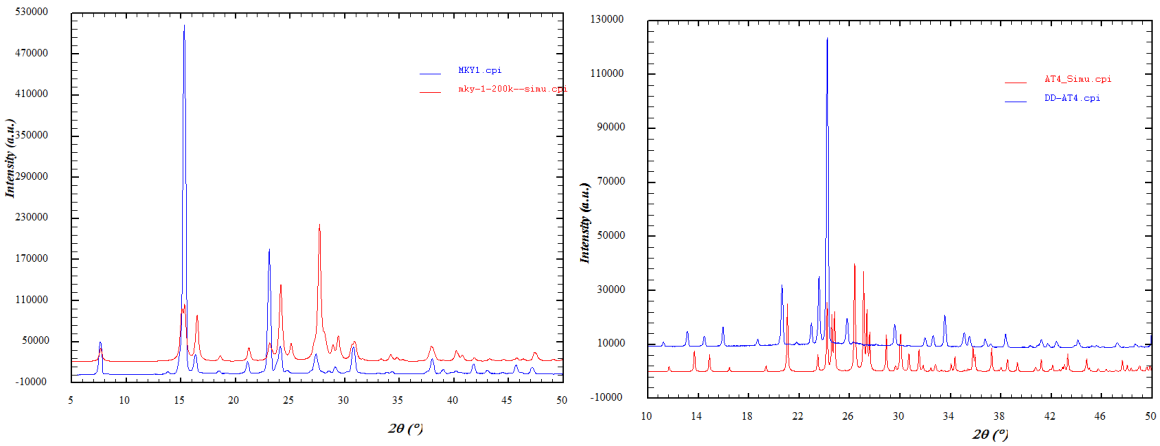

Experimental (blue) and simulated (red) PXRD pattern of **5a,5b**

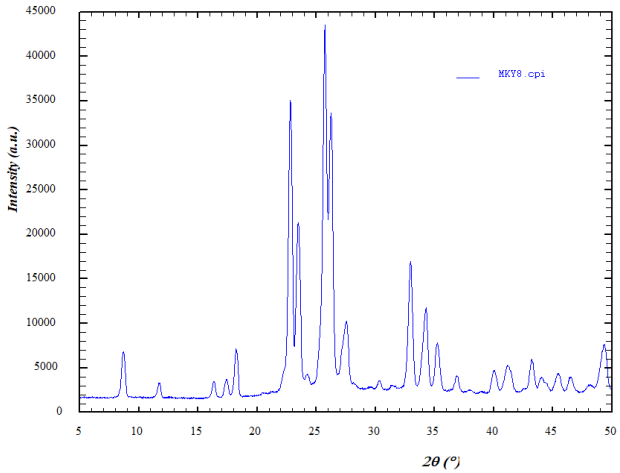

Experimental PXRD pattern of **5c**

Figure 2.10 Experimental (blue) and simulated (red) PXRD pattern of compound **(1a,1b,1c) (2a,2b,2c), (3a,3b,3c), (4a,4c)** and **(5a,5b)** Experimental (blue) PXRD pattern of **4b,5c**

2.1.4 Single-crystal X-ray diffraction study

Crystal Growth, Single crystal data Collection, Structure solution and Refinement

Good quality crystals were grown from methanol/ethyl acetate or dichloromethane solvents by slow solvent evaporation techniques at 4 to 6 ºC, and single-crystal X-ray diffraction data for the crystals of compounds **1b**, **2a, 2b, 2c, 3b, 4a,** and **5b,** were recorded using Bruker AXS KAPPA APEX-II CCD diffratometer (monochromatic Mo K_α radiation) equipped with Oxford cryosystem 700 Plus at 100 K. Data collection and unit cell refinement for the data sets were done using Bruker APEX-II suit, data reduction and integration were reduced using SAINT V7.685A (Bruker AXS, 2009), and absorption corrections and scaling were done using

SADABS V2008/1 (Bruker AXS, 2009). The crystals of compounds **1a, 1c, 3a, 3c, 4c,** and **5a** were recorded using a Rigaku XtaLAB mini diffractometer with Mercury375/M CCD detector, Mo-K_α radiation, a sample-to-detector distance of 4.95 cm, and 2θ fixed at 29.85° using the CrysAlis Pro software. The 100 K data were collected using Oxford Cryosystem. The crystal structure were solved using Olex2[38] packages using XT,[39] and the structures were refined using XS.[40] Single crystal data and refinement parameters for all these compounds are listed in Table 2. All hydrogen atoms were geometrically fixed and refined using the riding model. The thermal ellipsoid plots and packing diagrams of all molecules are drawn at 50% probability for non-H atoms using Mercury[41] and are shown with respective atomic labels.

2.1.5 Photo-isomerization

2.1.5 (A) Nuclear Magnetic Resonance (NMR) study:

During the analysis of ^{1}H NMR spectra of the compounds in their *trans*- isomeric form (as synthesized), some small peaks along with the peaks of the *trans*- isomer in the aromatic region were observed. Those small peaks become prominent when the samples were irradiated by 365 nm UV light. NMR spectra of the freshly irradiated samples were also recorded immediately. This confirmed that very small amount of the *cis*- isomer was present even in the freshly prepared trans material at room temperature. ^{1}H NMR spectra of the ABs were taken before and after irradiation to get further confirmation for *trans*- → *cis*- isomerization upon irradiation using 365 nm UV light. Such type of characteristic shift is observed for all the compounds reported herein.

2.1.5 (B) UV-Vis Study for Understanding of Kinetic stability

Photo-switching properties of all the compounds were studied in the solution state by irradiating a solution (in DMSO solvent) of the respective compound under UV light (365 nm) for 1 - 10 minutes. After the irradiation, it was observed that the *trans*- isomers were transformed to the corresponding *cis*- isomer. The solution of the *cis*- isomer was then exposed to white light in the laboratory for long hours and the UV-Vis spectrum of the solution was measured at regular intervals up to 4 days. The kinetics of transformation of *cis*-isomer to *trans*-isomer was then studied using a UV-Vis spectrophotometer and the rate constant for this transformation was calculated.

2.2 Computational Study:

All the computations have been done using Gaussian 09 program. Gauss View 05[42] has been used as a graphical interface. The transitions states of these compounds have larger number of probable geometries, all the probable geometries of the the transition states (TS) were first optimized without any constraints. All the optimized TS geometries showed only one negative imaginary frequency vibrating in the directions of the reaction coordinate. The optimizations of the *trans*-, *cis*- isomers and the probable transition states were conducted using DFT/B3LYP level of theory and 6-311++G(d,p) as basis set. The effect of the solvents (DMSO) were modelled with the polarizable continuum model (PCM).[43]

2.2.1 Intrinsic Reaction Coordinate (IRC) Calculation

The reaction paths were traced using intrinsic reaction coordinates (IRC) in both forward as well as backward direction from all the probable optimised TSs. Intrinsic Reaction Coordinate (IRC) was followed to establish the transformation TS to *trans*- and TS to *cis*- isomers. A few of the transition state geometries do not follow the reaction co-ordinates leading to both *cis*- and *trans*- isomer as shown by Intrinsic Reaction Coordinates (IRC) .These structures were not included for further calculation. There are 2 probable conformers for the *trans*- and *cis*- isomers of 1(a-c) and 2(a-c), 4 probable conformers for 3(a-c) and 4(a-c) and only one conformer is possible for 5(a-c).

2.2.2 Density Functional Theory calculation

The *cis*- and *trans*- isomers obtained after IRC calculations were optimised further with frequency calculation using DFT/B3LYP level and 6-311++G(d,p) basis set The optimised geometry of the probable transition states and the corresponding *cis*- and *trans*- isomers of all the compounds are shown in the (Table 16). The activation energy for the *cis*- → *trans*- isomerization was calculated from the energy of the optimized geometries of the conformer of the *cis*- isomer obtained after IRC calculation and the corresponding transition state for most of the compounds the fluoro compounds show larger E_{act} value compared to bromo and chloro analogues.

2.2.3 Time dependent density functional theory calculation

Time-Dependent Density Functional Theory (TD-DFT) calculations were conducted to compare the wavelength and the nature of transitions observed in the experimental UV-Vis spectra. The calculations predict an intense $\pi \rightarrow \pi^*$ transition at approximately 355nm for the *trans*- compound involving HOMO and LUMO. The absorption band for $n \rightarrow \pi^*$ transition around 480 nm for *trans*- isomer is dipole forbidden as indicated by very low oscillation strength (f). This prediction matches quite well with the experimentally observed spectra. On the other hand, the *cis*- compound predicts transitions approximately at 470nm and 300nm which represent $n \rightarrow \pi^*$ and $\pi \rightarrow \pi^*$ transitions respectively. The $n \rightarrow \pi^*$ transition is allowed in *cis*- isomer and the oscillator strength is relatively higher than that in the *trans*- isomer. The intensity of $\pi \rightarrow \pi^*$ transition in *trans*- isomers is greater than *cis*- isomers. This observation also matches well with the experimentally observed spectra of the *cis*- and *trans*- compounds. Major orbital contributions of the *cis*- and *trans* - isomers were calculated for these $\pi \rightarrow \pi^*$ and $n \rightarrow \pi^*$ transition

CHAPTER 3

Results and Discussion

3.1 Structural analysis of all 5 sets of halogenated azo-benzenes

Among the fifteen molecules synthesized, we could structurally characterized thirteen of them. The compounds **4b** and **5c** did not yield suitable single crystals for structure determination.

3.1.1. Structure of 1(a, b, c)

In this series of asymmetrical halogenated azobenzene compound **1a.** 1-(3-fluorophenyl)-2-phenyldiazene was crystallized in monoclinic centrosymmetric $P2_1/c$ space group with Z = 2 and have C –H···F hydrogen bonds[44] in the solid-state. We observed pseudo centre of inversion disorder in the crystal structure of *trans*- isomer of the fluorinated azobenzene **1a**. Compound **1b** (1-(3-chlorophenyl)-2-phenyldiazene) and **1c** (1-(3-bromophenyl)-2-phenyldiazene) both were crystalized in the orthorhombic crystal system, $Pca2_1$ space group with Z = 4. Compound **1b** have C –H····Cl[45] and π····π[46] interactions in the solid-state and compound 1c have C –H····Br,[47] C –Br····π[48] and π····π interactions in the solid-state .(The experimental PXRD pattern of these compounds are found to match with the corresponding simulated PXRD pattern from the CIF of the single crystal structure solution. it indicates that raw material and recrystallized phases were same. Significant intermolecular interaction of these compounds are reported herein.

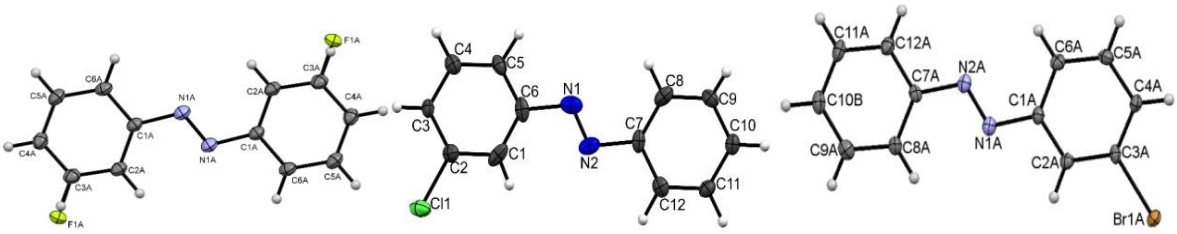

1a 1b 1c

. **Figure 3.1**. ORTEP of **1a,1b,1c** compounds

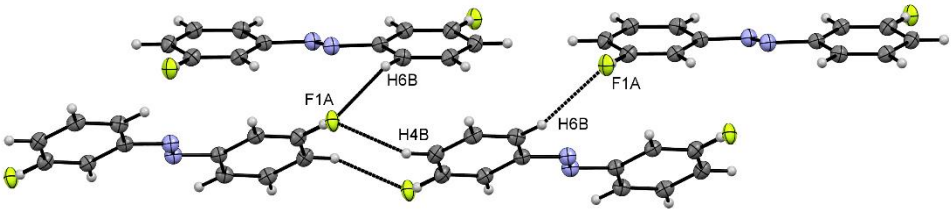

Figure 3.2. H····F interactions in the solid-state in **1a.**

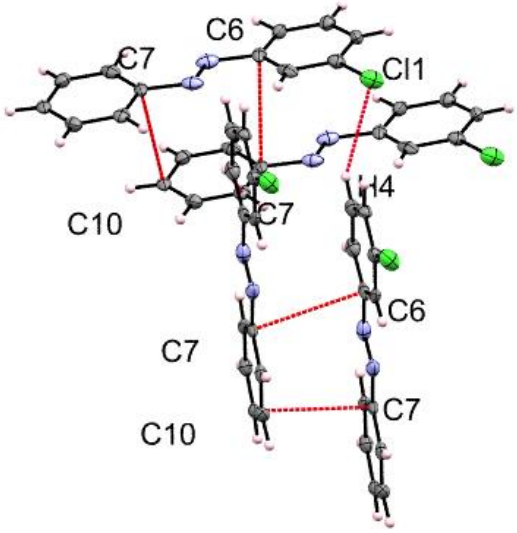

Figure 3.3. H····Cl and π····π interactions in the solid-state in **1b.**

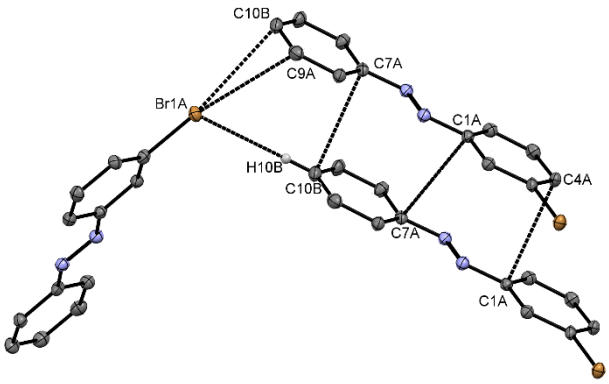

Figure 3.4. H····Br, Br····π and π····π interactions in the solid-state in **1c**.

Table 2. Crystallographic and Refinement data for the compounds

Samples	**1a**	**1b**	**1c**	**2a**	**2b**
CCDC no.	1952357	1952358	1952359	1952360	1952361
Empirical formula	$C_{12}H_9FN_2$	$C_{12}H_9N_2Cl$	$C_{12}H_9BrN_2$	$C_{12}H_6F_2N_2$	$C_{12}H_{10}N_2Cl_2$
Formula weight	200.12	216.67	261.12	216.19	251.12
Temperature/K	100.0(2)	100.0(2)	100.0(2)	296.0(2)	296.0(2)
Crystal system	monoclinic	orthorhombic	orthorhombic	monoclinic	monoclinic
Space group	$P2_1/c$	$Pca2_1$	$Pca2_1$	$P2_1/c$	$P2_1/c$
a/Å	11.8769(12)	11.9759(2)	11.8827(3)	12.0362(8)	20.3732(5)
b/Å	5.8555(3)	4.51200(10)	4.5273(1)	5.8230(4)	4.59290(10)
c/Å	12.2150(14)	18.7655(4)	19.2353(5)	12.2683(10)	11.5971(3)
α/°	90	90	90	90	90
β/°	145.347(10)	90	90	145.744(5)	101.723(2)
γ/°	90	90	90	90	90
V/Å^3	483.02(10)	1014.00(4)	1034.79(4)	483.99(7)	1062.53(5)
Z	2	4	4	2	4
ρ_{calc} g/cm^3	1.376	1.4192	1.675	1.483	1.5697
μ/mm^{-1}	0.097	0.340	3.936	0.117	0.579
F(000)	208	448.7	519	220.0	513.3
2Θ range for data collection/°	6.032 to 65.396	4.34 to 57.38	3.4 to 32.8	6.014 to 50.268	2.04 to 57.4
Index ranges	$-16 \leq h \leq 16$, $-8 \leq k \leq 8$, $-18 \leq l \leq 16$	$-16 \leq h \leq 15$, $-2 \leq k \leq 6$, $-24 \leq l \leq 25$	$-14 \leq h \leq 17$, $-6 \leq k \leq 6$, $-27 \leq l \leq 27$	$-14 \leq h \leq 14$, $-6 \leq k \leq 6$, $-14 \leq l \leq 14$	$-27 \leq h \leq 26$, $-6 \leq k \leq 3$, $-15 \leq l \leq 15$
Reflections collected	4424	7583	7611	3865	7518
Independent reflections	1585 [R_{int}=0.0198, R_{sigma}=0.0217]	2481 [R_{int} = 0.0189, R_{sigma} =0.0222]	3516 [R_{int} = 0.022, R_{sigma} = 0.03]	861 [R_{int} = 0.0147, R_{sigma}=0.0128]	2728 [R_{int} = 0.0263, R_{sigma} = 0.0345]
Data/restraints/parameters	1585/0/75	2481/1/172	3516/0/264	861/0/82	2728/0/145
Goodness-of-fit on F^2	1.094	1.044	1.05	1.082	1.049
Final R indexes [$I>=2\sigma(I)$]	R_1 = 0.0489, wR_2 = 0.1419	R_1 = 0.0500, wR_2 = 0.1167	R_1 = 0.0299, wR_2 = 0.0770	R_1 = 0.0334, wR_2 = 0.0918	R_1 = 0.0483, wR_2 = 0.1140
Largest diff. Peak/hole/e (Å^{-3})	0.36/-0.26	0.48/-0.38	0.6/-0.6	0.14/-0.23	1.62/-0.71

Compound No.	**2c**	**3a**	**3b**	**3c**
CCDC no.	1952519	1952362	1952363	1952364
Empirical formula	$C_{12}H_{10.5}N_2Br_2$	$C_{12}H_6F_4N_2$	$C_{12}H_6Cl_4N_2$	$C_{12}H_6Br_4N_2$
Formula weight	340.02	127.09	320.00	497.83
Temperature/*K*	100.0(2)	298.0(2)	296.0(2)	298.0(2)
Crystal system	monoclinic	monoclinic	monoclinic	monoclinic
Space group	$P2_1/c$	$P2_1/c$	$P2_1/c$	$P2_1/c$
a/Å	21.089(2)	12.152(3)	3.8774(5)	12.570(2)
b/Å	4.5236(4)	9.341(2)	6.7859(9)	12.6296(10)
c/Å	11.6930(10)	12.229(3)	23.572(3)	13.341(2)
α/°	90	90	90	90
β/°	95.678(8)	157.61(3)	91.221(2)	160.195(11)
γ/°	90	90	90	90
V/Å^3	1110.08(17)	528.7(3)	620.08(14)	717.6(2)
Z	4	4	2	2
ρ_{calc} g/cm^3	2.035	1.597	1.7138	2.304
μ/mm^{-1}	7.272	0.146	0.933	11.199
F(000)	656.0	256	321.3	464
2Θ range for data collection/°	3.882 to 49.996	5.534 to 65.582	3.46 to 50	6.452 to 65.632
Index ranges	$-23 \leq h \leq 25$, $-2 \leq k \leq 5$, $-13 \leq l \leq 13$	$-17 \leq h \leq 11$, $-13 \leq k \leq 13$, $-14 \leq l \leq 18$	$-2 \leq h \leq 4$, $-8 \leq k \leq 7$, $-27 \leq l \leq 27$	$-17 \leq h \leq 9$, $-15 \leq k \leq 18$, $-6 \leq l \leq 18$
Reflections collected	4939	4863	1933	4548
Independent reflections	1933 [R_{int} = 0.0327, R_{sigma} = 0.0255]	1844 [R_{int} = 0.0338, R_{sigma} = 0.0380]	1049 [R_{int} = 0.0359, R_{sigma} = 0.0278]	2414 [R_{int} = 0.0323, R_{sigma} = 0.0546]
Data/restraints/parameters	1933/0/145	1844/0/83	1049/0/82	2414/0/82
Goodness-of-fit on F^2	1.106	1.026	1.069	1.098
Final *R* indexes [$I>=2\sigma(I)$]	R_1 = 0.0654, wR_2 = 0.1681	R_1 = 0.0659, wR_2 = 0.1878	R_1 = 0.0227, wR_2 = 0.0628	R_1 = 0.0783, wR_2 = 0.2213
Largest diff. Peak/hole/e (Å^{-3})	2.17/-2.08	0.37/-0.24	0.27/-0.22	0.81/-1.02

Compound No.	**4a**	**4c**	**5a**	**5b**
CCDC no.	1952365	1952366	1952367	1952368
Empirical formula	$C_{12}H_8N_2F_4$	$C_{24}H_{12}Br_8N_4$	$C_{12}H_6F_4N_2$	$C_{12}H_6Cl_4N_2$
Formula weight	254.19	995.66	254.19	320.00
Temperature/*K*	296.0(2)	298.0(2)	200.0(2)	100.0(2)
Crystal system	monoclinic	monoclinic	monoclinic	monoclinic
Space group	$P2_1/c$	$P2_1/c$	$P2_1/c$	$P2_1/c$
a/Å	3.7549(12)	17.645(2)	3.8151(3)	13.749(3)
b/Å	6.1126(15)	4.0942(7)	6.0756(6)	3.7695(8)
c/Å	21.725(6)	17.898(3)	23.1225(14)	15.209(4)
α/°	90	90	90	90
β/°	91.329(10)	147.706(15)	93.759(7)	128.475(3)
γ/°	90	90	90	90
V/Å^3	498.5(3)	690.8(2)	534.80(7)	617.1(3)
Z	2	1	2	2
ρ_{calc} g/cm^3	1.6933	2.393	1.579	1.7220
μ/mm^{-1}	0.155	11.633	0.145	0.938
F(000)	256.2	464.0	256	321.3
2Θ range for data collection/°	6.92 to 49.98	5.388 to 55.072	3.5 to 32.7	3.78 to 50
Index ranges	$-1 \leq h \leq 4$, $-4 \leq k \leq 4$, $-25 \leq l \leq 5$	$-22 \leq h \leq 22$, $-4 \leq k \leq 5$, $-23 \leq l \leq 23$	$-5 \leq h \leq 5$, $-7 \leq k \leq 8$, $-32 \leq l \leq 35$	$-16 \leq h \leq 16$, $-4 \leq k \leq 2$, $-18 \leq l \leq 16$
Reflections collected	420	4594	4871	2902
Independent reflections	283 [R_{int} = 0.0719, R_{sigma} = 0.0591]	1560 [R_{int} = 0.0653, R_{sigma} = 0.0693]	1836 [R_{int} = 0.036, R_{sigma} = 0.05]	1070 [R_{int} = 0.0217, R_{sigma} = 0.0233]
Data/restraints/parameters	283/0/37	1560/0/82	1836/0/82	1070/0/82
Goodness-of-fit on F^2	1.050	1.094	1.05	1.058
Final *R* indexes [$I>=2\sigma(I)$]	R_1 = 0.0448, wR_2 = 0.1074	R_1 = 0.0792, wR_2 = 0.2493	R_1 = 0.0517, wR_2 = 0.1599	R_1 = 0.0253, wR_2 = 0.0679
Largest diff. Peak/hole/e (Å^{-3})	0.21/-0.24	1.51/-1.24	0.2/-0.3	0.30/-0.34

Table 3. Interactions in the solid state in the crystal structures

Serial no	D–H⋯A	*D*(D⋯A)/Å	*d*(H⋯A)/Å	∠D–H⋯A/º	SYMMETRY
1a	**C4–** H4 ⋯F1	3.360	2.469	134.10	1-x,1-y,-z+2
1b	C2 – H2⋯Cl1	3.664	2.810	135.89	x + ½, 1 -y, z
	C7– H7⋯N9	2.744	2.521	90.05	x, y ,z
	C11 – H11⋯N8	2.705	2.584	84.61	x, y, z
1c	C10– H10 ⋯Br1	3.421	3.5463	132.21	1-x, 1-y,+z+½
2b	C5 – H5⋯N1	2.742	2.494	91.38	x, y, z
	C8 – H8⋯N2	2.744	2.505	90.93	x, y, z
2c	C6– H6⋯N1	2.739	2.508	90.50	x, y, z
	C9– H9⋯N2	2.714	2.470	91.04	x, y, z
3a	C6– H6⋯N1	2.701	2.445	91.63	2 - x, 1 - y, 1 -z
	C4– H4 ⋯F1	3.399	2.547	135.14	x- ½,-y+ ½,+z+ ½
	C3– H3⋯F2	3.360	2.593	127.37	-x+ ½,+y- ½,-z+ ½+1
3b	C2– H2⋯N1	2.697	2.430	92.18	-x, 1-y, 1-z
3c	C6– H6⋯N1	2.659	2.396	91.81	2-x, 1-y, 1-z
4a	C5– H5⋯N1	2.730	2.434	93.98	2-x, -y, 2- z
	C6– H6⋯F2	3.401	2.578	132.38	x-1, y+1,+z
	C2– H2⋯F1	3.213	2.542	119.46	1-x, y-½, -z+½+1
4c	C9– H9 ⋯N3	2.698	2.426	92.47	1-x,-y,1-z
5a	C5– H5⋯F2	3.361	2.520	134.03	x-1, y+1, z
	C8– H8⋯F1	3.401	2.494	140.92	1-x, y-½, -z + ½+1

	C5– H5⋯N3	2.712	2.464	91.28	-x, 1-y, 1-z
5b	C4– H4 ⋯Cl1	3.816	2.893	143.55	-x,-y,1-z
	C6– H6⋯N1	2.710	2.459	91.42	1-x,1-y,1-z
	C6– H6 ⋯Cl2	3.539	2.905	117.68	- x + ½,+y- ½,-z + ½

3.1.2 Structure of 2(a, b, c)

All three compound **2a** (1-(3-fluorophenyl-2-(4-fluorophenyl)diazene), **2b** (1-(3-chlorophenyl-2-(4-chlorophenyl)diazene) and **2c** (1-(3-bromophenyl-2-(4-bromophenyl)diazene) were crystallized in monoclinic centrosymmetric $P2_1/c$ space group but for compound **2a**, Z = 2 and for **2b** and **2c,** Z = 4 . The compound **2a** displayed different static disorder across the –N=N– bond. The crystal structure of **2b** contains C–Cl⋯Cl–C,[49] while **2c** displays C–Br⋯Br–C[49] interactions. **2b** and **2c** exhibits Type II halogen⋯halogen interaction[49] where θ_1 (= 95.09° and 100.32°) and θ_2 (= 166.07° and 167.43°) are close 90° and 180° ($\theta_1 - \theta_2 \geq 30^o$). The experimental PXRD pattern of 2(a, b, c) is found to match with the corresponding simulated PXRD pattern from the CIF of the single crystal structure solution.

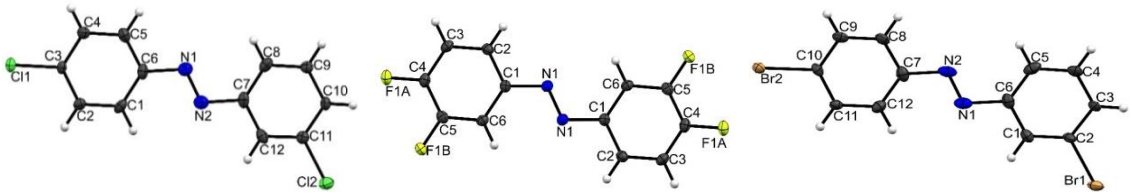

2a **2b** **2c**

Figure 3.5. ORTEP of **2a, 2b, 2c** compounds.

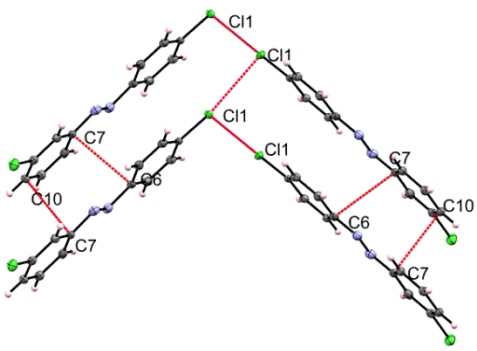

Figure 3.6. Type –II and π⋯π interactions in the solid-state in **2b**.

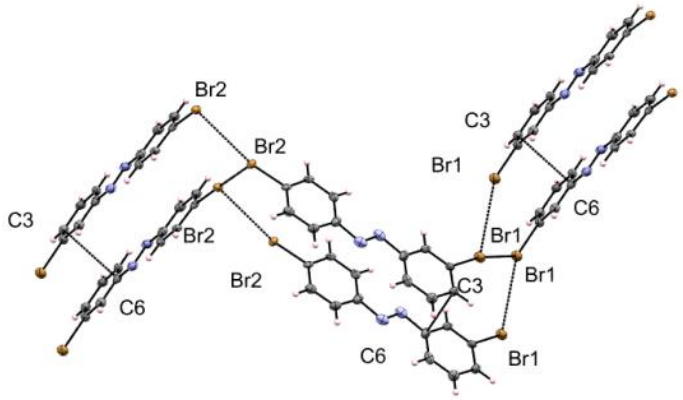

Figure 3.7. Type –II and π⋯π interactions in the solid-state in **2c**.

3.1.3. Structural analysis of 3a, 3b and 3c

All three compound **3a** (bis(2,5-difluorophenyl)diazene), **3b** (bis(2,5-dichlorophenyl)diazene) and **3c** (bis(2,5-dibromophenyl)diazene) were crystallized in monoclinic centrosymmetric *P2₁/c* space group although 3a has Z = 4 while 3b and 3c has Z = 2 (Z′ = 0.5). These symmetrical molecules possessing an inversion centre and the crystallographic centre of inversion coincided with the molecular centre of inversion laying at the midpoint of the -N=N- bond. The ORTEPs ABs are shown herein. In the crystal structure of **3a** C–H⋯F and π⋯π interactions were observed. The crystal structure of **3b** contains Type I C–Cl⋯Cl–C interaction where $\theta_1 = \theta_2$ (= 144.48°). The experimental PXRD pattern of all 3(a, b, c) is found to match with the corresponding simulated PXRD pattern from the CIF of the single crystal structure solution.

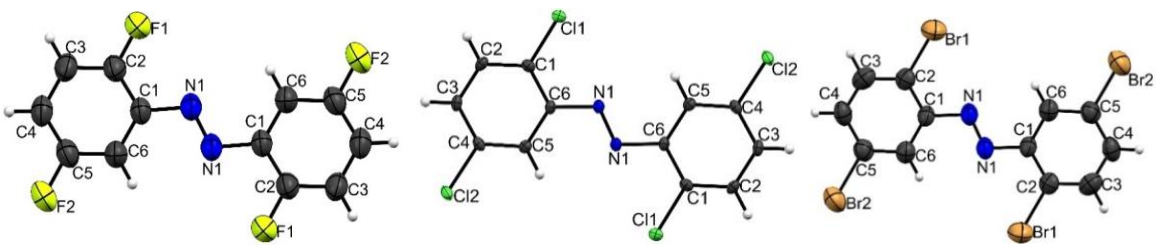

3a **3b** **3c**

Figure 3.8. ORTEP of **3a, 3b, 3c** compounds.

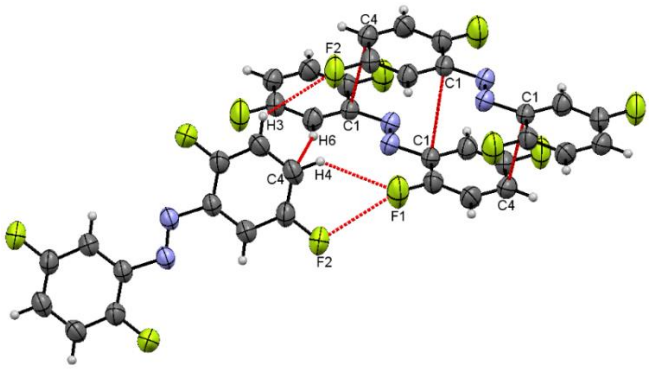

Figure 3.9. H⋯F and π⋯π interactions in the solid-state in **3a**.

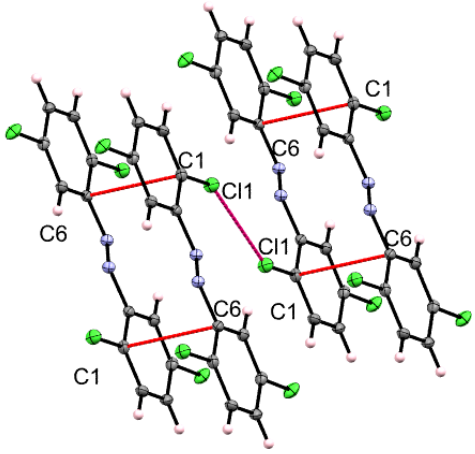

Figure 3.10. Type –I and π⋯π interactions in the solid-state in **3b**.

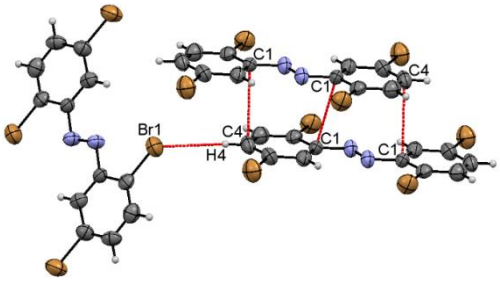

Figure 3.11. H⋯Br and π⋯π interactions in the solid-state in **3c**.

3.1.4. Structural analysis of 4a and 4c

Compound **4a** (bis(2,4-difluorophenyl)diazene) and **4c** (bis(2,4-dibromophenyl)diazene) were crystallized in the monoclinic centrosymmetric $P2_1/c$ space group with Z = 2 for **4a** and Z = 1 for 4c. The compounds **4b** did not yield suitable single crystals for structure determination. **4a** and **4c** possessing an inversion centre, and the crystallographic centre of inversion coincided with the molecular centre of inversion laying at the midpoint of the -N=N- bond. Significant intermolecular C–H⋯F interactions in the solid-state was observed in 4a**.** The experimental

PXRD pattern of both 4(a, c) are found to match with the simulated PXRD pattern from the CIF of the single crystal structure solution.

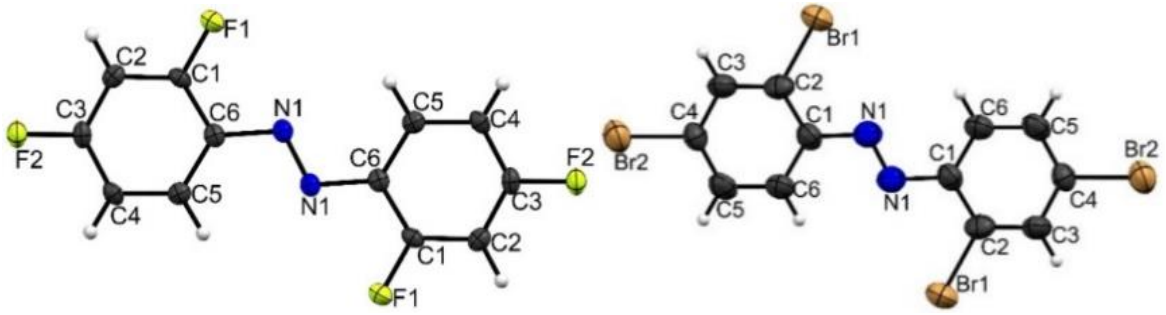

4a **4c**

Figure 3.12. ORTEP of **4a, 4c** compounds.

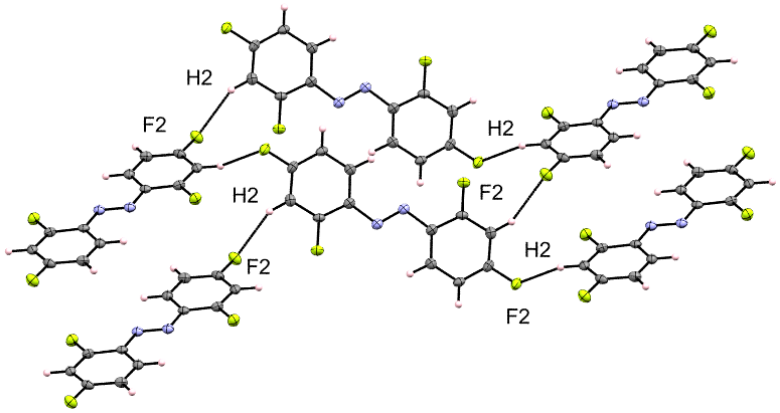

Figure 3.13 H⋯F interactions in the solid-state in **4a.**

3.1.5. Structural analysis of 5a and 5c

Compound **5a** (bis(3,5difluorophenyl)diazene) and **5b** (bis(2,4-dichlorophenyl)diazene) were crystallized in monoclinic centrosymmetric $P2_1/c$ space. The compounds **5c** (bis(3,5-dibromophenyl)diazene) did not yield suitable single crystals for structure determination. Both **5a** and **5b** possessing an inversion centre with Z = 2, and the crystallographic centre of inversion coincided with the molecular centre of inversion laying at the midpoint of the –N=N– bond. The ORTEPs of **5a** and **5b** are shown herein. Significant C–H⋯F and π⋯π interactions in the solid-state in **5a,** C–H⋯Cl and C–H⋯N interactions in the solid-state in **5b** was observed. The experimental PXRD pattern of both 5(a, b) are found to match with the simulated PXRD pattern from the CIF of the single crystal structure solution

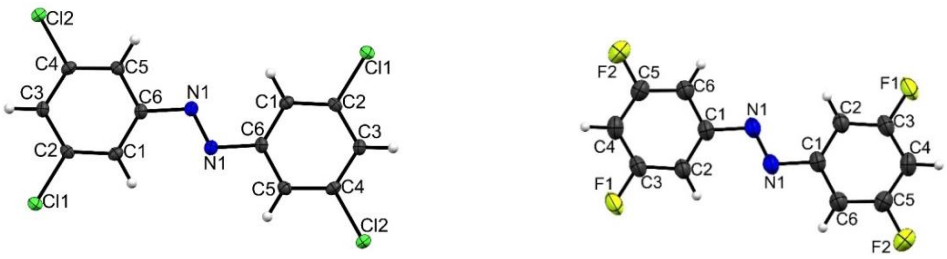

5a **5b**

Figure 3.14. ORTEP of **5a, 5b** compounds.

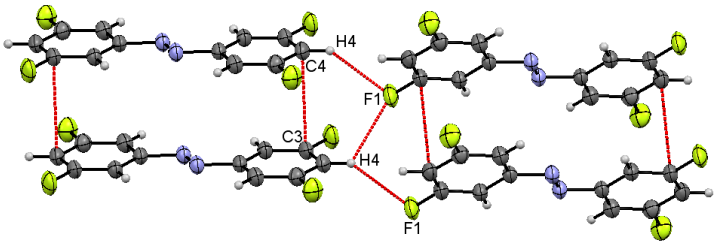

Figure 3.15 H····F and π····π interactions in the solid-state in **5a**.

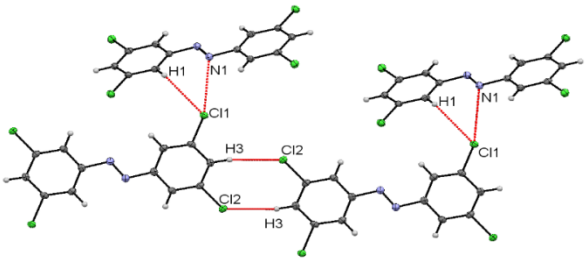

Figure3.16 H····Cl and N····Cl interactions in the solid-state in **5b.**

3.2: UV-VIS analysis of *cis*-/*trans*- isomerization of all the compounds

The results of kinetic study of *cis*- to *trans*- isomerization of the fifteen compounds by UV-Vis study are listed in the Table 13. UV-Vis spectrum of the compound are shown herein. The absorption spectrum of the *trans*- isomers exhibited $\pi \rightarrow \pi^*$ transitions at ~320-330 nm (For 4b and 4c the transition at around 350 nm) whereas very weak $n \rightarrow \pi^*$ transitions appeared at ~450-460 nm. After irradiation by 365 nm UV light, the compounds have shown shifting of $\pi \rightarrow \pi^*$ transitions below 330 nm with a large reduction in intensity of the peak while the weak $n \rightarrow \pi^*$ transitions shifted below 440 nm. All the ABs exhibited hyper chromic shift both in the $\pi \rightarrow \pi^*$ and in the $n \rightarrow \pi^*$ region. It has been observed that $n \rightarrow \pi^*$ is greatly affected due to the –N=N– bond orbital involvement during photo-isomerization.[38] UV-Vis spectra of all the compounds show complete conversion of *trans*- isomers to *cis*- isomers. The *cis*- isomers have been found to remain unaltered for long time (few hours) if kept in the dark and below 4

°C in a refrigerator. When the solutions were exposed to the visible light in the laboratory, spontaneous *cis*- → *trans*- isomerization was observed at different rate and approximately 15-30% of *cis*– isomer was found to remain unconverted even after exposure to visible light for several days (except for compounds 3(c), 4(c), 5(b) and 5(c)) .All the compounds followed first order kinetics. The rate constants (k) were calculated using standard procedure (Table 13). All the kinetic data were reproduced twice.

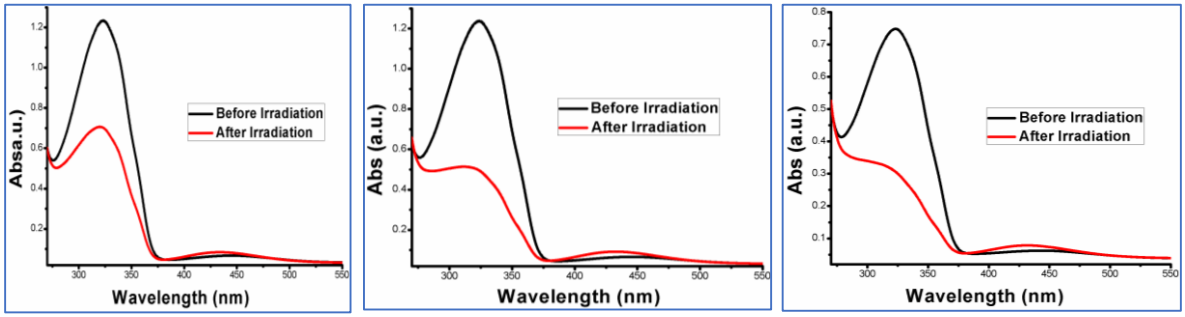

(a) (b) (c)

Figure 3.17: Time evolution of the UV-Vis spectra of (a) 1a (10^{-5} M), (b) 1b (10^{-5} M) and (c) 1c (10^{-5} M).

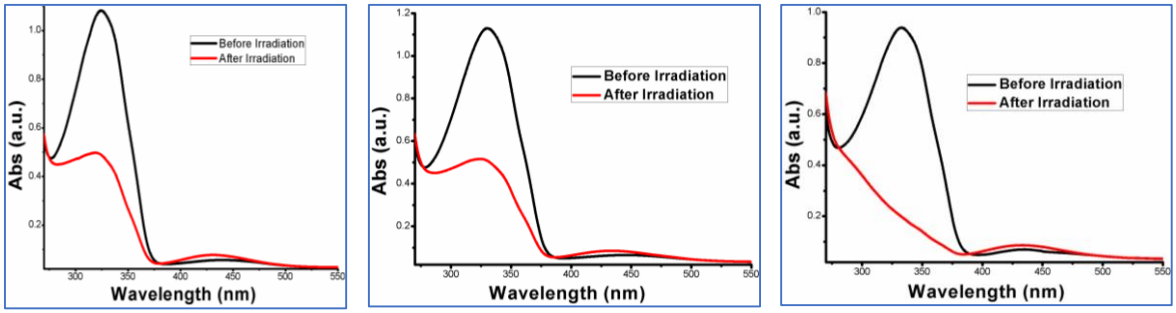

(a) (b) (c)

Figure 3.18: Time evolution of the UV-Vis spectra of (a) 2a (10^{-5} M), (b) 2b (10^{-5} M) and (c) 2c (10^{-5} M).

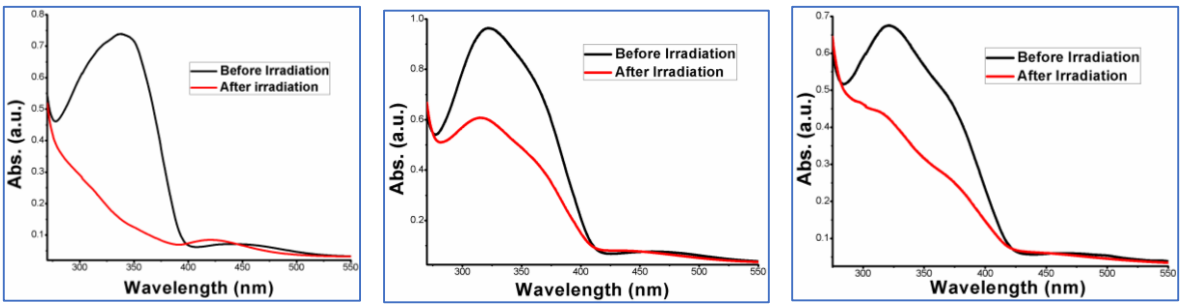

(a) (b) (c)

Figure 3.19: Time evolution of the UV-Vis spectra of (a) 3a (10^{-5} M), (b) 3b (10^{-5} M) and (c) 3c (10^{-5} M).

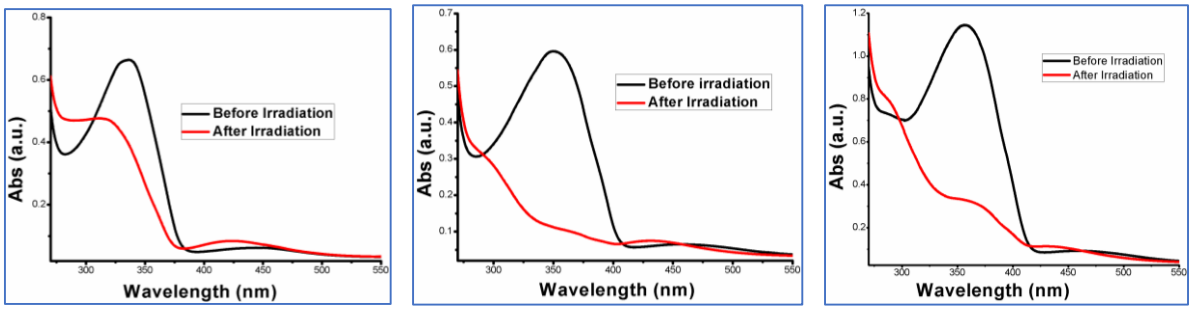

(a) (b) (c)

Figure 3.20: Time evolution of the UV-Vis spectra of (a) 4a (10^{-5} M), (b) 4b (10^{-5} M) and (c) 4c (10^{-5} M).

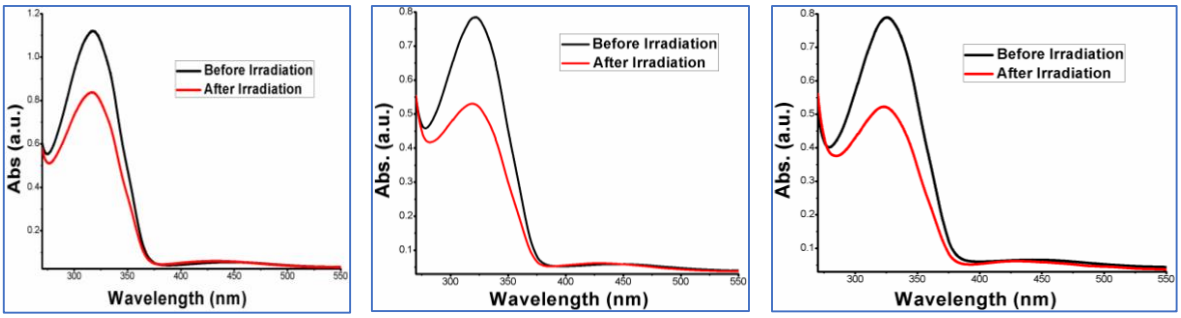

(a) (b) (c)

Figure 3.21: Time evolution of the UV-Vis spectra of (a) 5a (10^{-5} M), (b) 5b (10^{-5} M), (c) 5c (10^{-5} M).

Table 4: Rate constants and % of unconverted *cis*- isomers.

Samples	Rate constant (k) (min^{-1})	Unconverted % of *cis*- after 4 days
1a	2.11×10^{-2}	21.1
1b	2.83×10^{-2}	20.7
1c	2.8×10^{-2}	18.3
2a	1.68×10^{-2}	22.82
2b	2.88×10^{-2}	21.5
2c	3.17×10^{-2}	16.6
3a	1.62×10^{-2}	33.3
3b	1.98×10^{-2}	22.0
3c	2.01×10^{-2}	0
4a	3.35×10^{-2}	31.9
4b	4.0×10^{-2}	16.6
4c	4.51×10^{-2}	0

5a	1.08×10^{-2}	18.1
5b	1.73×10^{-2}	0
5c	2.52×10^{-2}	0

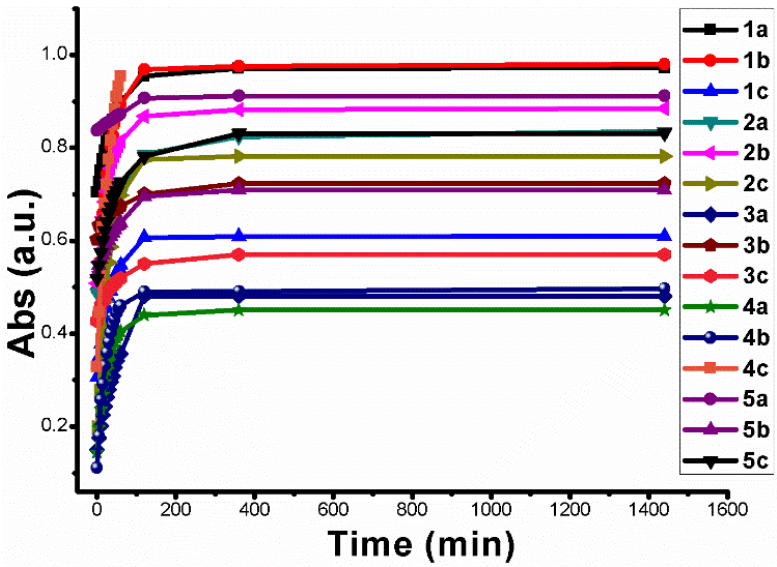

Figure 3.22. Kinetic study of the compounds.

Table 5. Azo compounds with their λ_{max} values for $\pi \rightarrow \pi^*$ and $n \rightarrow \pi^*$ transitions.

Samples	*trans*-isomer		*cis*-isomer	
	λ_{max} (nm) for $\pi \rightarrow \pi^*$	λ_{max} (nm) for $n \rightarrow \pi^*$	λ_{max} (nm) for $\pi \rightarrow \pi^*$	λ_{max} (nm) for $n \rightarrow \pi^*$
1a	322.0	445.0	320.0	433.0
1b	324.0	446.0	318.0	434.0
1c	323.0	445.0	308.0	430.0
2a	324.0	445.0	320.0	430.0
2b	330.0	445.0	325.0	433.0
2c	333.0	434.0	#	432.0
3a	338.0	450.0	#	420.0
3b	320.0	468.0	315.0	430.0
3c	320.0	455.0	300.0	430.0
4a	336.0	446.0	317.0	422.0
4b	350.0	460.0	#	430.0
4c	356.0	463.0	360.0	435.0
5a	318.0	449.0	317.0	429.0
5b	322.0	452.0	320.0	426.0

5c	325.0	444.0	324.0	432.0
# No peak was observed				

3.3 Theoretical Calculations

The transitions states of these compounds have larger number of probable geometries (Table-6). The optimised geometry of the probable transition states and the corresponding *trans*- and *cis*- isomers of all the compounds are shown in the (Table-7). There are 2 probable conformers for the *trans*- and *cis*- isomers of **1(a-c)** and **2(a-c)**, 4 probable conformers for **3(a-c)** and **4(a-c)** and only one conformer is possible for **5(a-c)**. The resultant *trans*- isomers were compared with the geometry of the *trans*- isomer observed in the crystal structure (for 13 compounds). Energy value of optimized geometry of all possible *cis*-, *trans*-, TS in (Table -8). We calculated the activation energy (E_{act}) for *trans*- → *cis*- ($\Delta E_{trans\text{-}TS}$) and *cis*- → *trans*- ($\Delta E_{cis\text{-}TS}$) isomerization from the energy of the optimized geometries of the conformer obtained after IRC calculation and the corresponding transition state for all the possible optimized geometries of *trans*- and *cis*- isomers (Table 9). For most of the compounds the fluoro compounds show larger E_{act} value compared to bromo and chloro analogues. Bond Length (Å) and bond angles (º) torsional angle (º) of the all possible *cis*- and *trans*- compounds are shown in (Table 10). We used optimized geometry for TD-DFT calculation to compare the wavelength and the nature of transitions observed in the experimental UV-Vis spectra.

Table 6. Input and optimized geometries of the Transition States

Sample ID	TS Input Geometries	TS Optimized Geometries
1a1	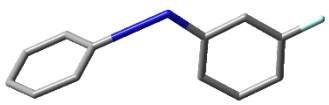	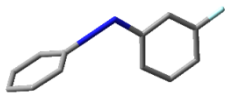
1a2	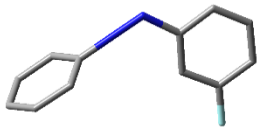	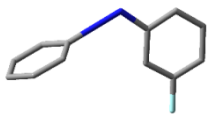
1a3	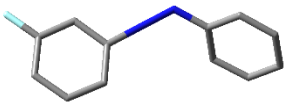	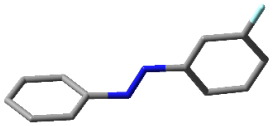

1a4	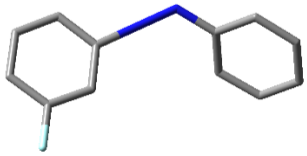	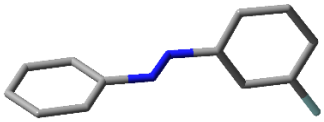
1b1	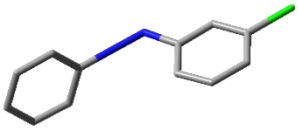	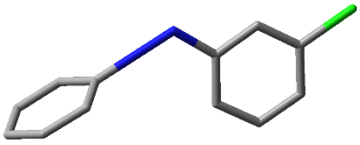
1b2	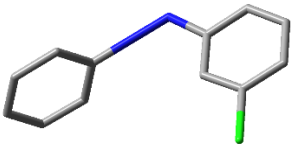	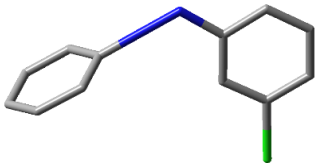
1b3	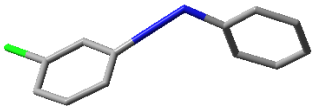	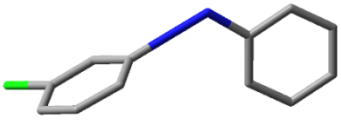
1b4	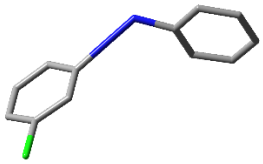	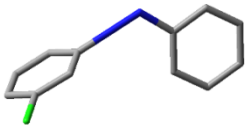
1c1	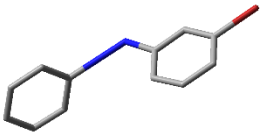	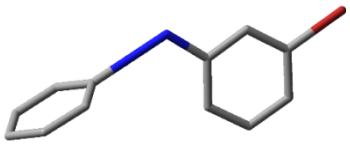
1c2	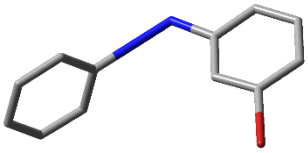	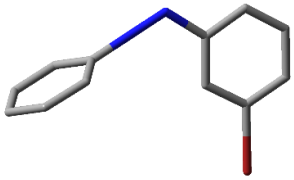
1c3	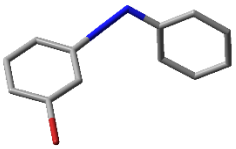	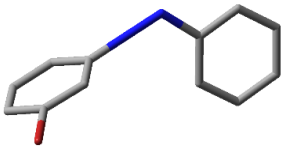

1c4	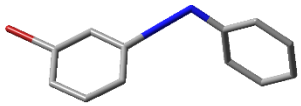	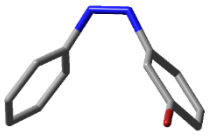
2a1		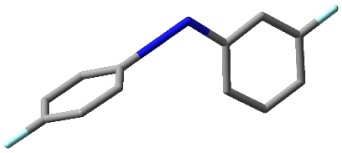
2a2	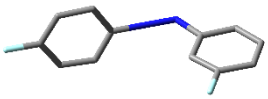	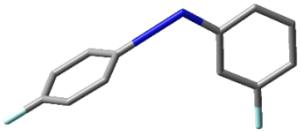
2a3	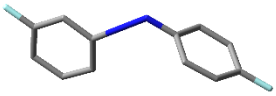	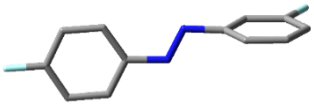
2a4	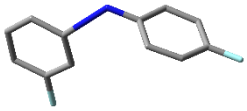	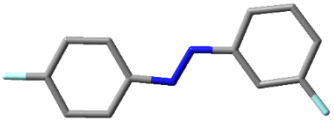
2b1	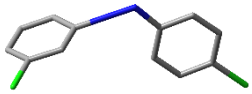	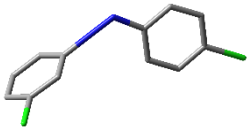
2b2	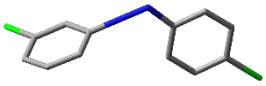	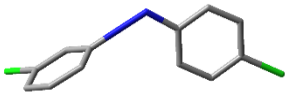
2b3	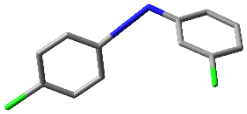	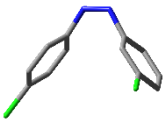
2b4	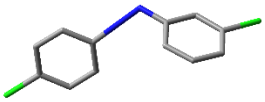	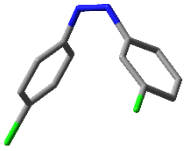

2c1	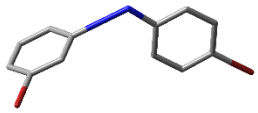	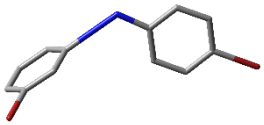
2c2	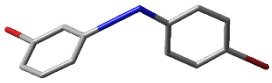	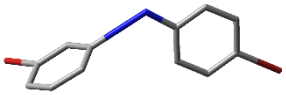
2c3	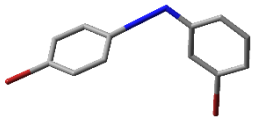	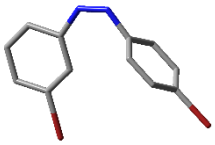
2c4	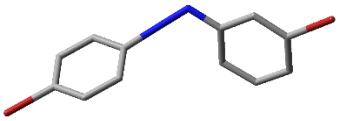	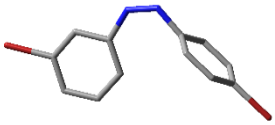
3a1	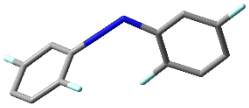	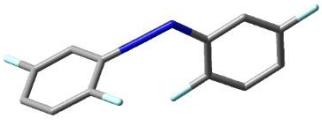
3a2	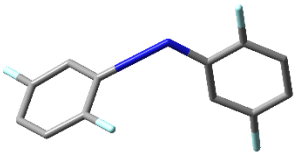	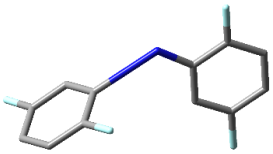
3a3	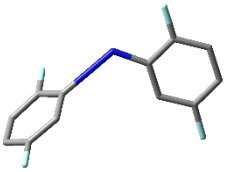	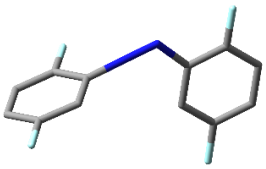
3a4	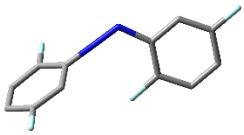	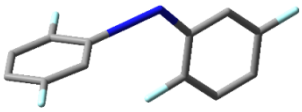
3b1	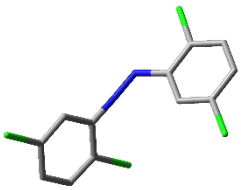	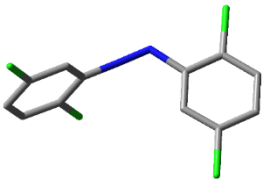

3b2	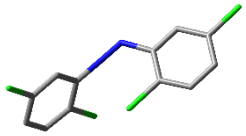	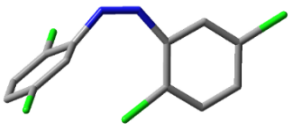
3b3	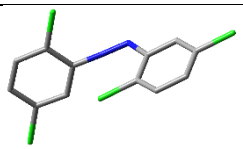	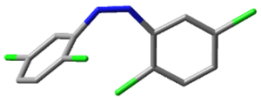
3b4	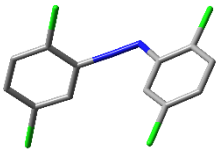	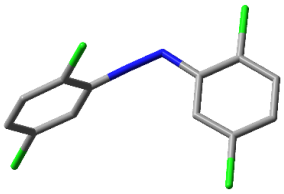
3c1	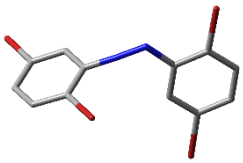	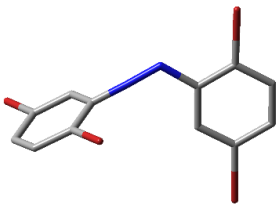
3c2	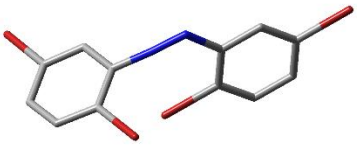	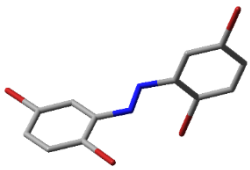
3c3	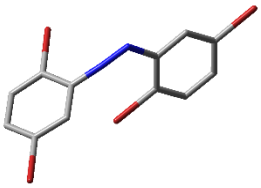	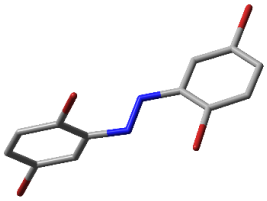
3c4	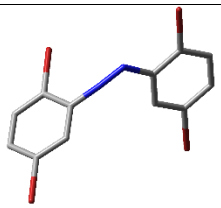	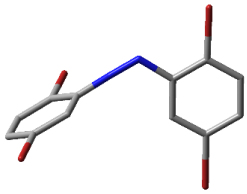
4a1	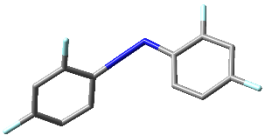	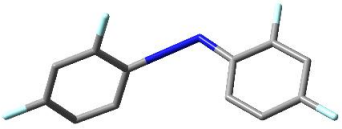

4a2	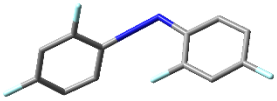	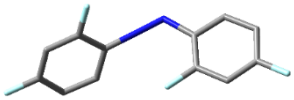
4a3	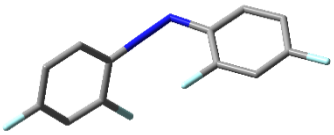	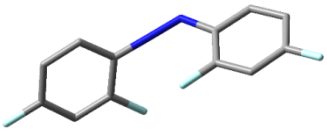
4a4	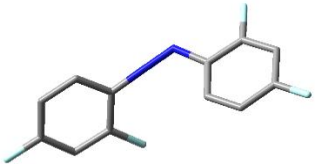	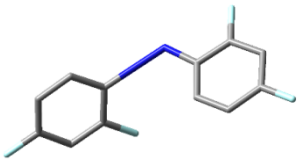
4b1	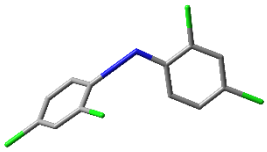	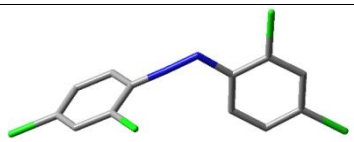
4b2	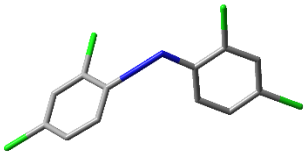	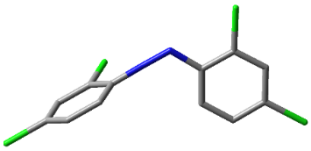
4b3	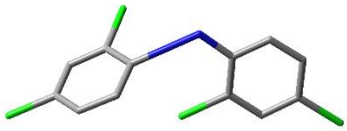	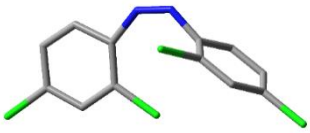
4b4	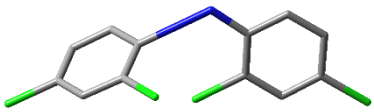	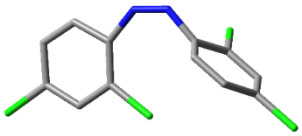
4c1	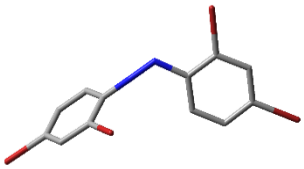	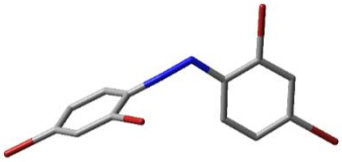
4c2	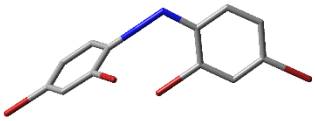	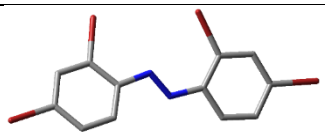

4c3	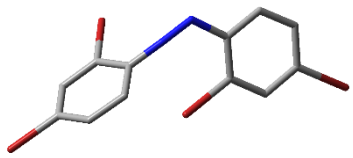	
4c4	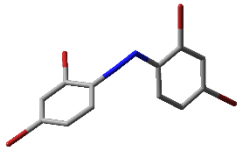	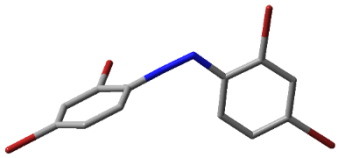
5a	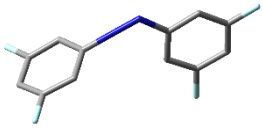	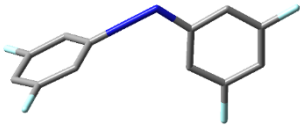
5b	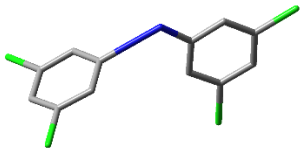	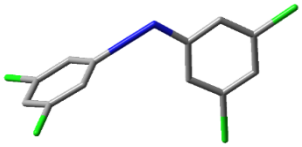
5c	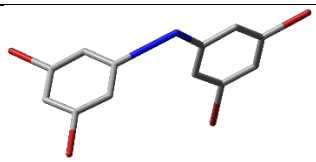	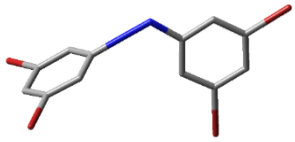

Table 7: Probable TS and corresponding optimized *Cis* and *Trans* Geometries

Sample ID	***Trans* Geometries obtained from TS after IRC (Optimized)**	**Probable TS Geometries (Optimized)**	***Cis* Geometries obtained from TS after IRC (Optimized)**
1a1	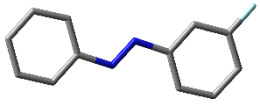	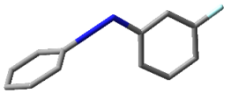	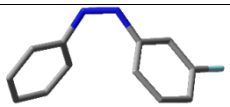
1a2	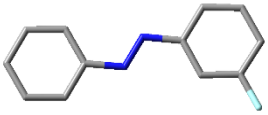	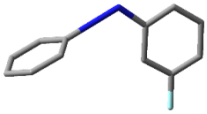	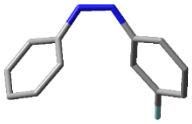
1a3	#	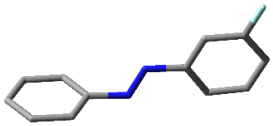	#

1a4	#	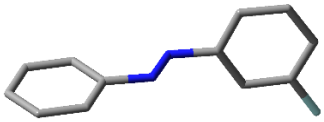	#
1b1	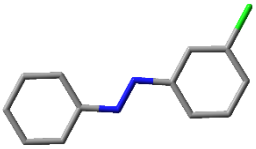	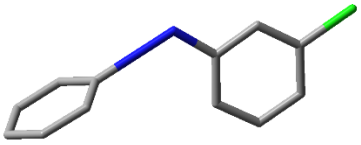	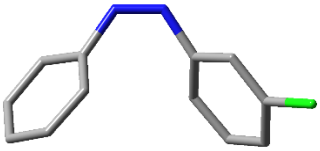
1b2	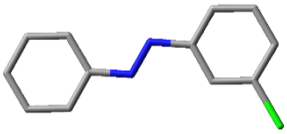	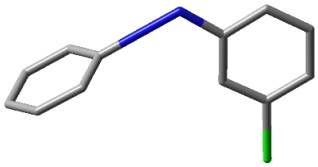	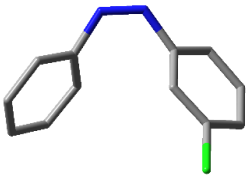
1b3	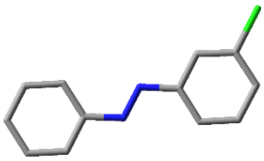	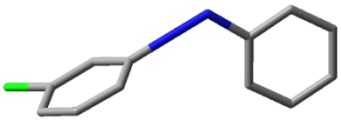	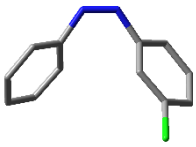
1b4	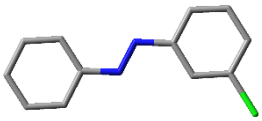	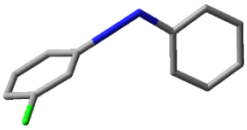	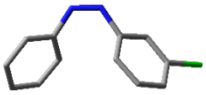
1c1	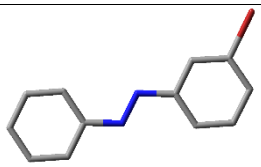	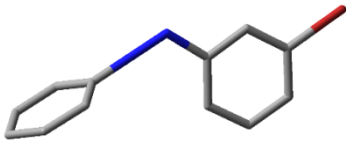	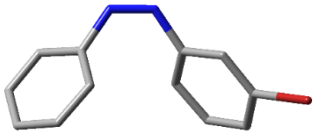
1c2	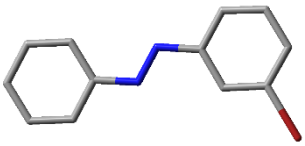	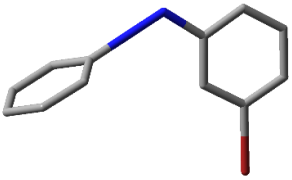	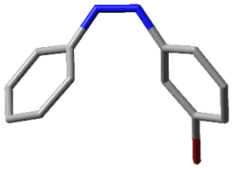
1c3	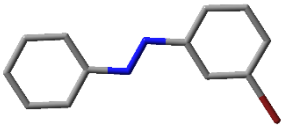	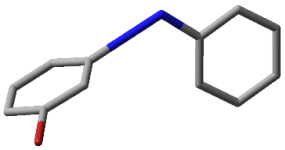	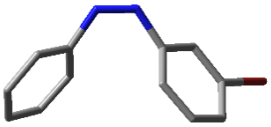
1c4	#	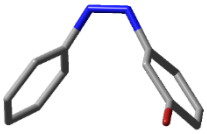	#

2a1	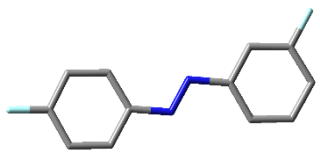	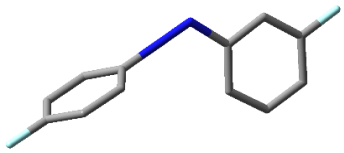	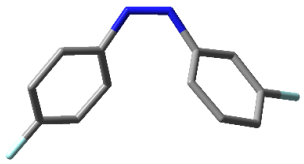
2a2	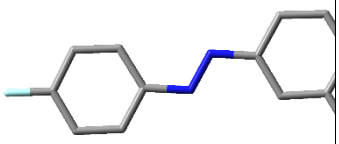	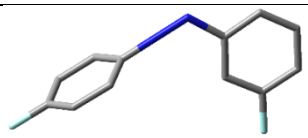	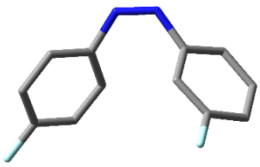
2a3	#	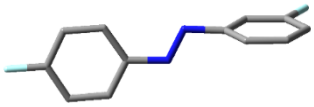	#
2a4	#	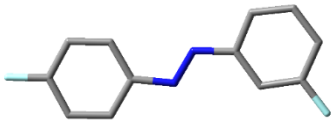	#
2b1	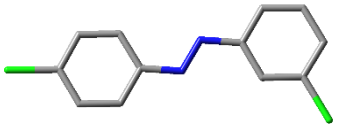	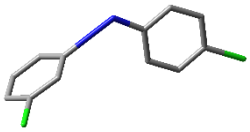	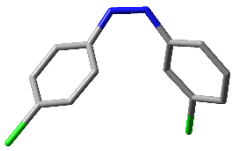
2b2	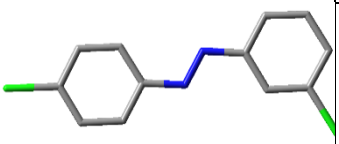	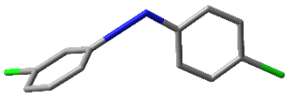	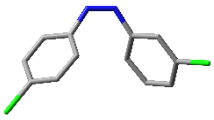
2b3	#	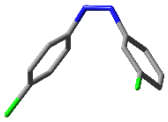	#
2b4	#	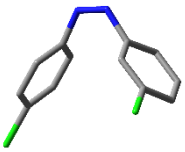	#
2c1	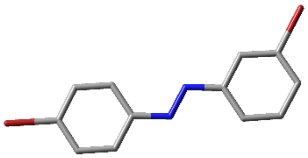	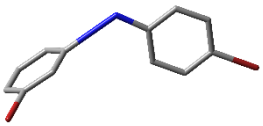	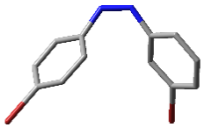

2c2	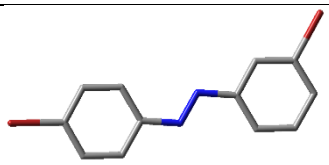	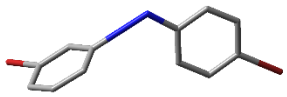	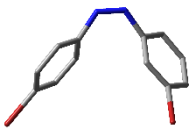
2c3	#	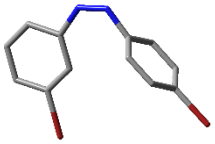	#
2c4	#	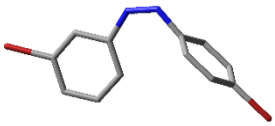	#
3a1	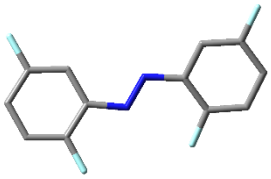	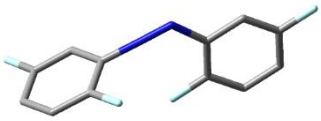	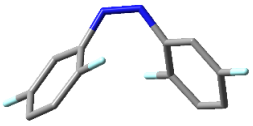
3a2	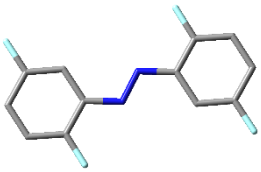	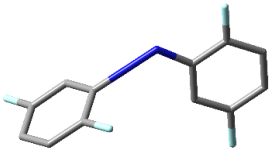	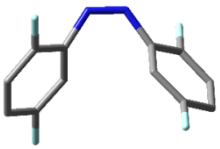
3a3	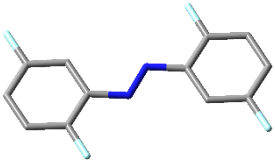	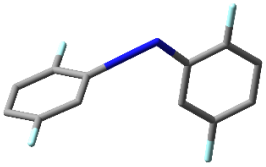	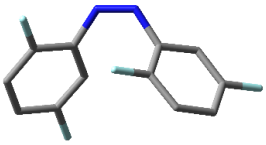
3a4	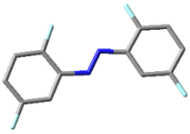	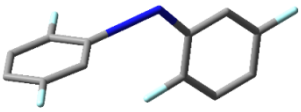	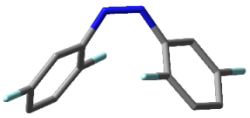
3b1	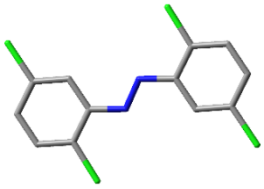	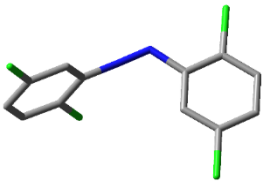	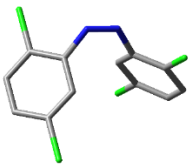

3b2	#	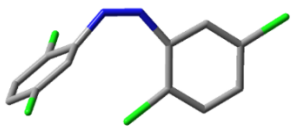	#
3b3	#	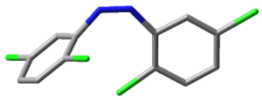	#
3b4	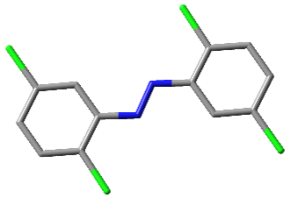	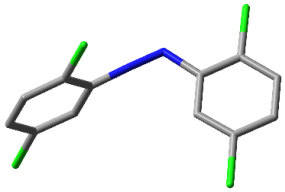	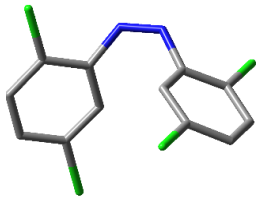
3c1	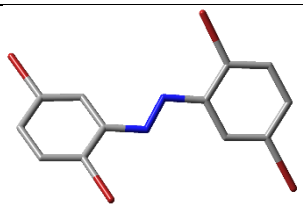	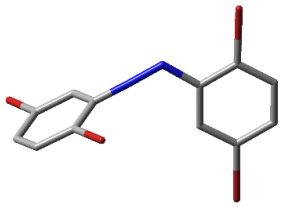	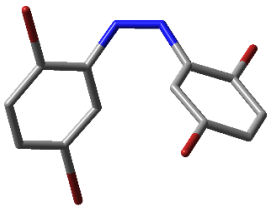
3c2	#	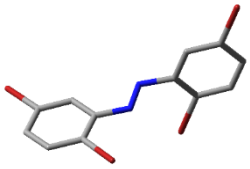	#
3c3	#	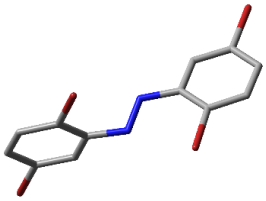	#
3c4	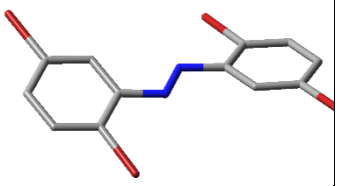	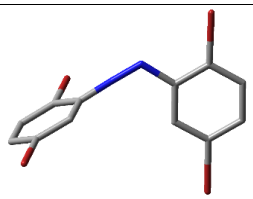	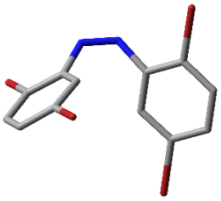
4a1	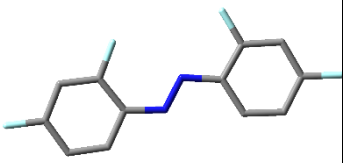	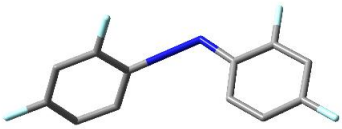	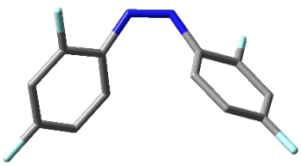

4a2	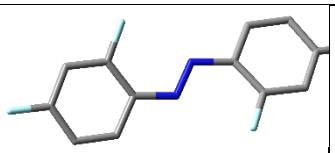	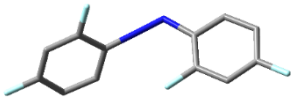	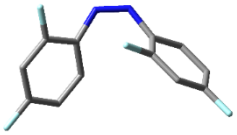
4a3	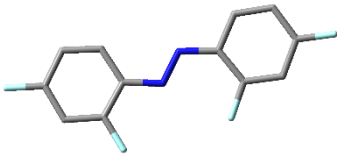	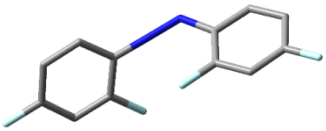	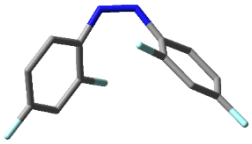
4a4	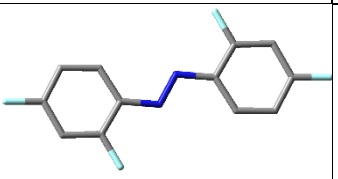	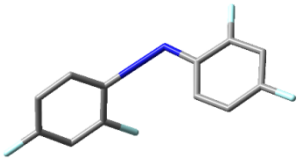	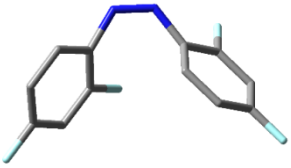
4b1	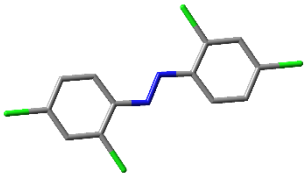	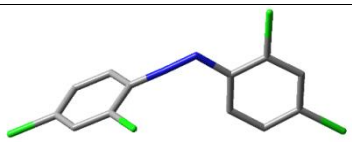	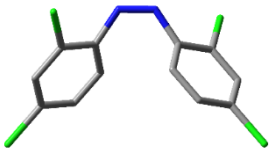
4b2	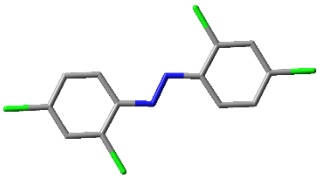	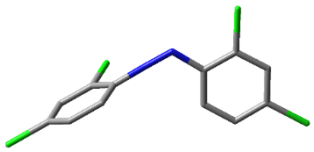	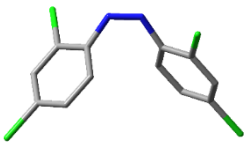
4b3	#	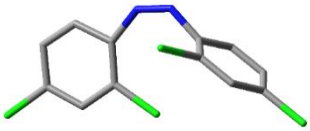	#
4b4	#	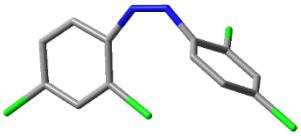	#
4c1	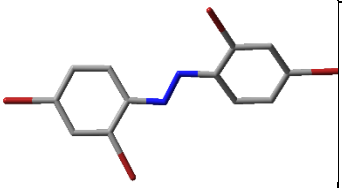	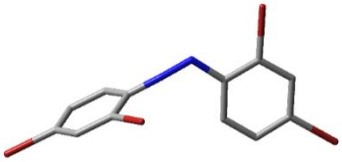	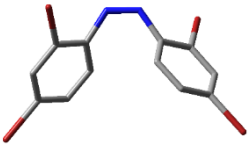
4c2	#	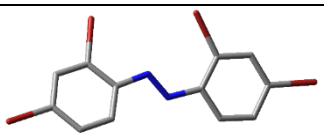	#

4c3	#		#
4c4	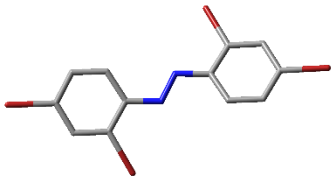	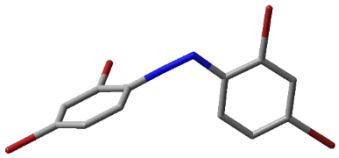	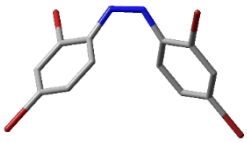
5a	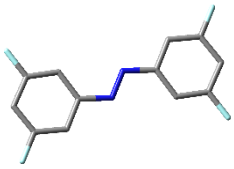	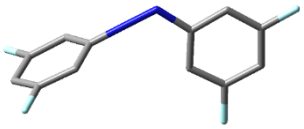	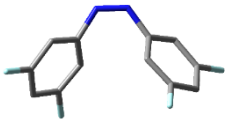
5b	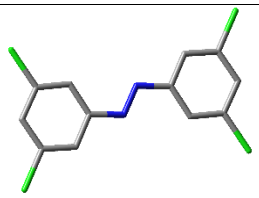	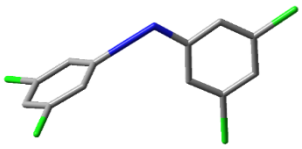	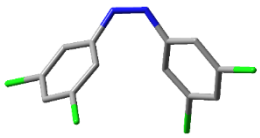
5c	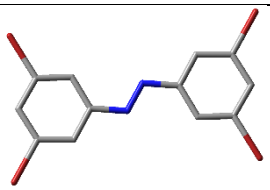	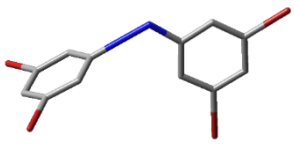	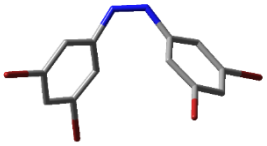

These transition states did not yield any corresponding cis/trans geometry in IRC calculation

Table 8. Energy value of optimized geometry of all possible *cis*-, *trans*-, TS.

Sample ID	***Cis* Energy (Kcal/mol)**	***Trans* Energy (Kcal/mol)**	**TS Energy (Kcal/mol)**
1a1	-421691.6326	-421705.6691	-421667.3785
1a2	-421691.6012	-421705.8725	-421667.4789
1b1	-647814.9768	-647828.9016	-647790.6599
1b2	-647815.049	-647829.0347	-647790.7685
1b3	-647815.0709	-647828.8489	-647792.2105
1b4	-647815.0119	-647829.211	-647792.2889
1c1	-1974300.7	-1974314.686	-1974276.448
1c2	-1974300.768	-1974314.78	-1974276.52
1c3	-1974300.722	-1974315.031	-1974278.177
2a1	-483988.5406	-484002.8909	-483963.4418
2a2	-483988.5525	-484003.1456	-483963.509
2b1	-936235.3174	-936249.4305	-936212.494

2b2	-936235.3124	-936249.6075	-936212.4984
2c1	-3589206.72	-3589220.726	-3589183.938
2c2	-3589206.693	-3589220.767	-3589183.926
3a1	-608574.9909	-608585.6145	-608550.7625
3a2	-608575.4948	-608589.3086	-608551.6391
3a3	-608575.4346	-608589.6619	-608551.5889
3a4	-608575.001	-608587.2379	-608550.7236
3b1	-1513070.789	-1513083.406	-1513047.24
3b4	-1513070.772	-1513083.47	-1513047.291
3c1	-6819014.215	-6819026.001	-6818990.354
3c4	-6819013.874	-6819026.374	-6818990.351
4a1	-608576.3419	-608588.7539	-608550.8579
4a2	-608576.2899	-608586.6787	-608550.0942
4a3	-608575.8606	-608588.8505	-608549.9129
4a4	-608576.2767	-608591.3436	-608550.8792
4b1	-1513070.758	-1513083.818	-1513047.977
4b2	-1513070.652	-1513084.36	-1513046.988
4c1	-6819014.2	-6819026.656	-6818990.28
4c4	-6819014.033	-6819026.669	-6818990.565
5a	-608579.8258	-608594.0525	-608557.3839
5b	-1513073.035	-1513087.032	-1513050.429
5c	-6819015.905	-6819029.93	-6818993.588

Table 9. Energy difference (Cis – Trans), activation energies $\mathbf{E_{act(\textit{trans- to TS})}}$ **and** $\mathbf{E_{act(\textit{cis- to TS})}}$

Sample ID	**(Cis-Trans) (Kcal/mol)**	$\mathbf{E_{act(\textit{trans- to TS})}}$ **(Kcal/mol)**	$\mathbf{E_{act(\textit{cis- to TS})}}$ **(Kcal/mol)**
1a1	14.036	38.290	24.254
1a2	14.271	38.393	24.122
1b1	13.924	38.241	24.316
1b2	13.985	38.266	24.280
1b3	13.778	36.638	22.860
1b4	14.199	36.922	22.723
1c1	13.985	38.237	24.252
1c2	14.011	38.259	24.248
1c3	14.308	36.853	22.545
2a1	14.350	39.449	25.098
2a2	14.593	39.636	25.043
2b1	14.113	36.936	22.823
2b2	14.295	37.109	22.814
2c1	14.006	36.788	22.782
2c2	14.073	36.840	22.766
3a1	10.623	34.851	24.228
3a2	13.813	37.669	23.855
3a3	14.227	38.072	23.845
3a4	12.236	36.514	24.277
3b1	12.617	36.166	23.549
3b4	12.698	36.179	23.480
3c1	11.785	35.647	23.861

3c4	12.499	36.022	23.523
4a1	12.411	37.895	25.484
4a2	10.388	36.584	26.195
4a3	12.989	38.937	25.947
4a4	15.066	40.464	25.397
4b1	13.060	35.840	22.780
4b2	13.707	37.372	23.664
4c1	12.456	36.376	23.919
4c4	12.635	36.103	23.468
5a	14.226	36.668	22.441
5b	13.997	36.602	22.605
5c	14.025	36.342	22.317

Table 10. DFT calculated parameters of all different conformers.

Sample ID	***cis* isomer**			***trans* isomer**		
	R (N1=N2) (Å)	A (N=N–C) (°)	D (C–N=N–C) (°)	R (N1=N2) (Å)	A (N=N–C) (°)	D (C–N=N–C) (°)
1a1	1.24	123.80	9.43	1.25	115.34	179.95
1a2	1.24	124.03	9.11	1.25	115.39	179.98
1b1	1.24	123.78	9.37	1.25	115.29	179.88
1b2	1.24	124.00	9.07	1.25	115.46	179.99
1b3	1.24	124.02	9.08	1.25	115.31	179.98
1b4	1.24	124.03	9.44	1.25	115.43	179.85
1c1	1.24	123.96	9.37	1.25	115.31	179.99
1c2	1.24	124.01	9.12	1.25	115.49	179.88
1c3	1.24	123.82	9.46	1.25	115.47	179.94
2a1	1.24	124.02	9.50	1.25	115.38	179.75
2a2	1.24	124.13	9.21	1.25	115.40	179.97
2b1	1.24	124.10	9.09	1.25	115.64	179.96
2b2	1.24	124.09	9.39	1.25	115.64	179.96
2c1	1.24	124.02	9.17	1.25	115.55	179.92
2c2	1.24	124.07	9.19	1.25	115.55	179.88
3a1	1.24	123.53	8.02	1.25	114.39	179.40
3a2	1.24	123.72	10.90	1.25	114.96	179.99
3a3	1.24	123.61	9.41	1.25	114.96	179.99
3a4	1.24	123.56	8.11	1.25	114.41	179.66
3b1	1.24	123.70	10.64	1.25	115.26	179.99
3b4	1.24	123.63	10.72	1.25	115.25	179.99
3c1	1.24	123.69	10.69	1.25	115.21	175.80
3c4	1.24	123.69	10.72	1.25	115.33	177.19
4a1	1.25	123.66	11.52	1.26	114.53	179.74

4a2	1.25	123.91	9.64	1.26	116.68	179.31
4a3	1.25	123.78	8.08	1.26	114.52	179.70
4a4	1.25	123.63	9.74	1.25	115.09	179.99
4b1	1.24	123.66	11.63	1.25	115.22	179.99
4b2	1.24	123.63	11.65	1.25	115.21	179.67
4c1	1.24	123.69	11.59	1.25	115.19	176.32
4c4	1.24	123.53	11.57	1.25	115.19	176.75
5a	1.24	123.84	8.67	1.25	115.24	179.99
5b	1.24	123.86	8.46	1.25	115.31	179.99
5c	1.24	123.93	8.60	1.25	115.35	179.99

3.3.1 Time dependent density functional theory

Time-Dependent Density Functional Theory (TD-DFT) calculations were conducted to compare the wavelength and the nature of transitions observed in the experimental UV-Vis spectra. Lowest unoccupied Molecular orbital (LUMO), highest occupied molecular orbital (LUMO) of all possible *cis*- isomer which are involved in $n \rightarrow \pi^*$ transitions approximately at 470nm are shown in (Table 11). Molecular orbital diagram of LUMO and all those occupied molecular orbital which has major contribution in $\pi \rightarrow \pi^*$ transitions approximately at 300nm for cis compound are reported in (Table- 12). HOMO and LUMO energies of *cis*- isomers in (Table -13) and HOMO and LUMO energies of *trans*- isomers in (Table -14)

TD-DFT calculated parameters and orbital contributions of the *cis* - isomers. ('H' stands for HOMO and 'L' stand for LUMO) are shown in (table-15) and orbital contributions of the *trans* – isomers in (Table 16). We observed that absorption band for $n \rightarrow \pi^*$ transition around 480 nm for *trans*- isomer is dipole forbidden as indicated by very low oscillation strength (f). On the other hand, the $n \rightarrow \pi^*$ transition is allowed in *cis*- isomer and the oscillator strength is relatively higher than that in the *trans*- isomer the *cis*- compound predicts transitions approximately at 470nm and 300nm which represent $n \rightarrow \pi^*$ and $\pi \rightarrow \pi^*$ transitions respectively. This prediction matches quite well with the experimentally observed spectra.

Table 11 Lowest unoccupied Molecular orbital (LUMO), highest occupied molecular orbital (HOMO) diagram of all possible *cis*- isomer which are involved in $n \rightarrow \pi^*$ transitions

Sample ID (Cis)	LUMO(L)	HOMO(H)
1a1	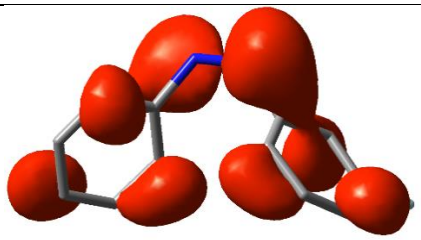	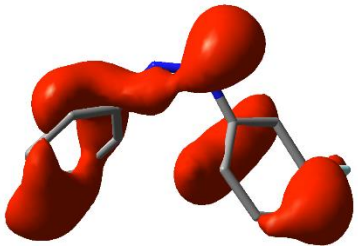
1a2	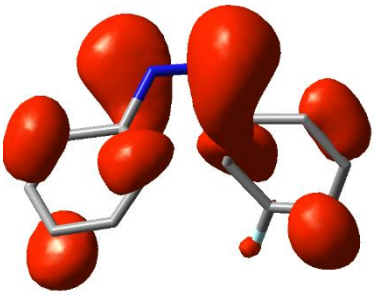	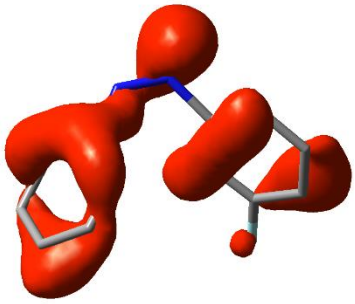
1b1	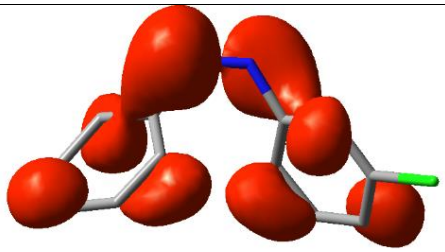	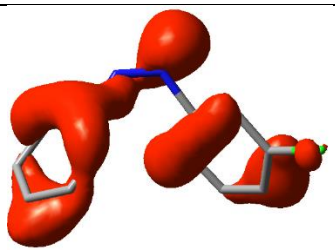
1b2	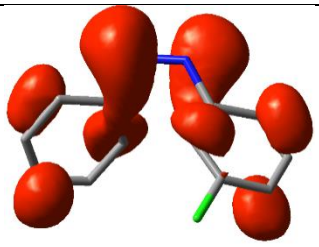	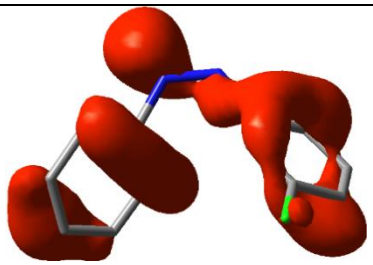
1b3	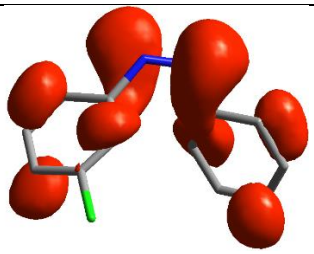	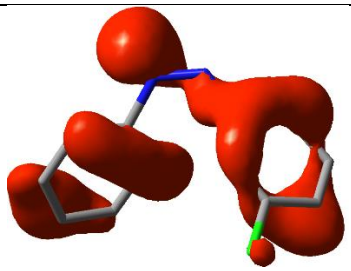

1b4	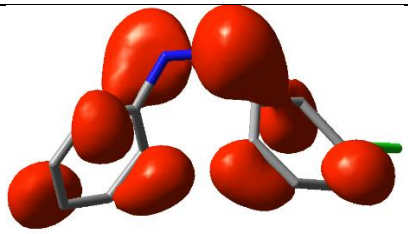	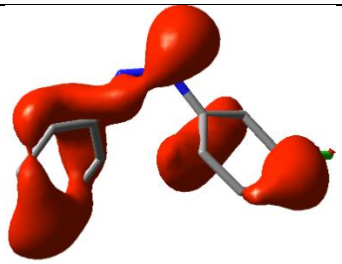
1c1	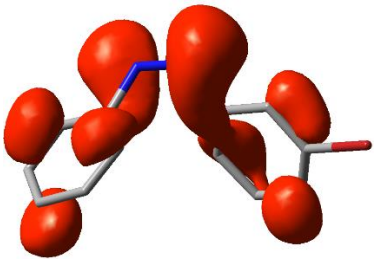	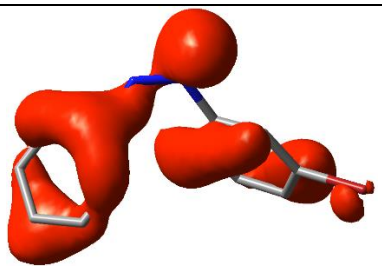
1c2	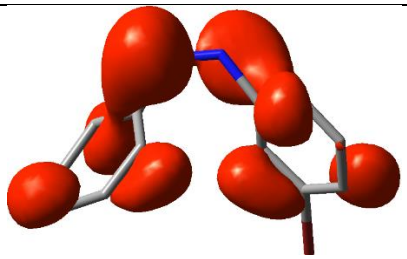	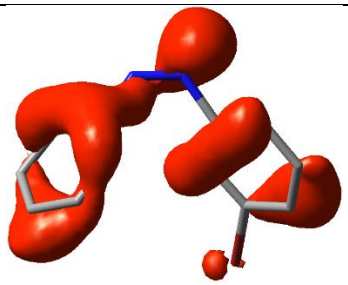
1c3	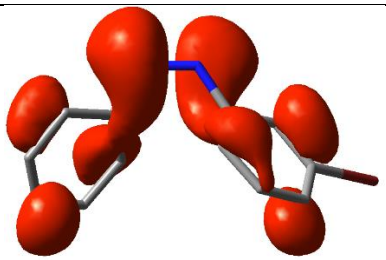	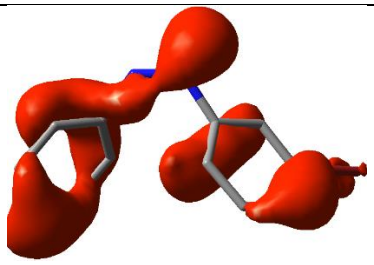
2a1	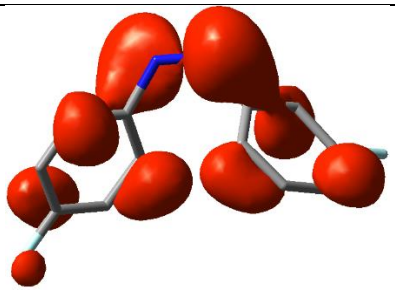	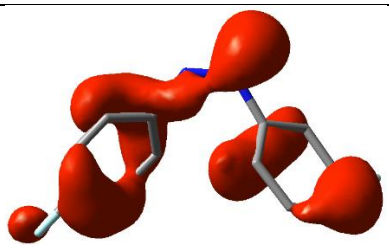
2a2	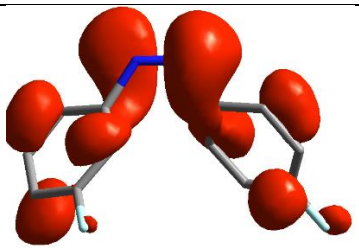	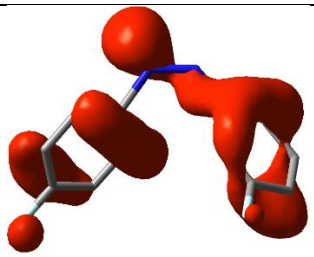

2b1	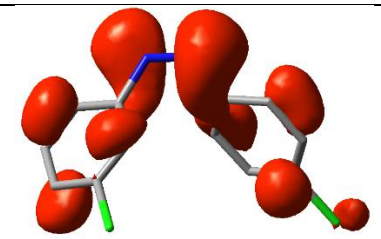	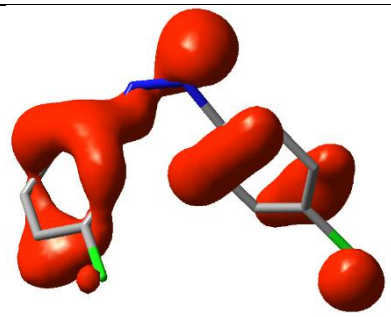
2b2	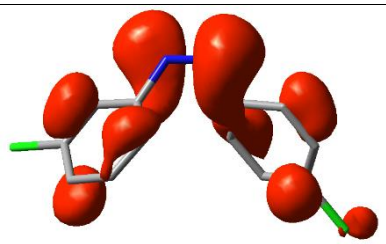	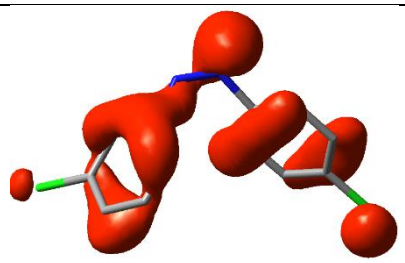
2c1	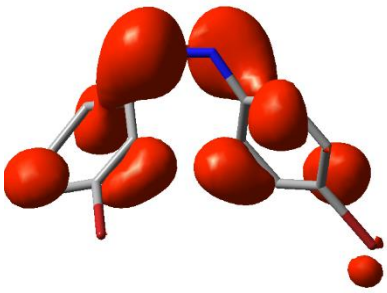	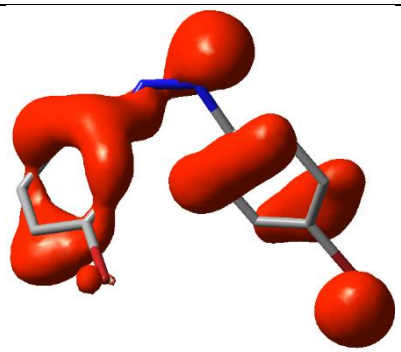
2c2	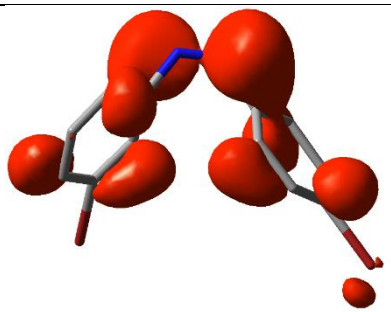	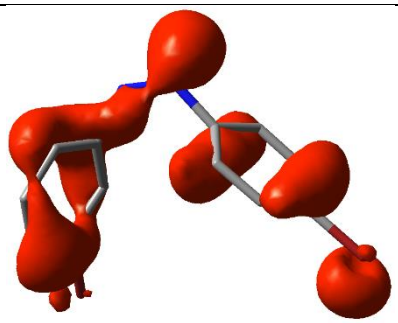
3a1	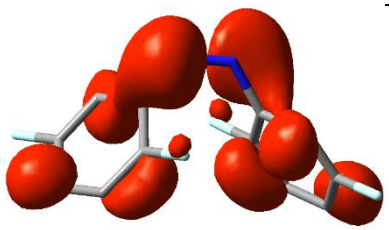	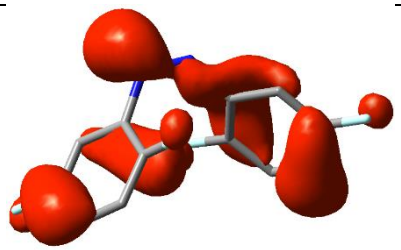

3a2	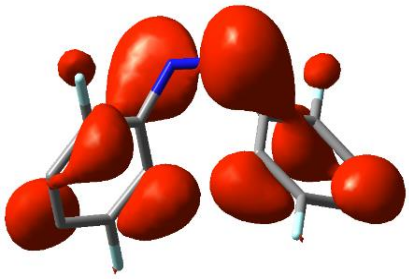	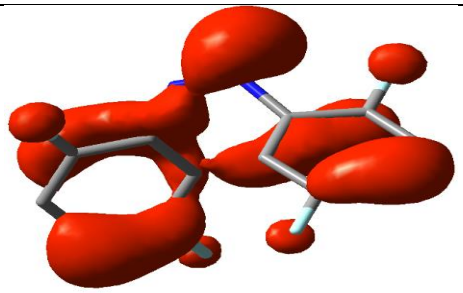
3a3	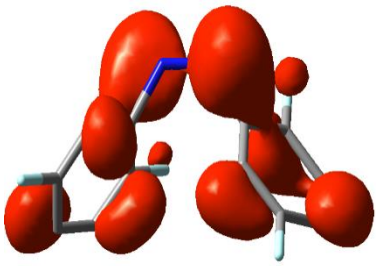	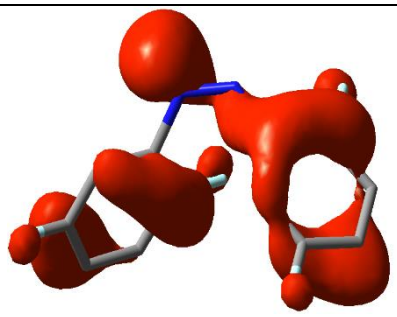
3a4	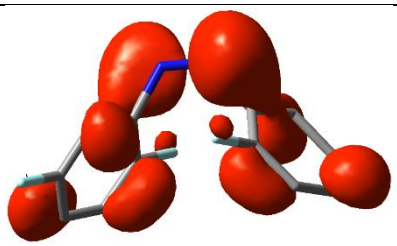	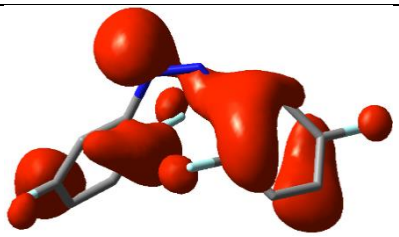
3b1	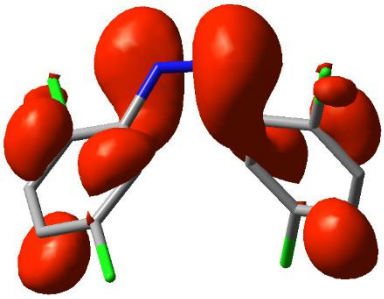	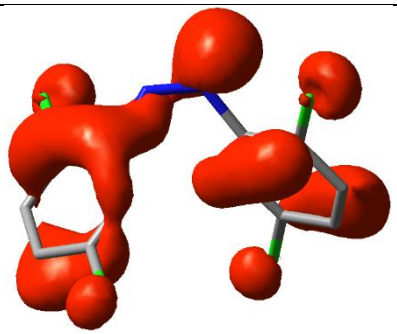
3b4	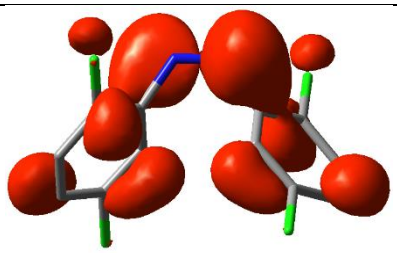	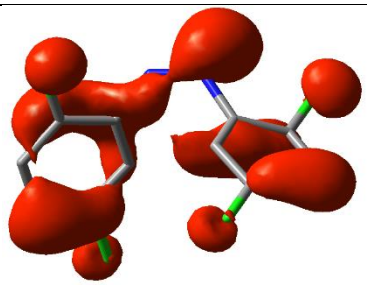

3c1	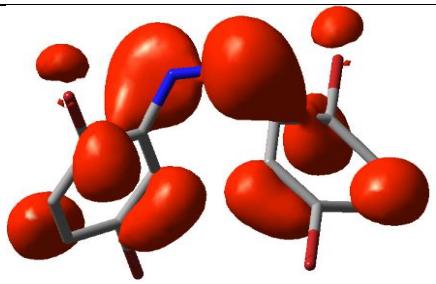	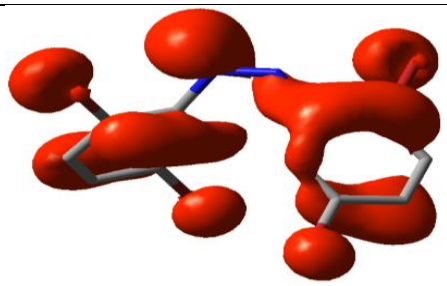
3c4	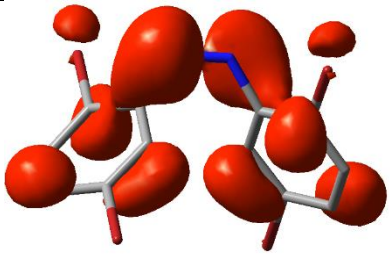	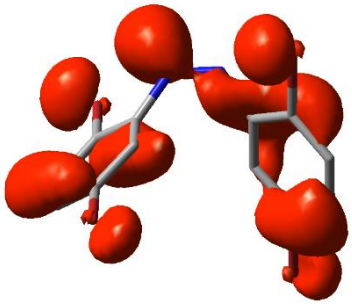
4a1	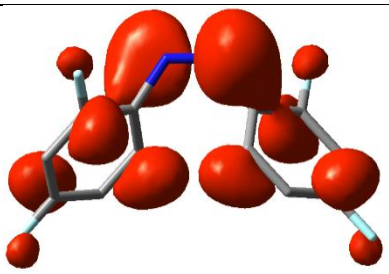	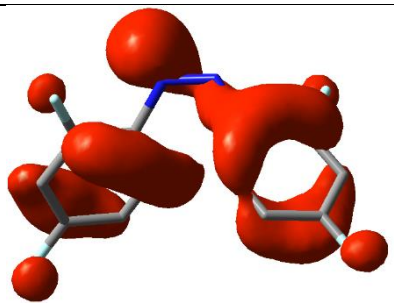
4a2	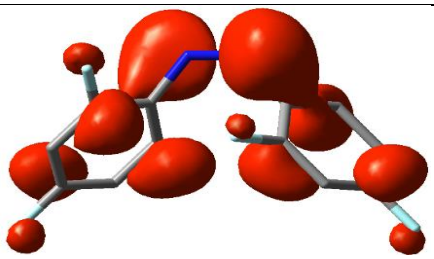	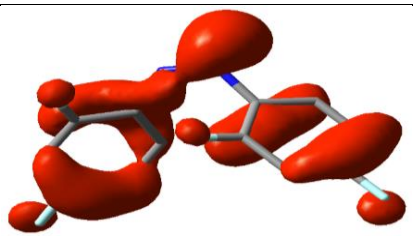
4a3	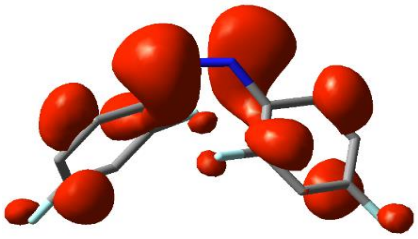	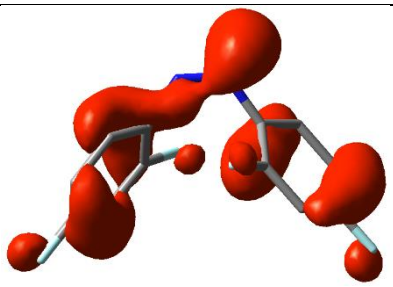
4a4	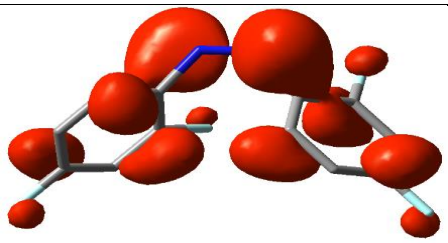	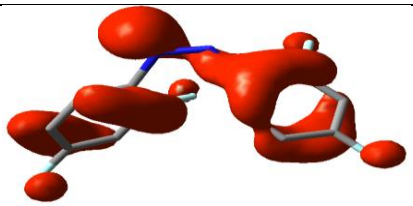

4b1	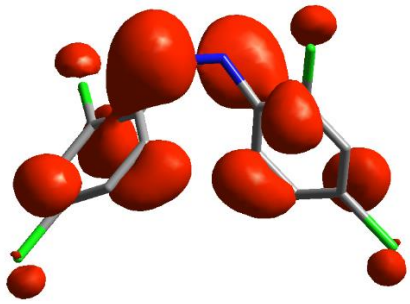	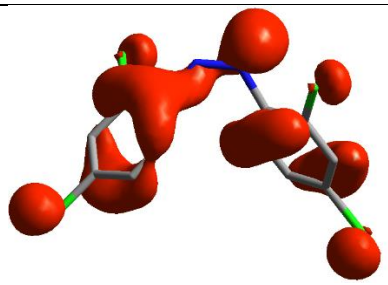
4b2	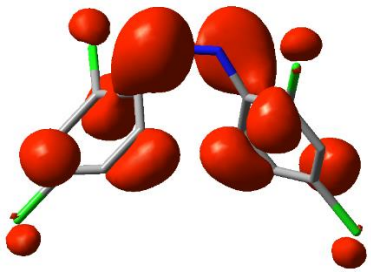	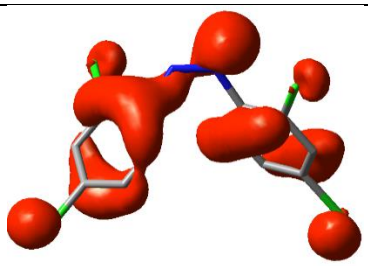
4c1	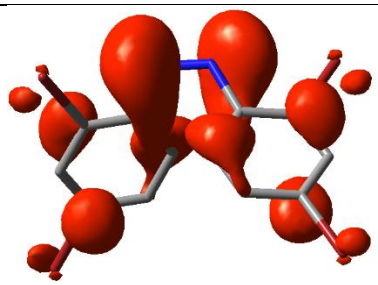	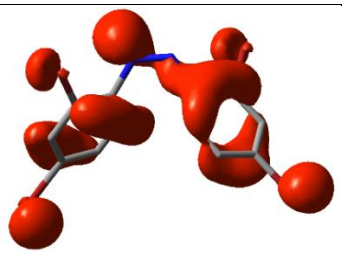
4c4	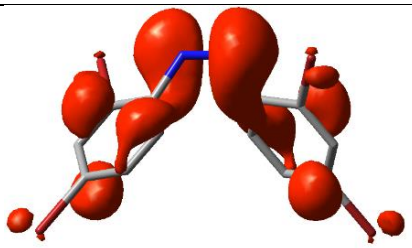	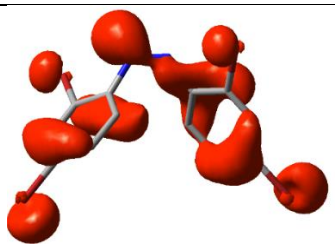
5a	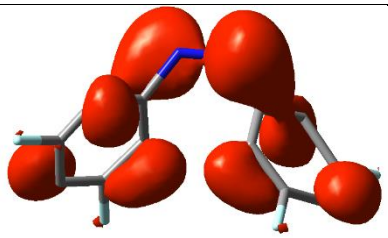	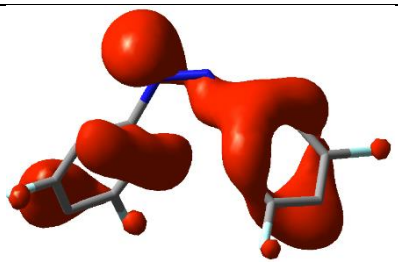
5b	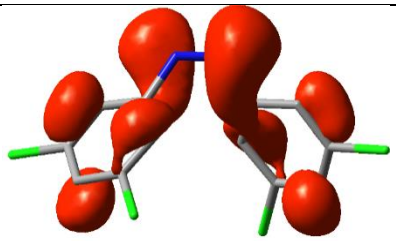	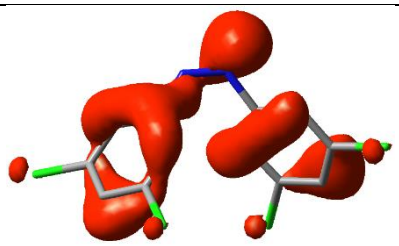

5c	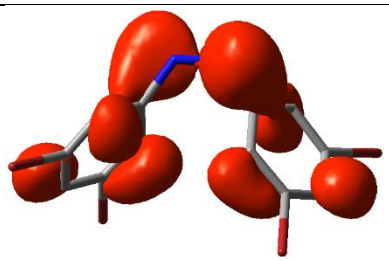	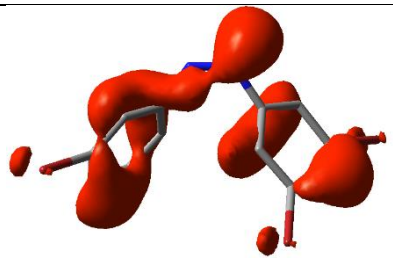

Table 12 Molecular orbital diagram of LUMO and all those occupied molecular orbital which has major contribution in $\pi \rightarrow \pi^*$ transitions approximately at 300nm for cis compound

Sample ID (Cis)	**LUMO(L)**	**MO diagram responsible for $\pi \rightarrow \pi^*$ transitions**
1a1	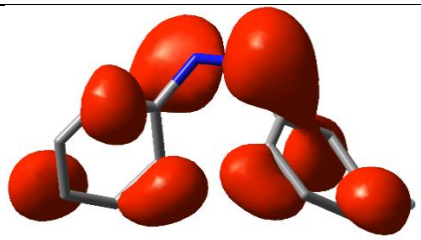	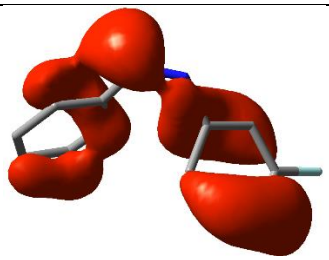 **H-4**
1a2	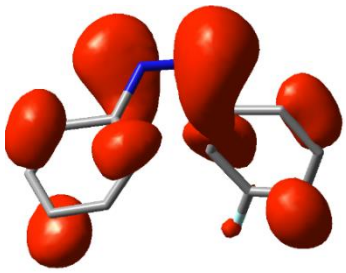	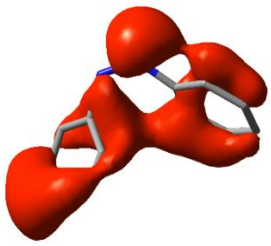 **H-3**
1b1	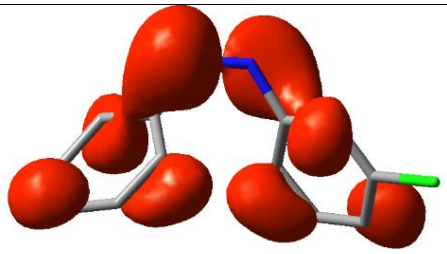	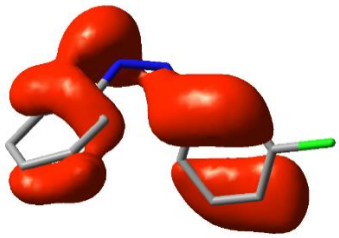 **H-4**
1b2	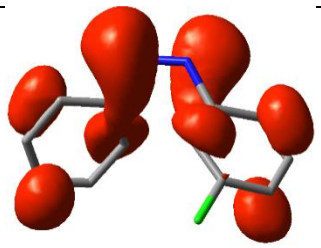	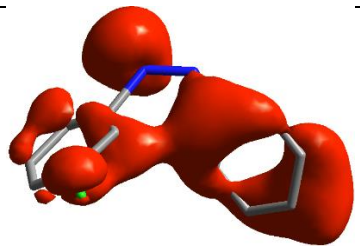 **H-3**

1b3	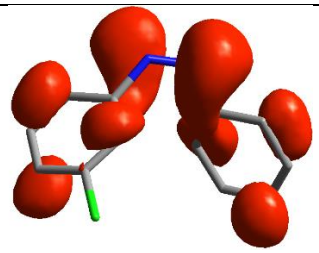	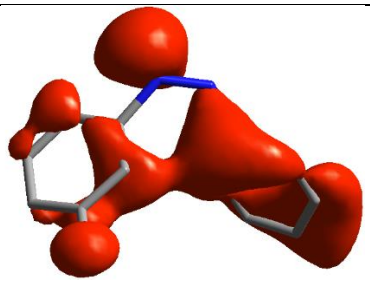	**H-3**
1b4	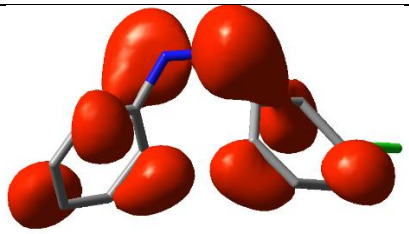	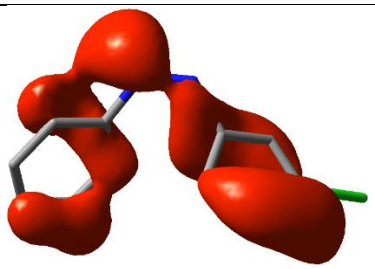	**H-4**
1c1	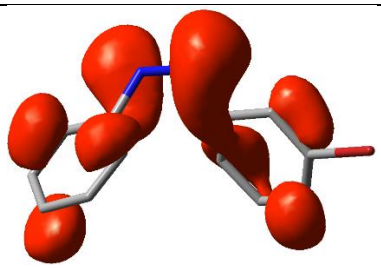	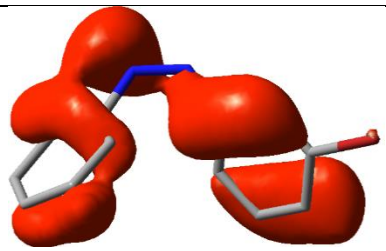	**H-4**
1c2	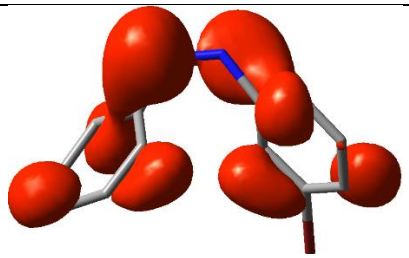	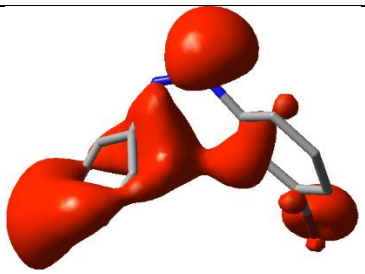	**H-3**
1c3	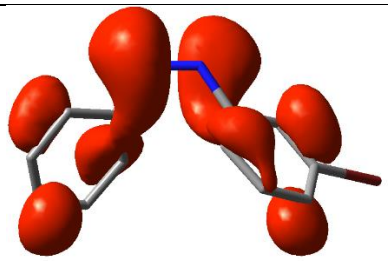	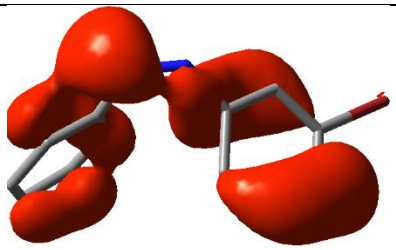	**H-4**
2a1	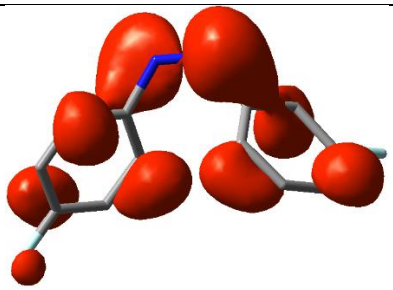	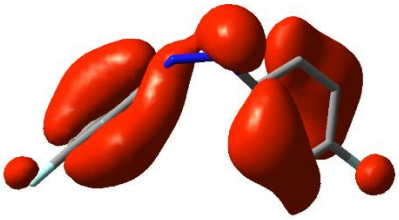	**H-3**

2a2	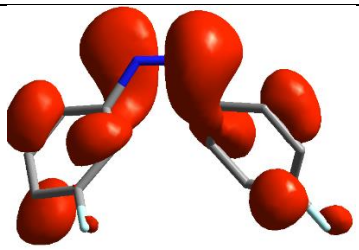	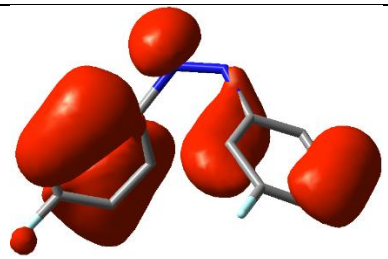 **H-2**
2b1	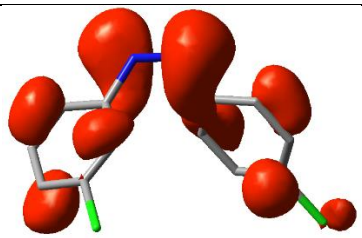	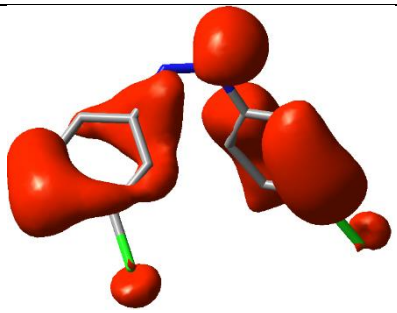 **H-3**
2b2	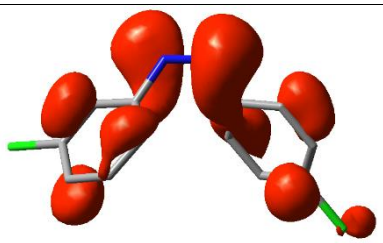	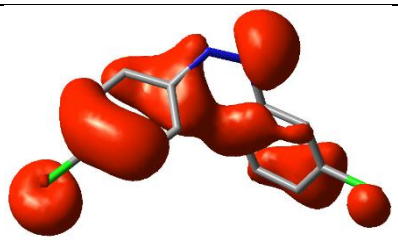 **H-2**
2c1	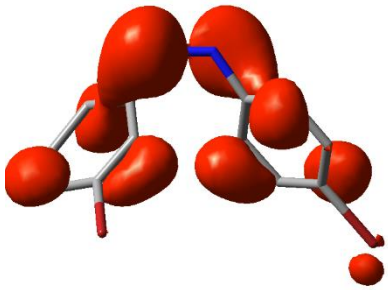	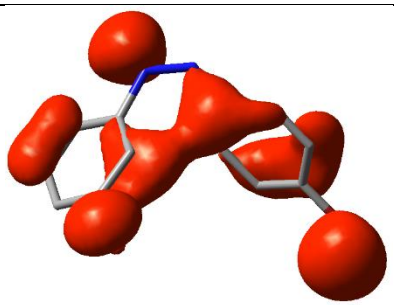 **H-2**
2c2	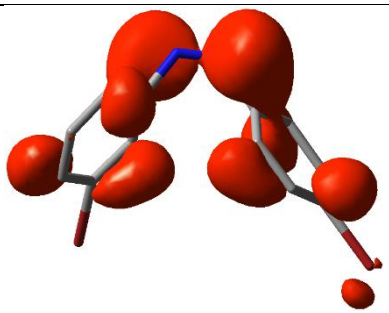	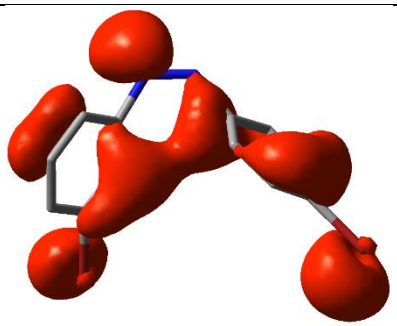 **H-2**
3a1	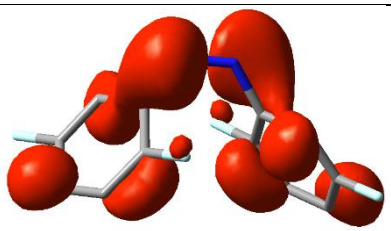	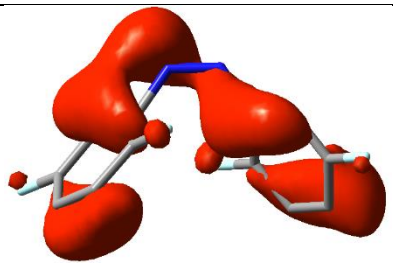 **H-4**

3a2	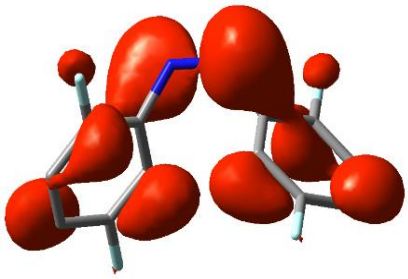	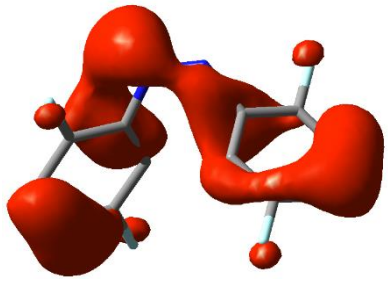 **H-3**
3a3	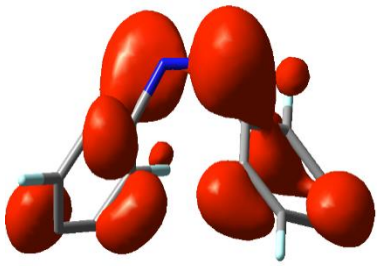	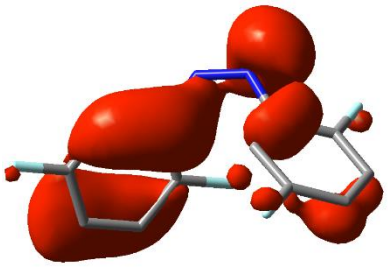 **H-4**
3a4	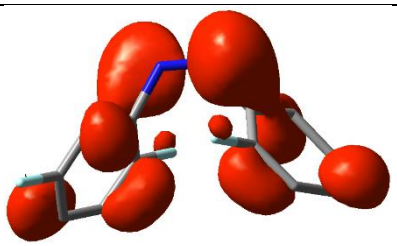	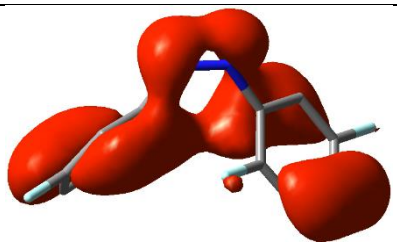 **H-3**
3b1	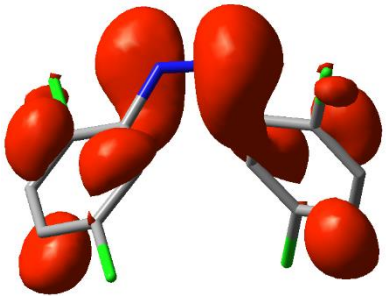	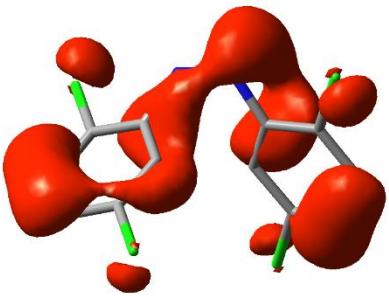 **H-2**
3b4	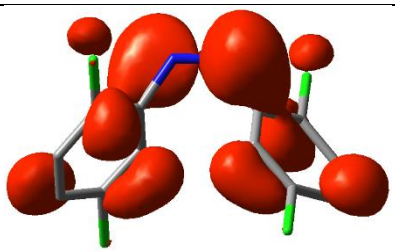	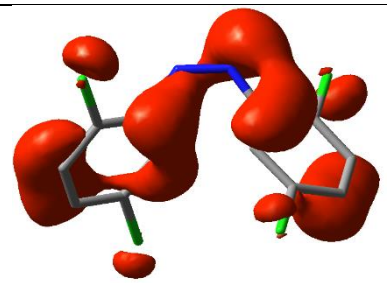 **H-3**
3c1	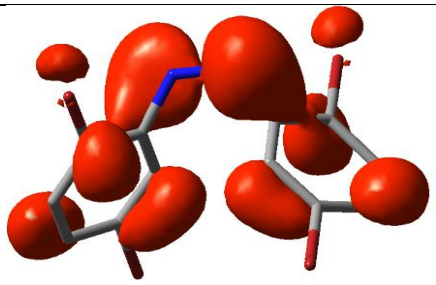	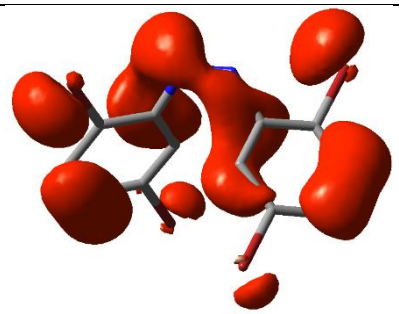 **H-3**

3c4	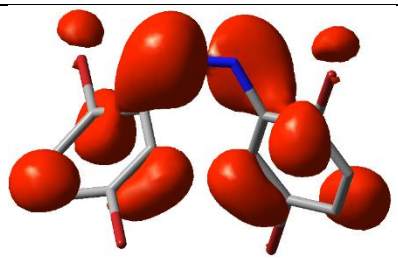	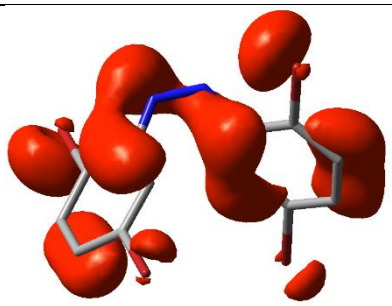 **H-3**
4a1	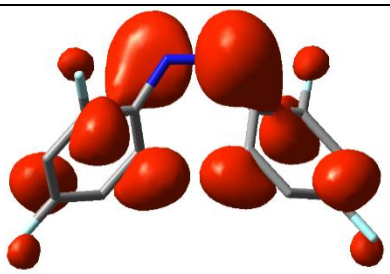	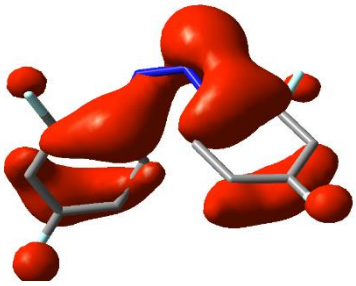 **H-3**
4a2	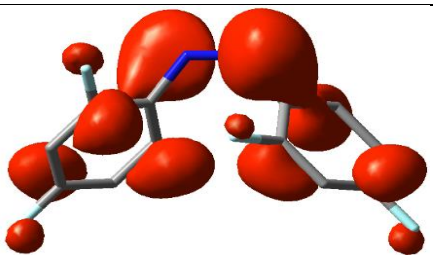	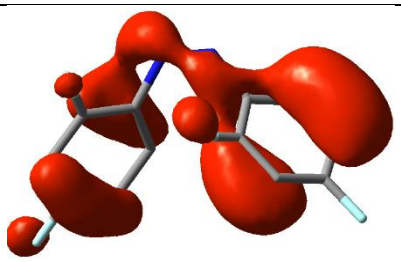 **H-2**
4a3	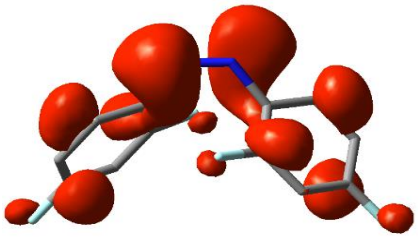	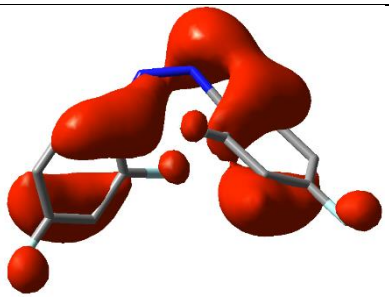 **H-4**
4a4	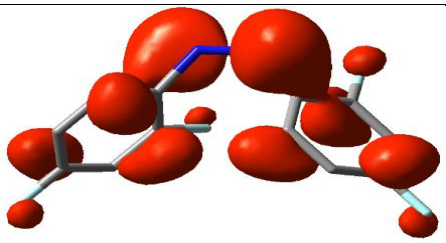	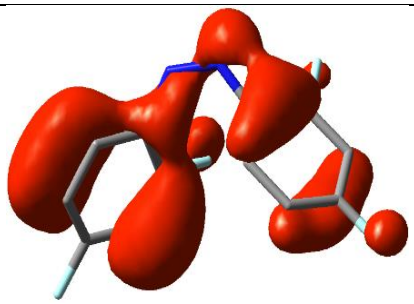 **H-2**

4b1	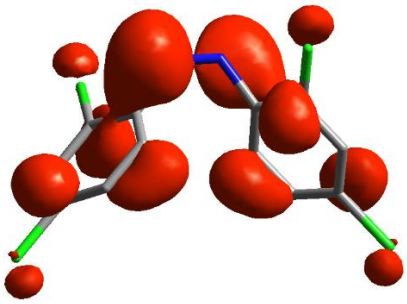	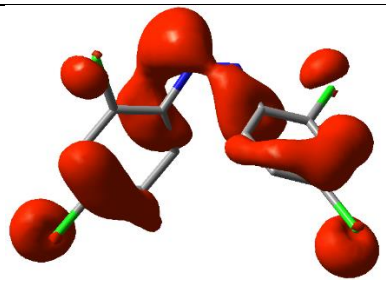 **H-3**
4b2	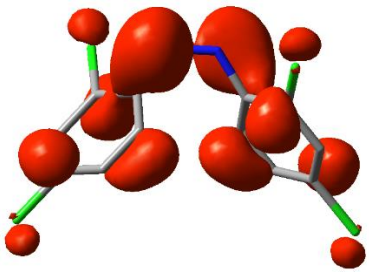	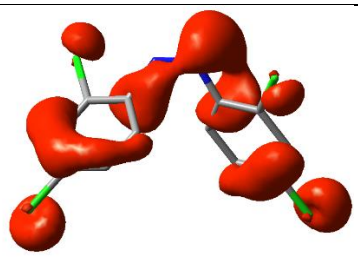 **H-3**
4c1	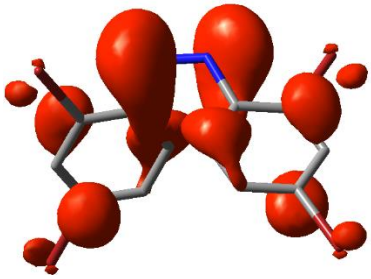	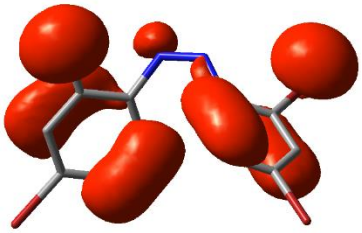 **H-2**
4c4	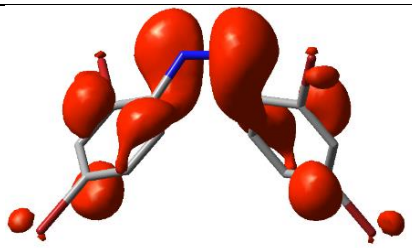	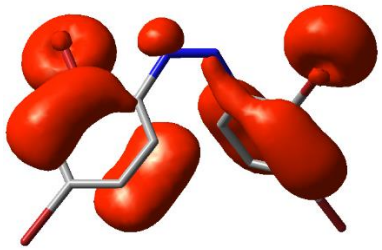 **H-2**
5a	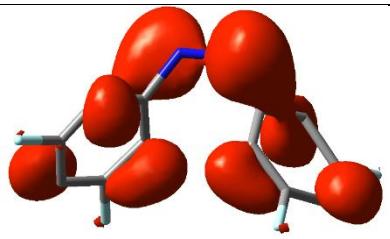	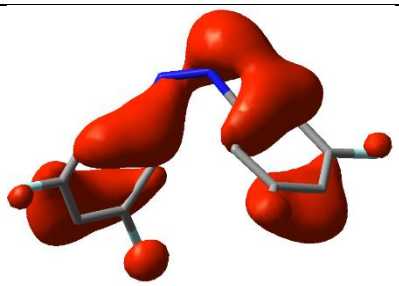 **H-4**
5b	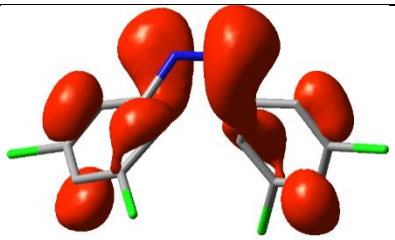	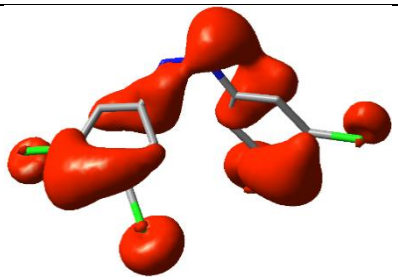 **H-4**

5c	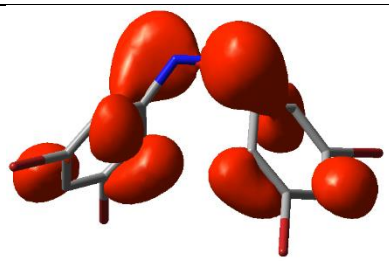	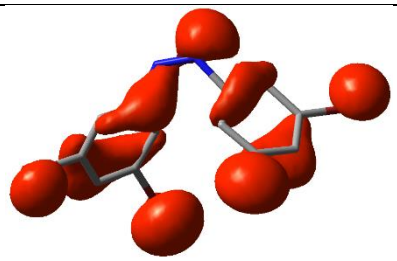 **H-4**

Table 13. HOMO and LUMO energies of *cis*- isomers

Cis-isomer	H (a.u.)	L (a.u.)	L-H (a.u.)	L-H (Kcal/mol)
1a1	-0.2353	-0.0955	0.1398	87.7245
1a2	-0.2354	-0.0959	0.1395	87.5362
1b1	-0.2355	-0.0959	0.1396	87.5990
1b2	-0.2357	-0.0961	0.1396	87.5990
1b3	-0.2357	-0.0962	0.1395	87.5362
1b4	-0.2355	-0.0960	0.1395	87.5362
1c1	-0.2356	-0.0959	0.1397	87.6617
1c2	-0.2357	-0.0962	0.1395	87.5362
1c3	-0.2355	-0.0961	0.1394	87.4735
2a1	-0.2359	-0.0967	0.1392	87.3480
2a2	-0.2361	-0.0971	0.1390	87.2225
2b1	-0.2370	-0.0993	0.1377	86.4067
2b2	-0.2368	-0.0991	0.1377	86.4067
2c1	-0.2369	-0.0998	0.1371	86.0302
2c2	-0.2369	-0.0997	0.1372	86.0930
3a1	-0.2494	-0.1067	0.1427	89.5442
3a2	-0.2476	-0.1095	0.1381	86.6577
3a3	-0.2488	-0.1086	0.1402	87.9755
3a4	-0.2494	-0.1067	0.1427	89.5442
3b1	-0.2480	-0.1095	0.1385	86.9087
3b4	-0.2481	-0.1094	0.1387	87.0342
3c1	-0.2473	-0.1094	0.1379	86.5322
3c4	-0.2472	-0.1095	0.1377	86.4067
4a1	-0.2410	-0.1035	0.1375	86.2812
4a2	-0.2422	-0.1029	0.1393	87.4107
4a3	-0.2436	-0.1015	0.1421	89.1677
4a4	-0.2423	-0.1028	0.1395	87.5362
4b1	-0.2421	-0.1072	0.1349	84.6497
4b2	-0.2421	-0.1071	0.1351	84.7752
4c1	-0.2414	-0.1078	0.1336	83.8340
4c4	-0.2416	-0.1075	0.1341	84.1477
5a	-0.2483	-0.1066	0.1417	88.9167
5b	-0.2485	-0.1077	0.1408	88.3520
5c	-0.2481	-0.1079	0.1402	87.9755

Table 14. HOMO and LUMO energies of *trans*- isomers

Trans- isomers	H (a.u.)	L (a.u.)	L-H (a.u.)	L-H (Kcal/mol)
1a1	-0.2495	-0.1057	0.1438	90.2345
1a2	-0.2496	-0.1062	0.1434	89.9835
1b1	-0.2496	-0.1061	0.1435	90.0462
1b2	-0.2498	-0.1064	0.1434	89.9835
1b3	-0.2496	-0.1061	0.1435	90.0462
1b4	-0.2497	-0.1065	0.1432	89.8580
1c1	-0.2493	-0.1062	0.1431	89.7952
1c2	-0.2495	-0.1065	0.1430	89.7325
1c3	-0.2495	-0.1065	0.1430	89.7325
2a1	-0.2487	-0.1062	0.1425	89.4187
2a2	-0.2488	-0.1068	0.1420	89.1050
2b1	-0.2488	-0.1094	0.1394	87.4735
2b2	-0.2488	-0.1094	0.1394	87.4735
2c1	-0.2477	-0.1095	0.1382	86.7205
2c2	-0.2477	-0.1095	0.1382	86.7205
3a1	-0.2542	-0.1163	0.1379	86.5322
3a2	-0.2557	-0.1199	0.1358	85.2145
3a3	-0.2557	-0.1199	0.1358	85.2145
3a4	-0.2552	-0.1163	0.1389	87.1597
3b1	-0.2545	-0.1220	0.1325	83.1437
3b4	-0.2545	-0.1220	0.1325	83.1437
3c1	-0.2495	-0.1203	0.1292	81.0730
3c4	-0.2504	-0.1214	0.1290	80.9475
4a1	-0.2498	-0.1084	0.1414	88.7285
4a2	-0.2448	-0.1048	0.1400	87.8500
4a3	-0.2497	-0.1084	0.1413	88.6657
4a4	-0.2495	-0.1118	0.1377	86.4067
4b1	-0.2491	-0.1185	0.1306	81.9515
4b2	-0.2491	-0.1185	0.1306	81.9515
4c1	-0.2457	-0.1181	0.1276	80.0690
4c4	-0.2459	-0.1184	0.1275	80.0062
5a	-0.2633	-0.1182	0.1451	91.0502
5b	-0.2627	-0.1189	0.1438	90.2345
5c	-0.2615	-0.1191	0.1424	89.3560

Table 15. TD-DFT calculated parameters and orbital contributions of the *cis* - isomers. ('H' stands for HOMO and 'L' stand for LUMO)

Sample	λ_{cal} (nm)	f(cal)	E (ev)	Major Contribution (%)
1a1 Cis	472.23	0.0536	2.6255	H -> L 91.95
	287.42	0.1278	4.3136	H-4>L 87.34
1a2 Cis	474.03	0.0541	2.6155	H -> L 92.74
	296.53	0.1762	4.1811	H-3 -> L 79.99

1b1 Cis	472.63	0.0560	2.6233	H -> L 91.79
	287.98	0.1215	4.3054	H-4 -> L 84.09
1b2 Cis	473.69	0.0526	2.6174	H -> L 92.60
	298.16	0.1583	4.1583	H-3 -> L 81.36
1b3 Cis	474.12	0.0528	2.6150	H -> L 92.61
	298.17	0.1626	4.1581	H-3 -> L 81.39
1b4 Cis	473.41	0.0565	2.6190	H-> L 91.79
	288.22	0.1218	4.3017	H-4 -> L 83.74
1c1 Cis	472.67	0.0574	2.6230	H -> L 91.51
	288.24	0.1228	4.3013	H-4 -> L 83.47
1c2 Cis	473.97	0.0516	2.6159	H-> L 92.51
	299.33	0.1500	4.1421	H-3 -> L 81.73
1c3 Cis	473.77	0.0582	2.6170	H-> L 91.53
	288.41	0.1232	4.2988	H-4 -> L 82.69
2a1 Cis	472.03	0.0562	2.6266	H-> L 91.32
	291.27	0.1146	4.2567	H-3 -> L 78.59
2a2 Cis	473.60	0.0567	2.6179	H-> L 92.14
	303.87	0.1343	4.0801	H-3 -> L 39.64 H-2 -> L 49.18
2b1 Cis	476.75	0.0640	2.6006	H-> L 91.13
	309.58	0.1916	4.0049	H-3 -> L 61.15 H-2 -> L 25.81
2b2 Cis	475.87	0.0682	2.6054	H-> L 90.25
	307.41	0.0855	4.0331	H-2 -> L 87.38
2c1 Cis	477.96	0.0670	2.5940	H -> L 90.25
	315.05	0.2050	3.9354	H-3 -> L 19.50 H-2 -> L 66.83
2c2 Cis	477.72	0.0669	2.5953	H-> L 90.25
	314.99	0.2032	3.9361	H-3 -> L 19.29 H-2 -> L 67.01
3a1 Cis	456.72	0.0497	2.7147	H-> L 88.39
	284.18	0.1821	4.3628	H-4 -> L 91.32
3a2 Cis	473.42	0.0665	2.6189	H-> L 91.15
	299.59	0.1801	4.1385	H-3-> L 90.28
3a3 Cis	467.20	0.0573	2.6538	H-> L 90.70
	290.16	0.1546	4.2729	H-4 -> L 89.90
3a4 Cis	457.08	0.0500	2.7125	H-> L 88.45
	299.34	0.1842	4.1420	H-3 -> L 93.86
3b1 Cis	473.58	0.0496	2.6180	H -> L 89.77
	302.02	0.1839	4.1052	H-3 -> L 90.51
3b4 Cis	472.68	0.0495	2.6230	H -> L 89.72
	301.88	0.1822	4.1071	H-3 -> L 90.41
3c1 Cis	474.44	0.0409	2.6133	H -> L 87.48
	304.58	0.1864	4.0706	H-3-> L 89.36
3c4 Cis	475.05	0.0414	2.6099	H-> L 87.52

	304.80	0.1882	4.0678	H-3-> L 89.46
4a1 Cis	472.30	0.0741	2.6251	H-3 -> L 7.79 H -> L 91.50
	306.78	0.2180	4.0414	H-3 -> L 89.29
4a2 Cis	466.99	0.0648	2.6550	H -> L 91.32
	308.17	0.1638	4.0233	H-2 -> L 72.21
4a3 Cis	457.59	0.0567	2.7095	H -> L 91.28
	290.49	0.1343	4.2682	H-4 -> L 81.37
4a4 Cis	466.25	0.0649	2.6592	H -> L 91.29
	308.18	0.1609	4.0232	H-2 -> L 73.55
4b1 Cis	481.04	0.0820	2.5774	H -> L 90.47
	321.25	0.2153	3.8594	H-3 -> L 57.93 H-2 -> L 32.57
4b2 Cis	480.16	0.0815	2.5821	H-> L 90.49
	320.78	0.2123	3.8650	H-3 -> L 58.01 H-2 -> L 32.50
4c1 Cis	484.48	0.0815	2.5591	H-> L 89.56
	332.21	0.1958	3.7321	H-4 -> L 35.56 H-2 -> L 54.64
4c4 Cis	482.37	0.0803	2.5703	H -> L 89.51
	331.45	0.1921	3.7407	H-4 -> L 36.78 H-2 -> L 53.33
5a Cis	467.01	0.0486	2.6548	H-> L 92.57
	292.36	0.1842	4.2408	H-4 -> L 87.41
5b Cis	469.88	0.0514	2.6386	H -> L 91.83
	299.93	0.1731	4.1338	H-4-> L 90.01
5c Cis	471.01	0.0523	2.6323	H-> L 91.06
	306.83	0.1419	4.0408	H-4 -> L 88.16

Table 16. TD-DFT calculated parameters and orbital contributions of the *trans* - isomers. ('H' stands for HOMO and 'L' stand for LUMO)

Sample	λcal (nm)	f(cal)	E (ev)	Major Contribution (%)
1a1 trans	354.51	0.8177	3.4973	H -> L 97.60
1a2 trans	354.0	0.9119	3.5024	H -> L 99.15
1b1 trans	355.52	0.7908	3.4874	H -> L 94.70
1b2 trans	355.22	0.9000	3.4904	H->L 98.93
1b3 trans	355.59	0.7912	3.4867	H->L 98.02
1b4 trans	355.23	0.9000	3.4902	H->L 94.46
1c1 trans	357.11	0.7249	3.4719	H -> L 97.28
1c2 trans	356.74	0.8636	3.4755	H -> L 96.47
1c3 trans	356.74	0.8645	3.4755	H -> L 97.53
2a1 trans	356.41	0.8309	3.4787	H->L 94.94
2a2 trans	356.22	0.9204	3.4805	H->L 99.45

2b1 trans	365.38	1.0181	3.3933	H->L	99.28
2b2 trans	365.36	1.0181	3.3935	H->L	99.30
2c1 trans	370.60	0.9338	3.3455	H->L	98.61
2c2 trans	370.59	0.9337	3.3455	H->L	98.57
3a1 trans	366.27	0.6111	3.3851	H-1-> L H->L	40.32 54.78
3a2 trans	376.69	0.7378	3.2914	H->L	96.57
3a3 trans	376.72	0.7386	3.2912	H->L	96.59
3a4 trans	366.75	0.6302	3.3806	H-1->L H->L	26.61 68.41
3b1 trans	344.95	0.3843	3.5943	H-3->L	95.43
3b4 trans	344.95	0.3844	3.5943	H-3->L	95.43
3c1 trans	339.86	0.4970	3.6481	H-3->L	96.04
3c4 trans	344.87	0.4790	3.5951	H-3->L	96.42
4a1 trans	355.47	0.9749	3.4879	H->L	96.05
4a2 trans	340.64	0.9672	3.6397	H-1->L H->L	67.37 31.79
4a3 trans	355.45	0.9746	3.4881	H->L	94.26
4a4 trans	367.67	0.9329	3.3722	H->L	99.47
4b1 trans	395.31	1.0078	3.1364	H->L	98.99
4b2 trans	395.24	1.0072	3.1369	H->L	98.05
4c1 trans	395.30	0.9076	3.1365	H-1->L H->L	44.58 53.19
4c4 trans	398.13	0.9257	3.1142	H-1->L H->L	39.61 58.29
5a trans	350.27	0.7043	3.5397	H-2->L H->L	10.23 89.35
5b trans	351.03	0.5057	3.5320	H-2->L H->L	64.01 33.62
5c trans	358.12	0.8601	3.4621	H->L	88.07

4. Conclusions

The rate constants for the *cis*- → *trans*- isomerization in solution for a series of halogenated azobenzenes were experimentally observed. These observations were further supported by theoretical calculations. It is interesting to note that there is a trend in the value of the rate constant for the transformation of *cis*- to *trans*- isomer for all the compounds. The value increases from fluoro to chloro to bromo derivative in general. Compounds 1(a-c) show similar trend in rate constant with the fluoro compound a slightly lower in value. The energy of activation is similar for all three compounds. A similar trend was observed for 2(a-c). The noticeable change was observed for 3a, 4a and 5a compounds. Approximately 20% of all of them remained unconverted even after 4 days. Approximately 30% of 3a and 4a while 18% of 5a remained unconverted for a long time.

The remarkable reduced rate constants of all the fluoro compounds compared to the Br and Cl analogues justified the kinetic stability of these fluoro derivatives over Br and Cl analogues. The resultant *trans*- isomers were compared with the geometry of the *trans*- isomer observed in the crystal structure (for 13 compounds). It is noteworthy that the conformation of the *trans*- isomers of the 13 compounds structurally characterized are found to be similar to those obtained by optimized conformation of the *trans*- isomers obtained after IRC calculations.Theoretical calculations of activation energy also predict the similar trend in most of the cases. The UV-Vis spectra were well predicted and analysed by theoretical calculations. Therefore, we conclude that the fluorinated ABs can be promising candidates for various applications in future.

5.Bibliography

(1) Hartley, G. S. The Cis-form of Azobenzene. *Nature* **1937**, *140,* 281

(2) Osorio-Planes, L.; Rodríguez, C.; Pericàs, M. A. Photoswitchable Thioureas for the External Manipulation of Catalytic Activity. *Org. Lett*. **2014**, *16*, 1704-1707.

(3) Dong, M.; Babalhavaeji, A.; Collins, C. V.; Jarrah, K.; Sadovski, O.; Dai, Q.; Woolley, G. A. Near-Infrared Photoswitching of Azobenzenes under Physiological Conditions. *J. Am. Chem. Soc*. **2017**, *139*, 13483-13486.

(4) Gerkman, M. A.; Sinha, S.; Warner, J. H.; Han, G. G. D. Direct Imaging of Photoswitching Molecular Conformations Using Individual Metal Atom Markers. *ACS nano* **2019**, *13*, 87-96.

(5) Malyar, I. V.; Titov, E.; Lomadze, N.; Saalfrank, P.; Santer, S. Photoswitching of azobenzene-containing self-assembled monolayers as a tool for control over silicon surface electronic properties. *J. Chem. Phys.* **2017**, 146, 104703.

(6) Nikolova, L.; Todorov, T.; Ivanov, M.; Andruzzi, F.; Hvilsted, S.; Ramanujam, P. S. Photoinduced Circular Anisotropy in Side-Chain Azobenzene Polyesters. *Opt. Mater.* **1997**, 8, 255-258.

(7) Ivanov, M.; Naydenova, I.; Todorov, T.; Nikolova, L.; Petrova, T.; Tomova, N.; Dragostinova, V. Light-induced optical activity in optically ordered amorphous side-chain azobenzene containing polymer. *J. Mod. Opt.* **2000**, *47,* 861-867.

(8) Nunzi, J.-M.; Fiorini, C.; Etilé, A.-C.; Kajzar, F. All-optical poling in polymers: dynamical aspects and perspectives. *Pure Appl. Opt*. **1998**, *7*, 141-150.

(9) Ichimura, K. Photoalignment of Liquid-Crystal Systems. *Chem. Rev*. **2000**, *100,* 1847-1874.

(10) Halabieh, R. H. El; Mermut, O.; Barrett, C. J. Using light to control physical properties of polymers and surfaces with azobenzene chromophores. *Pure Appl. Chem*. **2004**, *76,* 1445-1465.

(11) Aoki, K. I.; Nakagawa, M.; Ichimura, K. Self-Assembly of Amphoteric Azopyridine Carboxylic Acids: Organized Structures and Macroscopic Organized Morphology Influenced by Heat, pH Change, and Light. *J. Am. Chem. Soc.* **2000**, *122*, 10997-11004.

(12) Delaire, J. A.; Nakatani, K. Linear and Nonlinear Optical Properties of Photochromic Molecules and Materials. *Chem. Rev*. **2000**, *100,* 1817-1846.

(13) Viswanathan, N. K.; Kim, D.Y.; Bian, S.; Williams, J.; Liu, W.; Li, L.; Samuelson, L. Kumar, J.; Tripathy, S. K. Surface relief structures on azo polymer films. *J. Mater. Chem*. **1999**, *9,* 1941-1955.

(14) Natansohn, A.; Rochon, P. Photoinduced Motions in Azo-Containing Polymers. *Chem. Rev.* **2002**, *102,* 4139-4176.

(15) Willner, I.; Rubin, S.; Riklin, A. Photoregulation of papain activity through anchoring photochromic azo groups to the enzyme backbone. *J. Am. Chem. Soc*. **1991**, *113,* 3321-3325.

(16) Liang, X.; Asanuma, H.; Kashida, H.; Takasu, A.; Sakamoto, T.; Kawai, G.; Komiyama, M. NMR Study on the Photoresponsive DNA Tethering an Azobenzene. Assignment of the Absolute Configuration of Two Diastereomers and Structure Determination of Their Duplexes in the trans-Form. *J. Am. Chem. Soc.* **2003**, *125*, 16408-16415.

(17) Yager, K. G.; Barrett. C. J. Novel photo-switching using azobenzene functional materials. *J. Photochem. Photobiol. A* **2006**, *182*, 250-261.

(18) Norikane, Y.; Kitamoto, K.; Tamaoki, N. Novel Crystal Structure, Cis−Trans Isomerization, and Host Property of Meta-Substituted Macrocyclic Azobenzenes with the Shortest Linkers. *J. Org. Chem*. **2003**, *6*, 8291-8304.

(19) Rottger, D.; Rau, H. Photochemistry of azobenzenophanes with three-membered bridges. *J. Photochem. Photobiol. A* **1996**, *101*, 205-214.

(20) Nagamani, S. A.; Norikane, Y.; Tamaoki, N. Photoinduced Hinge-Like Molecular Motion: Studies on Xanthene-Based Cyclic Azobenzene Dimers. *J. Org. Chem*. **2005**, *70*, 9304-9313.

(21) Vollmer, M. S.; Clark, T. D.; Steinem, C.; Ghadiri, M. R. Photoswitchable Hydrogen-Bonding in Self-Organized Cylindrical Peptide Systems. *Angew. Chem. Int. Ed.* **1999**, *38*, 1598-1601.

(22) Shirota, Y.; Moriwaki, K.; Yoshikawa, S.; Ujike, T.; Nakano, H. 4-[Di(biphenyl-4-yl) amino]azobenzene and 4,4′-bis[bis(4′-tert-butylbiphenyl-4-yl)amino]azobenzene as a novel family of photochromic amorphous molecular materials. *J. Mater. Chem.* **1998**, *8*, 2579-2581.

(23) Funke, U.; Gruetzmacher, H. F. Dithia-diaza[n. 2] paracyclophane-enes *Tetrahedron* **1987**, *43,* 3787-3795.

(24) Rabek, J. F. *Photochemistry and Photophysics*; CRC Press, **1990**.

(25) Brown, E. V.: Granneman, G.R. *J. Am. Chem. Soc*. **1975**, 97, 621-627.

(26) Koshima, H.; Ojima, N.; Uchimoto, H. Mechanical Motion of Azobenzene Crystals upon Photoirradiation. *J. Am. Chem. Soc.* **2009**, *131* (20), 6890–6891.

(27) Nägele, T.; Hoche, R.; Zinth, W.; Wachtveitl, J. Femtosecond Photoisomerization of Cis-Azobenzene. *Chem. Phys. Lett.* **1997**, *272* (5–6), 489–495.

(28) Karanam, M.; Choudhury, A. R. *Cryst. Growth Des*., **2013**, *13*, 4803-4814.

(29) Schuster, S.; Fu¨ser, M.; Asyuda, A.; Cyganik, P.; Andreas Terfort, A.; Zharnikov, M.; *Phys. Chem. Chem. Phys.*, **2019**, *21*, 9098—9105.

(30) Yin, T. T.; Zhao, Z. X.; Zhang, H. X.; *RSC Adv*., **2016**, *6*, 79879–79889.

(31) Yin, T. T.; Zhao, Z. X.; Zhang, H. X.; *New J. Chem*., **2017**, *41*, 1659—1669.

(32) Samanta, D.; Gemen, J.; Chu, Z.; Posner, Y. D.; Linda J. W. Shimon, L. J. W.; Klajn. R; *PNAS* September 18, **2018** *115* (38) 9379-9384.

(33) Chu .Z.; Han. Y.; Bian. T.; De. S.; Král. P.; Klajn.R.; *J Am Chem Soc*. **2019** Feb 6;*141*(5):1949-196.

(34) Kennedy. A. D. W.; Sandler. I.; Andréasson. J.; Ho. J.; Beves. J. E.; *Chem.- Eur. J.* **2020**, *26*, 1103–1110.

(35) Frisch, M. J.; Trucks, G. W.; Schlegel, H. B.; Scuseria, G. E.; Robb, M. A.; Cheeseman, J. R.; Scalmani, G.; Barone, V.; Mennucci, B.; Petersson, G. A.; Nakatsuji, H.; Caricato, M.; Li, X.; Hratchian, H. P.; Izmaylov, A. F.; Bloino, J.; Zheng, G.; Sonnenberg, J. L.; Hada, M.; Ehara, M.; Toyota, K.; Fukuda, R.; Hasegawa, J.; Ishida, M.; Nakajima, T.; Honda, Y.; Kitao, O.; Nakai, H.; Vreven, T.; Jr.Montgomery, J. A.; Peralta, J. E.; Ogliaro, F.; Bearpark, M.; Heyd, J. J.; Brothers, E.; Kudin, K. N.; Staroverov, V. N.; Kobayashi, R.; Normand, J.; Raghavachari, K.; Rendell, A.; Burant, J. C.; Iyengar, S. S.; Tomasi, J.; Cossi, M.; Rega, N.; Millam, J. M.; Klene, M.; Knox, J. E.; Cross, J. B.; Bakken, V.; Adamo, C.; Jaramillo, J.; Gomperts, R.; Stratmann, R. E.; Yazyev, O.; Austin, A. J.; Cammi, R.; Pomelli, C.; Ochterski, J. W.; Martin, R. L.; Morokuma, K.; Zakrzewski, V. G.; Voth, G. A.; Salvador, P.; Dannenberg, J. J.; Dapprich, S.; Daniels, A. D.; Farkas, Ö.; Foresman, J. B.; Ortiz, J. V.; Cioslowski, J.; Fox, D. J. *Gaussian 09*, revision A.1; Gaussian, Inc.: Wallingford, CT, **2009.**

(36) Priewisch, B.; Ruck-Braun, K. Efficient Preparation of Nitrosoarenes for the Synthesis of Azobenzenes. *J. Org. Chem*. **2005**, *70*, 2350-2352.

(37) Knie, C.; Utecht, M.; Zhao, F.; Kulla, H.; Kovalenko, S.; Brouwer, A. M.; Saalfrank, P.; Hecht, S.; Bleger, D. ortho-Fluoroazobenzenes: Visible Light Switches with Very Long-Lived Z Isomers. *Chem. Eur. J*. **2014**, *20*, 16492-16501.

(38) Dolomanov, O. V.; Bourhis, L. J.; Gildea, R. J.; Howard, J. A. K.; Puschmann, H. J. *Appl. Cryst.* **2009,***42* ,339

(39) Sheldrick, G. M. *Acta Cryst* **2015**. *A71*,3-8

(40) Sheldrick, G. M. *Acta Crystallogr* . **2008**, *A64* ,112

(41) Macrae, C. F.; bruno, I.J.; Chisholm, J. A.; Edgington, P. R.; McCabe, P.;Pidcock, E.; Rodriguez-Monge, L.; Taylor,R .; Streek, J.; Wood, P.A *J.Appl.Crystallogr*.**2008**,*41*,466-470

(42) Denninng, R.; Keith, T.; Millam, J. *GaussView*, version 5; Semichem, Inc.: Shswnee Mission KS, **2009**.

(43) Cances, E.; Mennucci, B.; Tomasi, J. *J. Chem. Phys.* **1997**,*107*, 3032-3041.

(44) Thalladi, V. R.;Weiss, H. C.; Bläser, D.; Boese, R.;Nangia, A.; Desiraju, G. R. *J. Am. Chem. Soc.* **1998**, *120* , 8702

(45) (a) Aakeroy, C. B.;Evans,T. A.; Seddon, K. R.; Palink, I. *NewJ.Chem*.**1999**,*23*,145-152. (b)Desiraju, G. R *Acc. Chem. Res* **1991**, *24*, 290-296 (c) Pedireddi, V. R. *Cryst Growth Des*. ***2001***, *1*, 383-385

(46) Hunter, A.C.; Sanders, K.M.J.; *J. Am. Chem. Soc.* **1990**, *112*, 14, 5525-5534

(47) Mazik, M.; Buthe, C.A.; Jones, G.P.; *Tetrahedron.* **2010**, *66*, 385-389.

(48) Matter, H.; Nazaré, M.; Güssregen, S.; Will, D.W.; Schreuder, H.; Bauer, A.; Urmann, M.; Ritter, K.; Wagner, M.; Wehner, V.; *Angew Chem Int Ed Engl*. **2009**, *48(16)*, 2911

(49) Cortada, C. M.; Castelló, J.; Novoa, J. J. *CrystEngComm*, **2014**, *16*, 8232